NUMERICAL MODELLING AND QUANTIFYING UNCERTAINTIES OF LANDSLIDE RUNOUT WITH ENTRAINMENT

Submitted in partial fulfilment of the
requirements for the award of the degree of

DOCTOR OF PHILOSOPHY
in
CIVIL ENGINEERING

by

KAVIN KUMAR C

(Roll No: 716108)

Supervisor

Dr. M. HEERALAL

Dr. RAKESH J PILLAI

DEPARTMENT OF CIVIL ENGINEERING

NATIONAL INSTITUTE OF TECHNOLOGY WARANGAL

WARANGAL - 506004

INDIA

JUNE - 2021

DEDICATION

Dedicated To my father

P M Chinnasamy (1957-2021)

"Sire greatest boon on son confers, who makes him meet, in councils of the wise to fill the highest seat" - Thiruvalluvar

Indebted to my mother C Rajeswari

THESIS APPROVAL FOR PH.D.

This Thesis entitled "**NUMERICAL MODELLING AND QUANTIFYING UNCERTAINTIES OF LANDSLIDE RUNOUT WITH ENTRAINMENT**" prepared by **Mr. KAVINKUMAR C** (Roll No. 716108) is approved for the degree of Doctor of Philosophy.

Examiners

_____

_____

_____

Supervisor/s

_____

_____

Chairman

_____

Date:

Place:

DECLARATION

This is to certify that the work presented in the thesis entitled **"NUMERICAL MODELLING AND QUANTIFYING UNCERTAINTIES OF LANDSLIDE RUNOUT WITH ENTRAINMENT"** is a bonafide work done by me under the supervision of **Dr. M. HEERALAL** and **Dr. RAKESH J PILLAI** and was not submitted elsewhere for the award of any degree. I declare that this written submission represents my ideas in my own words and where others' ideas or words have been included, I have adequately cited and referenced the original sources. I also declare that I have adhered to all principles of academic honesty and integrity and have not misrepresented or fabricated or falsified any idea / data / fact /source in my submission. I understand that any violation of the above will be a cause for disciplinary action by the Institute and can also evoke penal action from the sources which have thus not been properly cited or from whom proper permission has not been taken when needed.

_____

(**Kavinkumar C**)

(Roll No: **716108**)

Date: _____

NATIONAL INSTITUTE OF TECHNOLOGY WARANGAL

CERTIFICATE

This is to certify that the thesis entitled **"NUMERICAL MODELLING AND QUANTIFYING UNCERTAINTIES OF LANDSLIDE RUNOUT WITH ENTRAINMENT"** being submitted by **Mr. KAVINKUMAR C** for the award of the degree of **DOCTOR OF PHILOSOPHY** to the Faculty of Engineering and Technology of **NATIONAL INSTITUTE OF TECHNOLOGY, WARANGAL** is a record of bonafide research work carried out by him under my supervision and, it has not been submitted elsewhere for the award of any degree.

Dr. M. Heeralal
Thesis Supervisor
Associate Professor
Department of Civil Engineering
National Institute of Technology
Warangal (T.S.) – INDIA

Dr. Rakesh J Pillai
Thesis Co-Supervisor
Assistant Professor
Department of Civil Engineering
Indian Institute of Technology
Palakkad – INDIA

ACKNOWLEDGEMENT

I express my sincere thanks and gratitude to my supervisors, **Dr. M. Heeralal and Dr. Rakesh J Pillai** for their generous help, support, guidance, encouragement and their invaluable professional guidance throughout my PhD research. They were always there to listen, to give advice, to talk and clarify my doubts. I would like to express my sincere thanks to the members of Doctoral Scrutiny Committee **Prof. K V Jayakumar, Dr. P. Muthu, Dr. M. Shashi** and Chairman of Doctoral Scrutiny Committee **Prof. P. Rathish Kumar** for their kind suggestion on the research.

I consider myself very much fortunate to have guidance from **Mr. G Sankar**, Scientist G (Rtd.), Senior Consultant, Crustal Processes (CrP), National Centre for Earth Science Studies (NCESS), and **Dr. Sekhar Lukose Kuriakose**, Member Secretary, Kerala State Disaster Management Authority (ex-officio) & Head (Scientist), State Emergency Operations Centre for sharing their valuable knowledge, guidance and support during the field visits. Their insights and ideas helped me to overcome a number of hurdles during the course of this research work. I thank both of them profusely from the bottom of my heart.

I am also very grateful to **Prof. V. Ramana Murthy, Dr. P. Hari Krishna, Dr. Arif Ali Baig Moghal, Dr. G. V. Ramana, Dr. Sudheer Kumar Yamsani** and **Dr.Sanjit Biswas** the faculty members of Geotechnical Division, Department of Civil Engineering, for their constructive inputs during the course of the semester review. I owe a very special thanks to **Dr. G Kalyan Kumar** and **Dr. B Umesh** the faculty members of Department of Civil Engineering for their extended moral support, advice and suggestions at critical times during my Ph.D life. I thank **Ms. M Anju, Ms. Sureka** and **Mr. Satya Narayana** for their sincere help during field visits and discussions on developing the model and conducting numerical experiments. I would like to thank **Dr. Y. Sudheer Kumar, Dr. Noolu Venkatesh, Dr. Mohammad Muzzaffar Khan, Dr. Y S J Yeswanth Paluri, Dr. Venkata Koteswara Rao, Dr. M Sudhakar, and Mr. Mohammed Ashfaq**, **Mrs V Bhavita Chowdary, Ms. A G Sharanya** and other fellow research scholars for their constant support. This acknowledgement cannot be complete without expressing a very special thanks to my friends **Mrs. Seenu P Z, Mr. Nikhil M Thoppil and Mr. Munaga Teja** who have always been there for me.

"AMMA and APPA…. Here Is My Ph.D Thesis"

ABSTRACT

The modelling of catastrophic landslides is critical for risk assessment in densely populated areas. It is important to create risk maps that lead to urban planning laws and regulations and mitigation strategies. Landslide hazard assessment mainly revolves around the initiation and runout of the landslide. The design of remedial measures and mitigation against rapid landslide requires analysis of the landslide runout behaviour. To achieve such an objective and to evaluate the effectiveness of mitigation measures, runout model is necessary which predicts the thickness of the flow, velocity of the flow and area affected by runout. The increase in the mass of runout caused by channel bed erosion is referred to as entrainment. Entrainment complicates the calculation of runout distances and velocities. The present study attempts to numerically simulate the landslide runout with entrainment model.

The present research includes numerical investigation of the behaviour of granular flows through granular column collapse model. The column is allowed to collapse on an erodible bed of granular particles to investigate the mechanism of entrainment. Discrete Element Method (DEM) was used to model the column collapse to investigate the run-out distance and velocity of granular flow. Simulations were performed at particulate level in this method. Particle-particle interaction in DEM helps in better understanding of entrainment phenomenon. Significant relation exists between column height and maximum run-out length. Simulations were carried out with granular columns of different aspect ratios and run-out distances were measured along the direction of flow in both rigid and erodible bed. The effect of entrainment on the granular flow was examined for different aspect ratios of columns, and parameters such as flow velocity, bulk coordination number, and kinetic energy are analysed and discussed. Run-out lengths were found to increase with increase in the initial column aspect ratio of the granular column with rigid bed. In this study, substantial variations were observed in final run-out lengths in the presence of erodible bed in the model. The force of impact induces frontal ploughing giving rise to entrainment of particles into the flowing mass and increased mean flow velocity. Column collapse over erodible bed resulted in thicker final deposits which was evident from the increased coordination number.

The main objective of this research is to apply and improve the use of dynamic runout model with incorporation of entrainment. The dynamic approach is used in this work to account for the entrainment phenomenon. The amount of newly entrained mass is determined by the amount of momentum available. Runout analysis are often needed to delineate depth of flowing mass, potentially affecting area, travel length and travel time of runout. Numerical

model based on continuum approach with the variety of rheologies are often used for runout analysis. A two dimensional single phase continuum numerical model with entrainment was formulated in the present study. The formulated runout model is implemented in PCRaster environment, a raster based Geographical Information System (GIS) package. The model was validated with the case studies of landslides at Peringalam and Kaipalli in Kerala, India by simulating the landslide flow kinematics based on depth-averaged form of the equation of motion. Depth of deposit, velocity, flow path and entrainment exerted by the flow on particular point in deposition zone were analysed and compared with the field observed data. Uncertainties associated with model due to rheological parameter were quantified by the application of Monte-Carlo method. Maps were generated for both case studies i.e Peringalam and Kaipalli event to show the probabilities for runout and runout with particular depth reaching deposition zone.

This research aimed at contributing to an improvement of existing runout model with entrainment. In this study, the effect of erodible bed on granular column collapse flow behaviour was numerically investigated using 3D-DEM. A new runout model with entrainment was developed, and the uncertainties were quantified using model parameters for the case studies of Peringalam and Kaipalli events.

CONTENTS

LIST OF FIGURES

LIST OF TABLES

Chapter 1

Introduction

The term *landslide* is defined as the movement of a mass of rock, earth or debris down a slope (Cruden, 1991). The increase in population density, human activity, global climate change and torrential rainfall in mountainous terrain, there is increase in occurrence of debris flows induced by landslides, causing loss of property and human lives in the base and valley of mountains. As a measure to reduce the casualties, protection measures are adopted. Protection measures can be classified as active protection and passive protection. Active protection measures involve stabilizing the slope by increasing its strength. Passive measures involve the construction of retaining walls, nets, and fences to hold the failure mass from spreading to the farthest distance. It can be taken as a measure to reduce the run-out distance covered by the failure mass. For the design of passive measures, the destructive power of landslide should be known. With no protection measures adopted, depiction of maximum run-out distance becomes the most essential one so that the loss of lives and properties can be minimized.

1.1 Landslide Runout Analysis

The nature of the slope failure and the post-failure movement, or landslide runout, are the most important aspects of landslide hazard assessment. It necessitates forecasting landslide intensity based on runout behaviour. The landslide intensity, which is determined as a

function of the expected velocity of runout and landslide volume, aids in quantitative hazard analysis (Hungr, 1995). The destructive potential of landslide is determined through parameters like thickness, velocity and volume of the material displaced. The design of remedial measures against rapid landslide also requires runout analysis. Runout analysis can be studied as the prediction and implications of landslide dynamics. Runout analysis is often needed to delineate potentially affected area, travel length and travel time of runout. Numerical simulations of runout analysis help to map the landslide hazard zones. Quantitative Risk Assessment studies on a range of parameters like runout distance, velocity, volume of sliding and entrained mass will be useful to design proper strategies for mitigation (Luna *et al.*, 2012). Once the risk is assessed, then mitigation measures can be taken.

Figure 1.1 A recent landslide at Adimali, Idukki District, Kerala, 2018

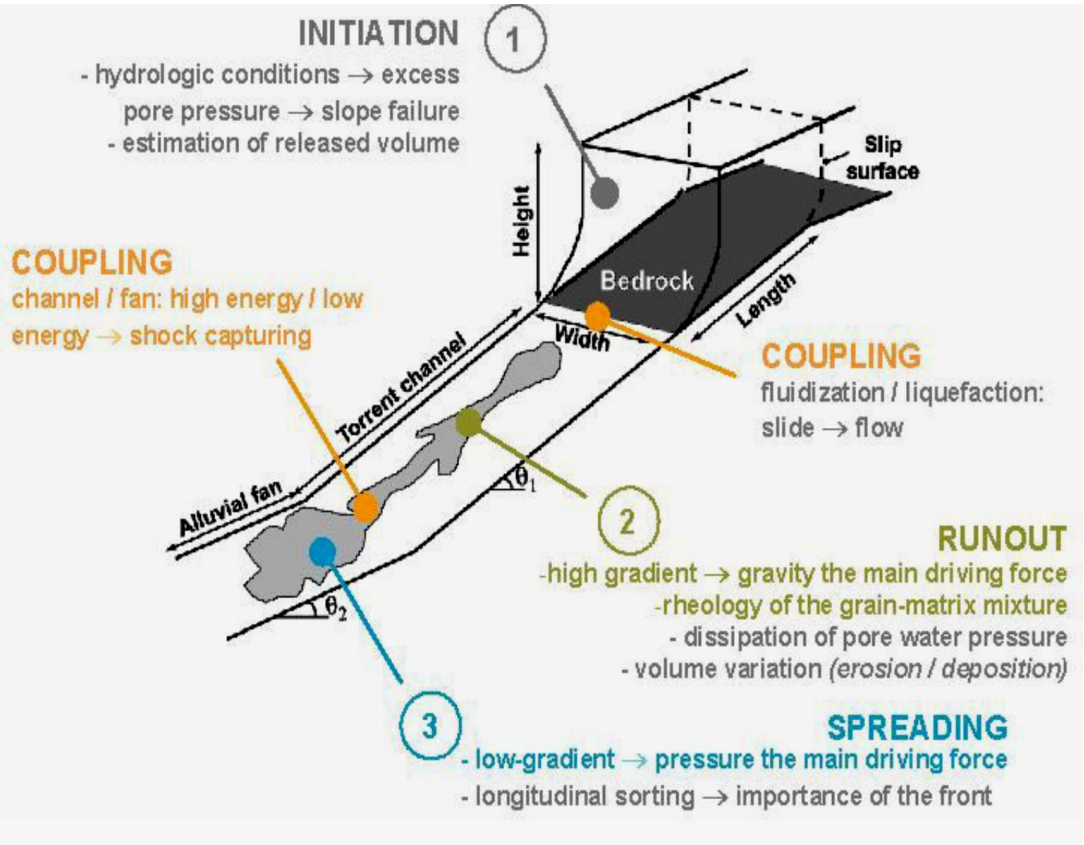

Figure 1.2 Schematic representation of landslide runout (Begueria, 2009)

The runout behaviour may be characterized by runout distance, velocity, runout width, depth of the moving mass and deposited material, pressure, volume of the material, scouring process, saturation. A landslide runout is theoretically divided into three components: an initiation zone, transport and deposition zone. Three components of the landslide runout is shown in Figure 1.1 and Figure 1.2.

Landslide runout model must include following parameters mainly (Hungr, 1995)

- Areas that could be affected by the landslide
- Depth of the moving mass
- Pressure
- Depth of the moving mass
- Maximum velocity

1.2 Methods of Runout Analysis

Approaches in landslide runout analysis are classified as empirical method, analytical method and numerical method. Empirical approach was based on data from field observation and past landslides. In empirical method, landslide runout distance is assessed by statistical analysis of extent of runout, flowing direction and initial volume of failure mass from past landslides (Hungr, McDougall and Bovis, 2005). The most basic analytical model is the sled model (Sassa, 1988) which is formulated on the premise that energy losses are due to friction and that the flow is regulated by a single resultant force. The Sled model was improved by taking into account the effect of pore fluid pressure. An analytical model based on basal friction and excessive fluid pressure was developed to predict the runout distance for loose, cohesive material (Hutchinson, 1986). Analytical methods have been used to measure the impact pressure from the velocity profile and the acceleration of the runout (Hungr, 1995). The purpose of a numerical model is to simulate the behaviour and development of landslide runout realistically. The advantage of numerical method is that they have the ability to simulate runout over complex topographic terrain. Along with Geographic Information System (GIS), semi-empirical numerical models have been used to map hazards of lahar, which were improved for unconfined flows (Iverson, Schilling and Vallance, 1998; Berti and Simoni, 2005). In numerical models using discontinuum approach, runout is studied by generating continuous assemblage of many small granular element that interact with each other (Poisel and Preh, 2008) . Though discrete element method gives realistic simulation, their main limitation is the computational cost considering the huge volume of mass involved in the debris flow. Depth averaged continuum models are the most widely used approach for landslide runout analysis. The continuum model considers the multiphase material of runout as a kind of single phase fluid with flow controlled by the rheological properties (Hungr and McDougall, 2009). In most of the catastrophic landslides, depth of the landslide will be smaller in comparison to length and width of the landslide, so depth average shallow water equation has been applied. The equations of the depth averaged model are obtained by integrating along the depth of the balance of mass and momentum equations. With rheological properties, bulk behaviour of the multiphase material is approximated to the single equivalent continuum fluid. The frictional force at the interface of the flow and bed is expressed by single term with rheologies used in the model and that frictional force denotes the flow resistance due to momentum dissipation resulting from frictional stress from the bed (Begueria et al. 2009). Different types of rheology will determine the different types of material characteristics and hence help determination of the movement of the material.

The Savage-Hutter model is a depth-averaged continuum approach consisting of hyperbolic partial differential equations to explain the depth distribution and topography of the mass of the granular media (Savage and Hutter, 1989, 1991; Hutter, 2005). Numerical techniques are used to solve the derived governing equations of mass and motion to calculate the velocity, depth of flow and depth of deposit of runout material.

1.3 Numerical Modelling in Landslide Runout

The numerical runout model can be categorized on the basis of Solution Dimension, Reference Frame and Rheology. Depth-averaging shallow water equation essentially eliminates one dimension from the governing mass and momentum balances (Savage and Hutter, 1991). 1-D depth-averaged models evaluate the flow as a longitudinal segment, whereas 2-D models consider the topography in both the flow as well as cross-stream directions. The Eulerian and Lagrangian approaches are two separate formulations of solution reference frames. The Eulerian approach is widely used to solve problems in fluid dynamics. It uses a fixed reference framework by separating it into a fixed spatial lattice. The solution of the partial differential equations is calculated by using a fixed computational grid. The most widely used rheology models for debris flows are Frictional model, Voellmy model, and Bingham model.

1.3.1 Entrainment in Runout Model

Entrainment plays a vital role in the run-out of a debris flow, as the entrainment mechanisms significantly change the mobility of the flow (Iverson, Reid and Lahusen, 1997). Figure 1.3 shows the schematic representation of landslide runout system (Shen et al., 2018). In many debris flow events, the flow channels are typically covered by surficial deposits, sometimes several meters thick granular material. Geological deposits that are less than 2.6 million years old are referred to as superficial deposits which include soil, sediment, regolith, and rock fragments.

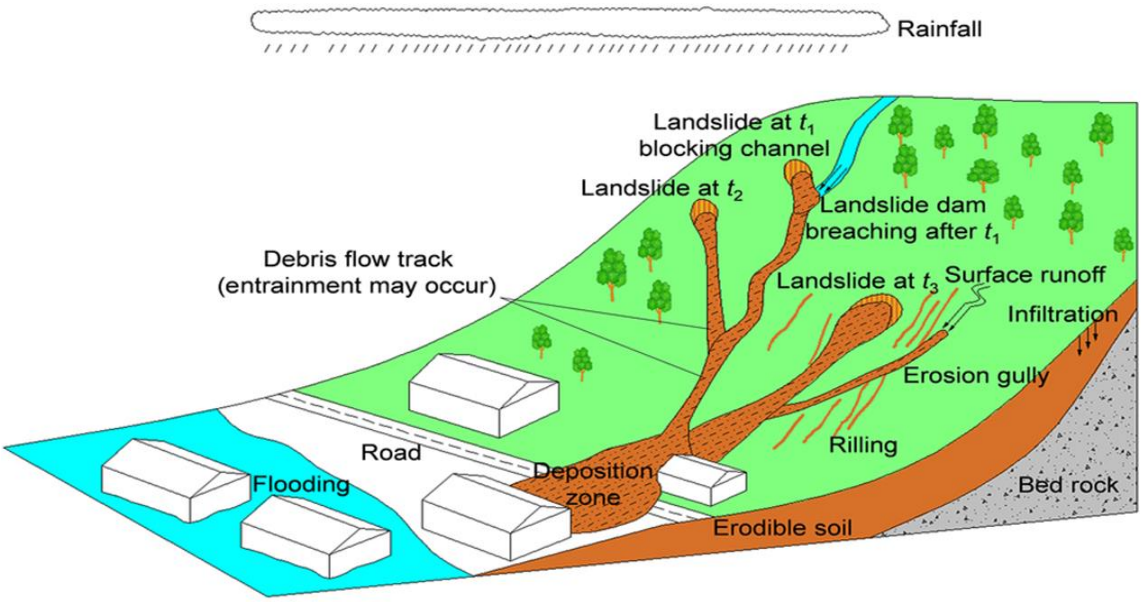

Figure 1.3 Schematic representation of landslide runout system, (Shen *et al.*, 2018)

Entrainment is defined as inclusion of solid and fluid from boundary of the flowing debris (Iverson, 2012). As the flow moves along the bed, the applied shear stress can exceed the strength of the material layer, causing bed material to be detached and accelerated by the flow (Gauer and Issler, 2004). The acceleration or deceleration of the moving mass as a result of entrained material, depend on the characteristics of the erodible material, topography and the dynamics of the flow (Mangeney *et al.*, 2010). According to Iverson, Logan and Denlinger, (2004) a flood can transform into a debris flow by entrainment of material. The entrainment materials can increase the volume of flow by several folds when the substrata is highly erodible (Iverson, Reid and Lahusen, 1997; VanDine and Bovis, 2002; McDougall and Hungr, 2005; Takahashi, 2007; Cuomo *et al.*, 2014). In the transport zone, entrainment of material increases the volume of the flow and this is where the highest velocity is reached. Erosion affects the motion by a decrease in bed friction force per unit mass, and the resistive force is generated due to a momentum transfer between the moving mass and the soil cover. The entrainment may accelerates or decelerate the flow velocity and hence the entrainment mechanism should be included in continuum models (Issler and Johannesson, 2011). Models using a constant volume without considering entrainment were not able to accurately forecast debris flow characteristics (Chen, Crosta and Lee, 2006). Different approaches for accounting material entrainment have been presented, varying from empirical methods that require the prescribed volume growth rates (McDougall and Hungr, 2005; Chen, Crosta and Lee, 2006) to process-based methods that simulate entrainment based on basal shear stress conditions (Crosta, Imposimato and Roddeman, 2009; Iverson, 2012). But still there is problem in accounting for the effect of entrainment in runout model.

1.4 Discrete Element Method (DEM) for Granular Flow Analysis

Researchers have advocated that the study of granular flow behaviour can be used to deduce the characteristics of debris flow (Iverson, Reid and Lahusen, 1997, Jaeger and Nagel, 1992, Savage and Hutter 1989; Zhang and Campbell, 1992). During landslides, the dense granular material flows through the surface covered with thick or thin deposits of erodible materials. These erodible materials get entrained into the flow thereby changing the flow mobility (Bouchut *et al.*, 2008, Mangeney *et al.*, 2010, Hungr and Evans, 2004, Crosta, Imposimato and Roddeman, 2009). Granular column collapse model is a simple approach widely used to study granular flows and has provided meaningful insights into flow behaviour. The effect of density, shape of grains, spreading velocity and final deposit was explored experimentally but the main purpose of the model is to relate the aspect ratio of the column and the final run-out distance covered by the final deposits.

The application of DEM in simulation of granular flow helps to understand the underlying physics in its flow (Cleary and Campbell, 1993; Lacaze, Phillips and Kerswell, 2008). Discrete Element Modelling (DEM) is a numerical modelling or computer simulation approach that can simulate soil and other granular materials (O'Sullivan, 2011). It has a unique feature in that it considers individual particles and their interactions. The typical approach in the simulation of mechanical behaviour of granular materials is by using the continuum mechanics framework wherein the relative movements and rotation of particles within the system are not considered. Constitutive models should be sophisticated enough to capture the complexity in the behaviour of materials due to the particulate nature. Whereas in DEM, many mechanical responses can be captured even if simple material models are used. By simplifying the particle shapes (e.g.: spherical) and adopting basic contact models, computational cost can be reduced and thereby comparatively large number of particles can be analysed.

DEM uses time discretization approach and hence numerical data are accessible at any stage of the test including the quantities that are difficult to assess. Finite displacements and rotation of discrete bodies can be simulated. Particles coming into contact and losing contact within the system can be automatically determined. In DEM, the numerical model is made of several discrete particles. In meshless or mesh free continuum methods including Smooth Particle Hydrodynamics (SPH), particles are interpolation points, rather than physical ones and hence they are similar to nodes in a finite element model. The philosophy behind DEM involves

modelling the actions at microscopic level and study its effect on the evolution of motion at the macroscopic level. In DEM, each particle is a single element whereas the continuous media is discretized into particle shaped elements.

The application of 2D DEM analysis in granular column collapse provides valuable clues about the correlation between aspect ratio and runout distance. Though 2D DEM model revealed fundamental knowledge about the influence of initial aspect ratio in the mechanism of granular flow, numerical results cannot match experimental observations. The effect of particle shape is not considered in 2D DEM model. Significant influence of particle shape in the flow mechanism and deposition of granular flow are clearly pointed out in 3D DEM analysis. Rolling resistance was employed for 3D DEM model to analyse the effect of particle shape. Though DEM is computationally costly, the aim is not to predict precisely what will happen to a system, but to predict the average behaviour of the system, 3D DEM works well in modelling the granular column collapse (Cleary and Frank, 2006; Girolami *et al.*, 2012; Zhao, 2014).

A granular column collapse model is used in the present study to gain more insights about entrainment phenomenon during granular flow. 3D DEM is used to model granular columns with different aspect ratios collapsing on an erodible layer made of particles similar to that of the column. The main objective of this study is to incorporate the effect of entrainment using a dynamic approach as reported by (Iverson *et al.*, 2011; Iverson, 2012; Iverson and Ouyang, 2015) in a two dimensional continuum model to perform a more realistic runout modelling. The newly formulated model was applied to the case studies in Peringalam and Kaipalli of Kerala, India and uncertainties associated with the model due to rheological parameters are quantified by the application of Monte-Carlo method.

1.5 Thesis Outline

Chapter 1 gives an introduction to landslide runout analysis, characteristics of runout analysis, and methods in runout analysis, formulation of entrainment in runout model and the application of DEM for granular flow analysis.

Chapter 2 presents a review of related research on landslide runout modelling. It discusses the work on runout models, Discrete Element Method (DEM), entrainment model and its use in

the numerical modelling of landslide runout. A short review of granular column collapse model, related numerical techniques involved in landslide research are presented. It also portrays the reasons to use DEM in the runout modelling, the need to incorporate entrainment phenomenon in landslide runout model and finally the research gaps involved in it are focused. The objectives of the present study based on the gaps identified from the literature review are mentioned at the end of the chapter

In Chapter 3 the theoretical background and methodology involved in DEM and the numerical tool used i.e., LIGGGHTS are discussed. It also explains the particle contact model used in it. The governing equation is used in the contact force formulation and time discretization is described. Description of granular column collapse model and flow on erodible layer are provided. The results of the numerical analysis of column collapse model using DEM and the effect of entrainment phenomenon on the granular flow are explained in detail in the later part of this chapter.

Chapter 4 focusses on the prediction of landslide initiation and propagation. Combined hydrological and slope stability model was used to analyse the landslide initiation. Dynamic entrainment model based on the availability of momentum was incorporated into the depth averaged continuum model and newly formulated runout model was applied to two case studies. Uncertainties in runout model due to rheological parameter were quantified by the application of Monte-Carlo method.

Chapter 5 discusses the results obtained in the granular column collapse model in erodible layer and the application of dynamic runout model for landslide runout case studies in Peringalam and Kaipalli. Finally this chapter summaries the results and the main points flowing from the research.

Chapter 2

Literature Review

The geophysical flows like rock and debris avalanches, landslides, and pyroclastic flows involve multiple principles of physics and can be characterized as large scale and transient, with complicated free surface behaviour on geometrically complex topography (Cleary and Prakash, 2004). Terrestrial landslides typically occurs with other natural hazards displacing solid materials causing soil collapsing, creeping, sliding, falling, spreading and flowing (Hungr, Evans and Hutchinson, 2001).The study of landslides and their effects has evolved into a multidisciplinary topic involving geographical, pedological, and urban planning considerations. We will only deal with engineering aspects here and will concentrate on the propagation process of quick landslides, especially debris flow. They can be catastrophic as because they can spread to longer distances in very short periods of time, reaching previously safe areas. Entrainment and deposition are critical processes in debris flow, but they are poorly understood due to uncertainties in debris flow characteristics. This chapter deals with the different approaches to analysing landslide runout, including entrainment models and numerical models.

2.1 Landslide Initiation and Slope Stability Analysis

The social and economic impact of slope failures and landslides worldwide is significant. Slope failures and landslides associated with extreme events have killed tens of thousands and their destructiveness can lead to loss of life that ranks with any natural disaster. As per Indian Meteorological Department, shallow landslides and slope failures are the major problems in tropical mountain cloud forests in India. Most of the slope failures in those regions are rainfall induced shallow with a depth of failure not more than 5m and steep slope of 35^{o} to 45^{o}. Landslides are natural hazards which happen without any warning, causing huge loss of public property and lives across the globe. Landslide evaluation and mitigation planning have become major concerns for geologists in developing countries. According to Geographical Survey of India, it is estimated that developing countries are facing economic losses which is of 1-2% of their gross national product and it has been reported that 80% of reported fatalities due to landslides occur in developing countries. In India, more than 12.6% of total land area (excluding snow covered) are vulnerable to landslide. In-depth assessments of variation of pore water pressure change in slopes during avalanche rainfalls are required for the purpose of mitigation.

Rainfall infiltration leads to pore water pressure built up at the soil bedrock interface. It resulted in downward movement due to gravity and sudden acceleration of failed soil mass caused by change in pore water pressure (Eichenberger, Ferrari and Laloui, 2013). The increase in pore water pressure due to rainfall leads to decrease in effective shearing resistance and reduction in frictional forces between soil particles. A rise in water table or decrease in matric suction due to rainfall infiltration causes instabilities in slope (Dhakal and Sidle, 2004). The infiltration model was proposed by Green and Ampt, 1911. Then the infiltration model was integrated along with slope stability analysis to predict the factor of safety and depth of failure by Chen and Young, (2006) and Muntohar and Liao, (2010). This infiltration model correlates saturated hydraulic conductivity (k_{sat}) and wetting front depth. Zhan and Ng, (2004) concluded that the coefficient of permeability is controlled by saturated hydraulic conductivity in lower suction range. De Campos and Menezes, (1992) and Rahardjo and Fredlund, (1995) observed failure in slopes without formation of positive pore water pressure, due to the loss of unsaturated shear strength. Ng and Shi, (1998), Rahardjo *et al.*, (2007) conducted various numerical analyses on rainfall induced slope failure mechanism. Many researchers from the past found that the response of suction to rainfall infiltration is mainly governed by the ratio of infiltration flux to saturated hydraulic conductivity k_{sat} and

soil water characteristic curve (SWCC). Since soil near the ground surface is usually unsaturated, the process of infiltration involves flow through the unsaturated zone. Unsaturated soil exhibits great spatial and temporal variation in properties with changes in moisture content. To investigate the effect of rainfall infiltration and stability of the slope, coupled infiltration and slope stability model have been used by most of the researchers (Anderson and Lloyd, 1991;Rahardjo *et al.*, 2007; Lumb, 1975; Mein and Larson, 1973). If flow condition changes with time, the flow is transient flow. Infiltration of rain water into unsaturated soil involves transient analysis. This transient flow of rainwater into the slope highly depends on SWCC and hydraulic conductivity function Darcy's law flow of water through unsaturated soil as well as saturated soil is applied by using the following partial differential water flow equation. Change in pore water pressure is related to the change in volumetric water content. SWCC, saturated hydraulic conductivity, compressibility and saturated water content are determined from laboratory tests Fredlund, Xing and Huang, (1994).

With the advancement of wetting front due to rainwater infiltration, there is reduction in matric suction. Reduction in shear strength eventually brings down the factor of safety lower than unity. Usually this kind of failure occurs in a plane of shallow slope failure. The range of the failure depth may vary from 1m to 5m. The most common failure plane is the one which is parallel to the slope surface Fourie, (1996); Muntohar and Liao, (2010).

There are lots of uncertainties in the parameters influencing the SWCC. Reliability considerations will incorporate the uncertainties associated design and analysis of engineering systems. The reliability of a system is usually evaluated with reference to a particular performance criterion. This leads to the failure of slope even the evaluated factor of safety is more than one. For that purpose, reliability analysis became necessary. Widely many researchers like Duncan, (2000), Griffiths, Huang and Fenton, (2009), Li and Lumb, (1987), and Whitman, (2000) used Monto- Carlo simulation is adopted in this study to calculate the probability of failure. Purpose of this reliability analysis is to quantify the effect of rainfall intensities on the slope in the form of probability of failure.

It is possible to describe the whole process (initiation and propagation) using a single mathematical model. When this mode of failure occurs in slopes, the mass of soil can traverse downhill, turning into mudflows. However, there exist a difficulty in the cases where the landslide evolves to flow type phenomena, where the problem of changing from solid-like to fluid-like type of behaviour presents important difficulties. This is why we will deal separately with both phases, using different approaches for them.

2.2 Landslide Runout Modelling

Models can be seen as a representation of the real world scenario. Models are also described as “a simplified representation of an object of investigation for the purposes of definition, interpretation, forecasting, or planning” (Fotheringham and Wegener, 1999). In general landslide consists of a three zones namely source zone, runout path and the deposition area (Chen and Lee, 2004). In other way it can also classified simply into depletion and accumulation zones. The post failure quantitative estimation of distance, material spreading and velocity with respect to initial condition plays a significance role landslide risk assessment. The main aspect is to forecast or reproduce the debris flow as accurately as possible. It is necessary to stress on the post failure runout hazard, rather than initiation of landslide which can directly influence on the overall loss in human lives. Brunsden, (1999) listed various modelling approaches in landslide studies such as Rheological models, slope stability models and hydrological landslide models. Dai, Lee and Ngai, (2002) explained the empirical, analytical and numerical methods in runout distance prediction runout behaviour of landslide material. Chen and Lee, (2004) classified the dynamic models into lumped mass models, continuum mechanics model and distinct element models. Lumped mass model was approached by analytical method, distinct element model and continuum mechanics model approached by numerical model. Hungr, McDougall and Bovis, (2005) has discussed the Discrete Element Method (DEM) and the continuum numerical methods. Mass and momentum conservation equations form the base of Continuum models. Distinct element methods represent a continuous assemblage of blocks formed due to connected fractures in the blocks of the region under consideration. Particle contacts and the discrete reaction forces on each particle is monitored and magnitude of contact forces is determined by the contact model. Forces created by external factors are also added at this point and the summation of total force is computed. Particles are then subjected to a small motion based on Newton’s law over a small-time interval (iteration).

Different methods are developed to model the mass movement of landslide runout. The movement of a runout is very complex and it is understood that many flow regime and different processes might be operating at any given time at different locations of a given event. Hence there is no run-out model which can be applied universally to predict the runout behaviour and movement types. But the models developed presents a method to measure the spreading, extension and velocity that generated by a runout. Based on Dai, Lee and Ngai,

(2002) these methods can be divided into (a) Empirical Methods, (b) Analytical Methods, (c) Numerical Methods.

2.2.1 Empirical Model

Empirical methods are developed on the basis of largescale field data, simplified assumptions and the statistical analysis done by forging relationships between the run-out distance, landslide mechanisms and parameters like the volume of failure mass and the characteristics of the terrain. Analysis of relationship between run-out distance and debris flow mechanics, e.g. volume and terrain, provide the basis of empirical models. Most empirical models often require volume estimation and topographic profiles. Empirical methods are sub classified into

(i) Heuristic Methods

(ii) The Mass-Change Method

(iii) The Angle-of Reach Method.

The basis for heuristic methods is on the assumption that spatial extent of past landslides on a given slope provides a first approximation of the spatial extent of potential landslides for a given frequency (Hungr, McDougall and Bovis, 2005). Observations in the field and photo analysis are traditional methods for determining the spatial distribution and magnitude of past landslides.

The mass-change approach is based on the landslide's initial volume or mass, which is modified by the loss or deposition of runout material. When the amount of actively moving debris becomes zero, runout comes to a halt (Cannon and Savage, 1988). The average volume or mass variation rate of runout is calculated by dividing the change in volume mobilised and final deposit volumes by trail runout length.

The angle of reach method is based on the angle of the line connecting the escarpment of the landslide source to the distal margin of the displaced mass. Runout length is estimated with the data on release source, direction, volume and selected angle of reach of the flow. When the data related to landslide and its source volume are known, the runout distance can be

calculated by following equation 2.1. *H* is the elevation difference between the escarpment and the toe of the deposit, and *L*.

$$L = \frac{H}{\tan \alpha} \qquad 2.1$$

Statistical techniques may be adopted to predict parameters associated with landslide run-out characteristics in addition to run-out duration. Rickenmann, (1999) have also used regression analysis and has suggested a set of empirical equations for debris flows in order to evaluate the peak flow, average flow rate, travel speed, and the run-out length.

Iverson, Schilling and Vallance, (1998) used the LAHARZ model (Schilling) to suggest statistical correlations between volume and deposit location (1998). LAHARZ was designed to delimit areas of possible lahar inundation caused by one or more user-specified lahar volumes. If the user enters several lahar volumes, LAHARZ generates a lahar-inundation hazard zone for each volume.

Fannin and Wise, (2001) designed a decision decision-support tool, intended to supplement judgement and experience. Changes in event magnitude caused by volumetric entrainment and deposition along the down slope direction of movement are used to calculate total travel distance for an expected initial failure volume. The model's volume-based approach includes the following controls. Initiation occurs for a user-defined initial failure volume. Following that, the flow behaviour is determined by the morphology of each subsequent reach, and the flow mode is determined by the reach's slope angle. Regression equations are used to measure the amount of entrainment and (or) deposition. The slope angle and flow form are used to calculate the change in flow rate. In the case of deposition, the volume change is negative, while in the case of entrainment, the volume change is positive

Berti and Simoni, (2014) established DFlowz, a generally accepted semi-empirical relationship for estimating the region potentially inundated by debris flow. The model is on the basis of the simple observation that the greater the volume of the flow, the larger the cross-sectional flow area and inundation of the planimetric area. When information on the flow behaviour is available, different combinations of the planimetric area and cross-sectional inundation width allow reproducing different predicted debris flow velocity and mobility. DFLOWZ computes the deposition area by assuming a constant cross-sectional flow area that stretches across a channel path that the consumer specifies. The path of the flow channel must be specified by a polyline shape file and evaluates the inundated area is computed by

connecting the inundation width computed at each cross-sectional profile. Profile traces can be specified manually or created automatically.

Horton *et al.,* (2013) developed Flow path assessment of gravitational hazards at a Regional scale (Flow-R) as a distributed empirical model for regional susceptibility assessments of debris flows at the University of Lausanne. Based on GIS instruments, the automated identification of source location and the estimate of debris flow mobilisation provide a solid foundation for a preliminary susceptibility assessment at the regional scale. The model's usability is one of its key advantages. In fact, the user has complete control over everything, from data selection to algorithm and parameter selection. It was shown that the quality of the DEM is the most important parameter to obtain reliable results for propagation, but also to identify potential debris flows sources. Although the model has advantages, it does not suit the research objective of obtaining flow path without field data and it needs friction parameters as input.

2.2.2 Analytical Model

Analytical methods comprise various formulation based primarily on lumped mass approaches in which the landslide failed mass is assumed to be concentrated in a single point. The sled (Sassa, 1988) is the most basic analytical approach for calculating energy loss due to friction, assuming that total loss in energy during debris mobilisation is due to friction and which can be defined as a movement of dimensionless body down the path. Eventually, mass is mobilised by a single resultant force. Hutchinson, (1986) designed a model to predict the run-out distance for loose, cohesion-less soil materials by relying on the type of a debris flow. The model assumes that the debris mass's basal resistance is mainly due to friction, and the excessive pressure exerted by fluid in the debris dissipates in line with the one-dimensional consolidation theory. The analytical methods include an estimation of the landslide's velocity profile and acceleration, which can be used to calculate impact pressures (Hungr, 1995).

2.2.3 Numerical Model

Numerical simulation of debris flow is an attempt to try and model a real-life situation, to estimate the development of a debris flow. The advantage of the numerical methods is the

ability to model the debris flow movement over irregular terrain. Based on the gravitational driving force and a constitutive law, governed by a rheology model describing the flow properties, run-out distance and velocity can be estimated. The majority of numerical models are based on a "continuum approach," which treats landslide material as a continuum. For numerical analysis of rapid mass flow over complex terrains, the depth-averaged shallow water equation method which aids in the representation of the flow rheology as a single frictional force.

2.3 Classification of Numerical Model

The numerical runout model can be classified based on Solution Dimension, Reference Frame, and the Rheology. The following section deals briefly about these three classification.

2.3.1 Based on Solution Dimension

The majority of dynamic models employ depth-averaging, which involves integrating the governing mass balance and momentum balance equations with respect to the flow depth. A linear increase in stress is predicted with the rise in depth of flow, which is typically assumed to be stress free top surface, and consequently the shear stresses induced along the depth are ignored. This observation is made on the premise that the change in depth is steady and minimal in comparison with the landslide's length and width. The shallow water depth-averaging equation effectively removes one factor from the governing mass and momentum balances (Savage and Hutter, 1991). 1-D depth-averaged models examine the flow as a pre-defined longitudinal segment of the terrain, while 2-D models adopt the topography in the flow and cross-stream directions.

2.3.2 Based on the Reference Frame

The Eulerian and Lagrangian method are two different formulations of solution reference frames. Euler's method is commonly used to describe fluid dynamics. It divides the space into a fixed spatial lattice to use a fixed reference scheme. This is equivalent to standing still and watching a debris flow move by. The partial differential equations' solutions are computed

using a fixed computational grid. The Eulerian method focuses on a fixed region in space and observes the material motion within this region as time progresses. The parameter of concern are denoted by the spatial coordinate x and time t. The acceleration and velocity are expressed in equations 2.2 and 2.3

$$\boldsymbol{a} = (\boldsymbol{x}, \boldsymbol{t}) \quad 2.2$$

$$\boldsymbol{v} = \boldsymbol{v}(\boldsymbol{x}, \boldsymbol{t}) \quad 2.3$$

The displacement u is denoted by

$$\boldsymbol{u}(\boldsymbol{x}, \boldsymbol{t}) = \boldsymbol{x} - \boldsymbol{\zeta}^{-1}(\boldsymbol{x}, \boldsymbol{t}) \quad 2.4$$

Another common approach is Lagrange's method. It divides the flow into deformable blocks. Accordingly, the motion in every block is described as well as the interfaces between the blocks. When adopting the Lagrangian approach (also named as the material reference), the acceleration and material velocity are presented in the form

$$\boldsymbol{A}(\boldsymbol{X}, \boldsymbol{t}) = \frac{\boldsymbol{D}\boldsymbol{\zeta}(\boldsymbol{X},\boldsymbol{t})}{\boldsymbol{D}\boldsymbol{t}} = \frac{\boldsymbol{D}^{\boldsymbol{2}}\boldsymbol{\zeta}(\boldsymbol{X},\boldsymbol{t})}{\boldsymbol{D}\boldsymbol{t}} \quad 2.5$$

$$\boldsymbol{V}(\boldsymbol{X}, \boldsymbol{t}) = \frac{\boldsymbol{D}\boldsymbol{\zeta}(\boldsymbol{X},\boldsymbol{t})}{\boldsymbol{D}\boldsymbol{t}} \quad 2.6$$

Where *V*, *A* denote velocity, acceleration respectively, **X** and **ζ** denote position and movement respectively that can be interpreted as a transport of points from the reference configuration to the current configuration during a specific time interval [0,*t*]. T the displacement **U** of a particle located at **X** is defined as

$$\boldsymbol{U}(\boldsymbol{X}, \boldsymbol{t}) = \boldsymbol{\zeta}(\boldsymbol{X}, \boldsymbol{t}) - \boldsymbol{X} \quad 2.7$$

The difference between Eulerian and Lagrangian is illustrated in Figure 2.1.

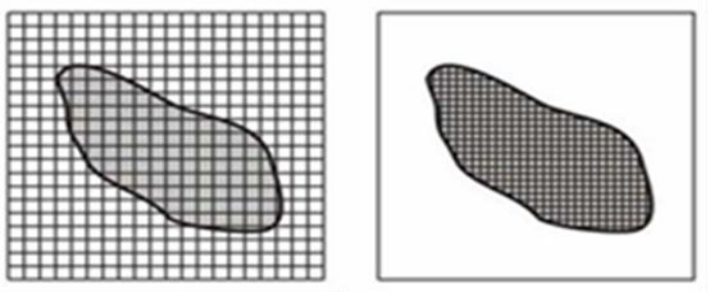

(a) Eulerian frame (b) Lagrangian frame

Figure 2.1 Reference frames (McDougall, 2006)

2.3.3 Based on the Rheology

Rheology is the analysis of the resultant flow and deformations of matter on the surface as a result of applied stress (Rifai, 2008). For rock avalanches, the rocks are assumed to be elastic to some extent and subsequently at higher stress. However, ductile substances deform plastically as stress increases, while the resistance force at the interaction between the bed path and flow is represented by the flow rheology. The most commonly used model are Frictional model (Hungr and McDougall, 2009), Voellmy model (Voellmy, 1955), Bingham model (Coussot, 1997).

Frictional (Coulomb) model is based on relation bed and normal stresses at the base. The pore pressure is also considered in this. Voellmy model is function of square of velocity of the flow and turbulent coefficient. Turbulent coefficient is very identical to the chezy resistance in flow of turbulent water in open channel flow and used for granular and cohesionless materials with or without the existence of a pore fluid. Several authors have estimated the friction coefficients of the Voellmy model using run-out from granular avalanches (McDougall and Hungr, 2005; Christen, Kowalski and Bartelt, 2010). Bingham model express resistance as a function of velocity, dynamic viscosity and yield stress. The Bingham-type resistance model applicable to material with rich plastic clay materials (Jiang and LeBlond, 1993; Imran, Harff and Parker, 2001; Malet, Remaître and Maquaire, 2004; Pastor *et al.*, 2009). Once the yield strength is extended, a linear stress-strain rate relationship is assumed. The average flow velocity is calculated by assuming the linear increase in shear stress with depth (Coussot, 1997). As per Rickenmann *et al.*, (2006), clay fraction (particles passing 45μ sieve) exceed than 10% is exential for a material to exhibit behaviour identical to Bingham fluid. Summary of above mentioned models are shown in following table 2.1

Table 2.1 Summary of rheological model

Model	**Expression**	**Remark**
Frictional or coulomb resistance	$s_f = \tan\phi'$ $\tan\phi' = (1-\gamma_u)\tan\phi$	$\boldsymbol{\gamma_u}$- Pore pressure ratio. Bed PWP/ bed normal total stress

Voellmy model	$s_f = \tan\phi' + \frac{u^2}{\xi h}$	u- flow velocity, ξ-turbulent coefficient. For granular cohesionless material
Visco-plastic Bingham (for plastic clay rich material)	$s_f = \frac{1}{\rho g h}\left(\frac{3}{2}\tau_c + 3\eta\frac{\| u \|}{h}\right)$	τ_c- strength due to cohesion η- viscosity coefficient

2.4 Overview on Dynamic Runout Model

The purpose of developing dynamic models is for risk evaluation and hazard assessment. One of the possible approaches to model landslide instability is modelling flow-like landslides and its flow development (Crosta, Imposimato and Roddeman, 2003). Prediction of landslide runout based on continuum mechanics is associated with a variety of rheological models. Numerical methods in this kind of modelling depend highly on the type of modelling approach, selection of constitutive models and model parameters. Several dynamic run-out models have been developed in the past and these models have been improved from the basic hydrodynamic models to models that account for internal strength, entrainment, and rheology variations. They were categorised depending on how they were implemented and how their entrainment rates were calculated. The amount of entrained material is specified by the user in a defined entrainment rate, whereas the amount of entrained material is estimated dynamically by dynamical variables such as velocity, flow height, and bed shear stress in a process-based entrainment rate.

The applicability of existing models has been tested for various scenarios around the world and details availed form International Forum on Landslide Disaster Management. Hong Kong Geotechnical Division, Hong Kong Geotechnical Society – Geotechnical Engineering Office, Hong Kong, 2007. Further the rheological parameters were back calculated for certain case histories and the models were assessed in various scenarios to identify the importance of the

above mentioned models in the application of forward prediction of landslides. Following the outcomes of these models were compared in order to comprehend their effectiveness for a given situation. Overview of model characteristics are summarised with reference frame of solution, solution approach, variation of rheology and basal rheology in table 2.2.

FLO-2D is a 3D Eulerian code developed by O'Brien, Julien and Fullerton, (1993) for the simulation of floods, mud flows, and debris flows. They used a generalised quadratic rheology model that allowed them to combine viscous, plastic/frictional and turbulent strengths. FLO-2D was validated using a real mud flow event and measured against a pre-existing hydrocode (the US Army Corps of Engineers).

Hungr, (1995) introduced DAN, a 2D Lagrangian model that synthesised several previous works, including the ability to accommodate the variation in entrainment, internal strength, and rheology. By modelling soil slides with the assumption that they behave as hypothetical material governed by simple rheological rules, Hungr formalised the idea of "equivalent fluid". Hungr, (1995) described the collection of rheologies that which can represent different zones within the sliding mass for the same or different segments which include frictional, Voellmy, and Bingham models. DAN allows the user to define different erodible material depths for each section along the path.

Iverson, Reid and Lahusen, (1997) raised objection to the application of rheological relationships in the dynamic modelling of debris flows and heavy influence of solid and fluid on the dynamic model. He suggested a generalisation for Savage-Hutter theory for granular material with fluid mixture theory to explicitly account for the viscous effects of fluid in pores, and adapted this concept into 2D representation of Lagrangian model.

MADFLOW, a 3D extension of DAN based on a Lagrangian finite element process, was proposed by Chen and Lee, (2000). Entrainment capability was not included. Internal stiffness and the compatibility of multidimensional internal stresses were not taken into account and depth integration was performed along vertical direction. Huber's channel tests (1980) were used to validate the model and bottom friction rheology was used to conduct back-analysis on two case studies. Later, the Bingham and Voellmy rheologies were used (Chen and Lee, 2004; Crosta et al., 2004). Chen, Crosta and Lee, (2006) integrated the entrainment potential and applied it to the back-analysis of actual landslides.

Denlinger and Iverson, (2001) and Iverson and Denlinger, (2001) proposed an extension of Iverson's theory, applied in an Eulerian frame of finite volumes. The theory was validated with simplified theoretical solutions to the governing equations. Small and large-scale channel experiments were used to validate computational model. They used a kinematic criterion to define zones of relative high strength near the edges of the frictional flow, which enabled the spatial distribution of pore pressures to evolve automatically in each simulation.

Denlinger and Iverson, (2004) proposed a dry-flow model based on an Eulerian-Lagrangian hybrid numerical model. The governing equations were solved in an Eulerian frame and the internal stresses were redistributed using a Lagrangian method of finite elements. Iverson et al. (2004) proposed additional experiments that included the movement of granular materials through a channel with an uneven surface in order to simulate natural terrain.

Pastor *et al.*, (2002) developed a 3D Eulerian finite element model for simulating rapid landslides of various types, including granular avalanches, landslide floods, and sliding flows. The code is based on a coupled nonlinear mathematical model based on mixture theory, and it allows the user to choose between Newtonian, frictional, Voellmy, and Bingham rheology. Haddad, (2008) and Pastor *et al.*, (2009) improved on the original by using the SPH technique to discretize the equations. They replaced the Eulerian formulation with a Pseudo-Lagrangian or Arbitrary Lagrangian Eulerian (ALE). They were among the first to apply the SPH approach to the study of the hydro-mechanical coupling.

DAN3D, a 3D alternative to DAN, was suggested by McDougall and Hungr, (2004). The DAN3D code is an SPH-based Lagrangian numerical system capable of handling large deformations. Internal stresses, like DAN, are functions of internal tension (limited between the passive state and the active state). (McDougall and Hungr, 2005) proposed a material entrainment potential based on the exponential volume growth model. The user can change the growth rate and maximum depth of erosion along the path, as well as the rheology at the beginning of the entrainment.

SHWCIN, a 3D model developed by Mangeney-Castelnau *et al.*, (2005), was used to simulate dry granular flows using a kinematic approach. The model is essentially based on the Savage-Hutter principle, with a Coulomb-type frictional law at the bottom and a frictional coefficient that can be constant or differ according to the empirical relationship suggested by Pouliquen, (1999). (Pirulli, 2005) suggested changes to SHWCIN in order to address mesh dependency issues. RASH3D, the updated model, allows simulation through irregular 3D terrains,

integrates the effect of internal strength. RASH3D, the updated model, allows simulation through irregular 3D terrains, integrates the effect of internal strength, and allows the selection of multiple strength relations for the bottom surface.

Pitman *et al.*, (2003) presented TITAN2D, an Eulerian 3D model for dry granular flows based on the Savage-Hutter principle. They used Iverson and Denlinger's, (2001) approach to account for non-hydrostatic internal stress conditions. The code was checked with simple and complex topography examples. E B Pitman *et al.*, (2003) used an empirical erosion rate to calculate entrainment potential. Sheridan *et al.*, (2005)evaluated the model using a back-analysis of a historical case of a rock avalanche.

VolcFlow (Kelfoun and Druitt, 2005) solves the equations of motion for a granular flow and this method has the benefit of accounting for basal friction, internal friction, and volumetric spreading action. It is used to describe the creation of the high topographic escarpment that is a prominent feature of the avalanche deposit in particular. The analysis offers some crude, but curious, constraints on the avalanche's rheological activity.

(Kwan and Sun, 2006) modified the original model of Hungr, (1995), allowing the selection of a trapezoidal section, giving birth to their model DMM. They performed back-analysis of a real case. Kwan and Sun, (2007) extended DMM to 3D, giving rise to 3dDMM. They used the Particle in Cell (PIC) technique Harlow, (1964)to solve two-dimensional equations integrated in depth and adopted the Savage-Hutter theory in the calculation of the internal stresses.

Crosta, Imposimato and Roddeman, (2003) proposed a 2D finite element model, without depth integration, which was then extended to 3D to consider the influence of the vertical component on flow behaviour. The model is based on the combined Eulerian-Lagrangian method where material displacements do not distort the Finite Element mesh Roddeman, (2001). The model takes into account erosion and entrainment as a function of the characteristics of the material, rather than empirical parameters.

Bateman *et al.*, (2007) developed a model based on finite volumes known as FLAT Model. The model is based on the equations of Savage and Hutter, (1989) and Iverson and Denlinger, (2001). They applied a correction factor to the hydrostatic pressures term, to take into account the difference between the direction of pressure and that of gravity. They also modified the pressure term depending on the thrust of the material (active or passive). They added a term due to the centripetal force derived from the curvature of the terrain, proposed by Hungr,

(1995). FLAT Model allows the application of viscoplastic, frictional and collisional rheologies. Medina, Hürlimann and Bateman, (2008) performed a reanalysis of the channel test performed by Iverson et al. (2004), and a back analyses of real cases of mudslides (Bateman *et al*., 2007; Medina, Bateman and Hürlimann, 2008).

A general purpose DEM based commercial software package called Particle Flow Code (PFC), developed by HCItasca, has been used by several authors (Calvetti, Crosta and Tatarella, 2000; Pirulli *et al.*, 2003; Herreros *et al.*, 2004; Tang *et al.*, 2019)) to model landslide-like processes.

RAMMS is a dynamic numerical modelling program, simulating run-out of mass movement in a three dimensional terrain. It was originally designed to model snow avalanche, but new models for debris ow and rock fall have subsequently been developed. The model is based on the Navier-Stokes equations modified by the Voellmy-Salm frictional relationship, and it describes the debris flow as a depth-averaged continuum model (Christen, Kowalski and Bartelt, 2010).

MassMov2D is a two dimensional model of mud and debris flow dynamics over a complex terrain developed by Beguería *et al.*, (2009) The model is built on the classic Savage-Hutter theory (Savage and Hutter, 1989), which assumes a one-phase homogeneous substance with rheological behaviour. An Eulerian reference frame is used in the model. The flow is described by a variation in the conservative variables at points of fixed coordinates as a function of time. The finite difference solution assumes continuity and smoothness of the surface.

Table 2.2 Review on existing dynamic runout models

Authors	**Solution Approach**	**Rheology**	**Variation Of Rheology**	**Reference Frame**	**Entrainment Rate**
Chen and Lee, (2007)	Continuum	Frictional, Voellmy,Bingham	No	Lagrangian approach with mesh	Defined

Crosta, Imposimato and Roddeman, (2003)	Continuum	Frictional (elastoplastic model)	Yes	Eulerian-Lagrangian approach (adaptive mess)	Process based
Christen, Kowalski and Bartelt, (2010)	Continuum	Voellmy	Yes	Eulerian approach	Process based and Defined
Hungr and McDougall, (2009)	Continuum	Frictional, Voellmy, Bingham	Yes	Lagrangian Meshless approach	Defined
Medina, Bateman and Hürlimann, (2008)	Continuum	Frictional, Voellmy	No	Eulerian approach	Process Based
D'Ambrosio, Gregorio and Iovine, (2003)		Energy based	No	Eulerian approach	Process Based
Kwan and Sun, (2006)	Continuum	Frictional, Voellmy	Yes	Eulerian approach	Defined
Pastor *et al.*, (2009)	Continuum	Frictional, Voellmy, Bingham	Yes	Lagrangian Meshless approach	Defined
Beguería *et*	Continuum	Voellmy,	Yes	Eulerian	Defined

al., (2009)		Bingham		approach	
Pirulli and Mangeney, (2008)	Continuum	Frictional, Voellmy Quadratic	No	Eulerian approach	No entrainment rate is used
O'Brien, Julien and Fullerton, (1993)	Continuum	Quadratic	No	Eulerian approach	No entrainment rate is used
Poisel and Preh, (2008)	Motion of particle	Inter-particle and particle wall interaction	No	Discrete Element Method	No entrainment rate is used

2.5 Entrainment of Debris Flow

Surficial deposits, sometimes several metres thick granular material, typically cover flow channels in numerous debris flow events. Superficial deposits are volcanic deposits that are usually of Quaternary age (less than 2.6 million years old). Usually soil, sediment, regolith, and rock fragments. As debris flows through a channel with loose deposit on the boundaries, the debris erodes the channel material which resulted in a significantly greater final volume than the initial volume. Entrainment – the inclusion of solid and fluid from boundary of the flowing debris is called entrainment (Iversion, 2012). As the flow moves along bed, the applied shear stress can exceed the strength of the material layer, causing bed material to be dislodge and accelerated by the flow (Gauer and Issler, 2004). Entrainment has the potential to greatly alter the dynamics of debris flow which makes back analysis and prediction much more difficult. The effect of entrainment in debris flow are studied by various researcher with numerical and experimental approaches.

There are various numerical models for calculating the amount and rate of entrainment in debris flow analysis. The entrainment rate or depth of erosion of the channel base is calculated using force equilibrium in the analytical technique. The entrainment rate is empirically connected to flow velocity or shear stress exerted on the erodible bed in the empirical approach. In following section, various models in analytical and empirical approach are discussed and summary of selected list of available entrainment model table 2.4

2.5.1 Analytical Approach

It is difficult to use the analytical approach to predict the complex entrainment phenomena but some researcher used analytical procedure by considering stresses and resistances in the debris flow channel (Jakob, Bovis and Oden, 2005). Entrainment rate can be expressed in two ways in analytical approach namely static analysis and dynamic analysis. The static model calculates the entrainment depth whereas the dynamic model calculates the rate of erosion to account the entrainment (Medina, Hürlimann and Bateman, (2008); Richard M. Iverson and Ouyang, (2015); Bouchut, Ionescu and Mangeney, (2016)).

Static Analysis

The static model calculates the entrainment depth according to the stress equilibrium or failure of the erodible layer. The depth of the failure is computed, as well as the amount of material that will be added into the flow. Medina, Hürlimann and Bateman, (2008) developed a static equation of entrainment by considering static equilibrium between the flow frictional stresses and the basal resistance stresses. Shear resistance is estimated using Mohr-Coulomb law.

Destabilisation is caused by drag forces acting at the flow's base (Medina, Bateman and Hürlimann, 2008), but it can also be assisted by strength loss due to rapid undrained loading (Sassa, 1988). The approach taken by De Joode and Van Steijn, (2003), according to Sassa, (1988), assumes that shearing at the bed is caused by the accumulation of pore water pressure. As a debris flow erodes a channel, the mass of the arriving flow causes a sudden increase of pore pressure within the sediment on the channel bottom.

Sovilla, Burlando and Bartelt, (2006) proposed a formula to calculate bed erosion of snow avalanche. The entrainment process has three modes: ploughing, step entrainment and basal

erosion modes. The snow pack is divided into several layers in the entrainment calculation. In the model, driving force for entrainment is calculated from the shear component of the normal force acting on the layer. The frictional force comes from the cohesion of the snow depending on the snow texture.

Dynamic analysis

The dynamic model computes the erosion rate using the net driving stress exerted at the interface between the debris and erodible layer. The velocity of the eroded material is presumed to be the average velocity of the debris in this process. Entrainment occurs when shear stress in the bed exceeds the shear resistance. As a result, the quantity of newly integrated mass is determined by the availability of momentum.

The difference between static and dynamic entrainment model is that the static model calculates the entrainment depth according to the stress equilibrium or failure of the erodible layer, while the dynamic model calculates the rate of erosion based on the net driving stress exerting at the interface between the debris and erodible layer.

The model proposed by van Asch et al. in 2004 is a one dimensional debris flow model that considers the entrainment concept based on the shear stress and shearing resistance which is affected by the development of pore pressure under undrained loading on the in-situ material. From top to bottom, the debris flow and channel bed are divided into three layers as the top layer (flowing debris), the erodible layer (erodible bed), and the substrate layer (rigid bed). A loading on the bed deposits is created as the moving mass overlays the erodible bed. This load on the soil is calculated by the model based on changes in normal stress and shear strength induced by debris flow. Then, factors of safety at the top and bottom of the erodible bed are calculated in equations 2.8 and 2.9 as follows

$$\boldsymbol{F_{bot}} = \frac{\boldsymbol{C_{bot}} + (\boldsymbol{\sigma_{bot}} - \boldsymbol{P_{bot}}) \tan \boldsymbol{\delta_{bot}}}{\boldsymbol{\tau_{bot}}} \qquad 2.8$$

$$\boldsymbol{F_{top}} = \frac{\boldsymbol{C_{bot}} + (\Delta\boldsymbol{\sigma_{bot}} - \boldsymbol{P_{bot}}) \tan \boldsymbol{\delta_{bot}}}{\Delta\boldsymbol{\tau}} \qquad \mathbf{2.9}$$

where c_{bot} is the cohesion and c_{bot} is the friction angle, $\Delta\sigma$ and $\Delta\tau$ are the changes in normal and shear stress caused by the variation characteristics of debris above the channel bed, and pore water pressure respectively, σ_{bot} and P_{bot} are the normal stress and pore water pressure at the bottom of the erodible bed respectively.

The depth of erosion can be calculated by analysing the factors of safety at the top and bottom of the erodible layer. In the case when Ftop < 1 and Fbot < 1, then dsc, thickness of eroded layer, equals the total thickness of the erodible layer d; In the case where Ftop > 1 and Fbot < 1, then dsc is again equal to the total thickness of in-situ material; In the case, where Ftop < 1 and Fbot > 1, it is showed that only a portion of d will fail and it can be calculated by equation 2.10 as follows.

$$d_{sc} = \frac{1-F_{top}}{F_{bot}-F_{top}} d \qquad 2.10$$

This model is identical to the dynamic model, with the exception that it includes the FOS for the erodible layer. The effect of debris flow velocity on entrainment is left out (Luna *et al.*, 2012). Furthermore, the impact of grain size is not taken into account in the entrainment calculation.

Iverson, 2012 investigated how a slide block descending on an erodible slope with the ability of incorporating soil. The sliding material is subjected to Newton's Second Law and The Coulomb friction rule is used to calculate basal frictional resistance, which also takes shear rate into account.

After analysing the slide-block problem, Iverson, 2012 considered mass and momentum exchange between three continuous layers, a flow layer, an erodible bed sediment layer, and deeper substrate that cannot be entrained, respectively. It is considered that the flow and erodible bed layers can exchange momentum and that momentum must be conserved during such an exchange.

The equation for determining basal erosion rate was improved by Richard M. Iverson and Ouyang, (2015). The derivation took into account jump conditions at the interfaces between each layer, which describe the abrupt change in shear stress and horizontal velocity in the debris. If no dilatancy exists, this model will reduce to the model proposed by Medina, Bateman and Hürlimann, (2008).

Kang and Chan, (2018) proposed a model to calculate entrainment with particle size, time taken for one particle to roll another particle and initial angle between channel bed and line connecting the centre of two particles. They stated that improvements are required on calculation of entrainment and total volume when lateral spreading of the debris flow is significant.

Empirical models

Empirical models are primarily developed based on the analysis of statistical data from field cases and laboratory experiments. Flow velocity, shear stress and solid concentration are generally used in the development of empirical entrainment model.

To measure the erosion rate, De Blasio, Breien and Elverhøi, (2011) proposed a semi-empirical model. The erosion rate of the model is solely determined by the tangent part of the weight at the base of channel and the average velocity of the debris. The critical shear stress is used to assess the occurrence of entrainment. Measurements from Fjaeland debris flow are utilised to calibrate the model. This model appears to be promising since it connects velocity of the debris flow and basal shear stress to entrainment.

McDougall and Hungr, (2005) built a new computer model to simulate rapid landslide motion through 3D terrain using a simple material entrainment algorithm based on the assumption of natural exponential growth with displacement. The bed erosion velocity (m/s) and the volume growth rate (s^{-1}), defined as bed-normal depth eroded per unit flow depth and unit displacement, can be accounted for by equation 2.11.

$$\frac{\partial z}{\partial t} = Ehv \qquad 2.11$$

Where E is volume growth rate (m^{-1}), h is flow depth and v is flow velocity.

The growth rate, E, is determined by trial and error. Therefore average volume growth rate, $\bar{E}$, is recommended to replace E as can be preliminary estimated from equation 2.12

$$\bar{E} = \frac{ln\left(\frac{V_f}{V_o}\right)}{\bar{S}} \qquad 2.12$$

Where V_0 - Estimated total volume entering, V_f is the estimated total volume exiting and $\bar{S}$ is the approximate average path length. Limitation of this equation is that it is assumed that material suffers even erosion along the channel.

In preliminary assessment, Chen, Crosta and Lee, (2006), proposed an equation to estimate the yield rate E (dimensionless) with total eroded volume, travel distance of the centre of mass and total erosion affected area. Correction coefficient was introduced to account for the system non-linearity and it should be determined before the application of the model.

E Bruce Pitman *et al.*, (2003) proposed an empirical formula to estimate the entrainment rate e_s (m/s) with velocity components and a constant to fit experimental results

Hsu, Dietrich and Sklar, (2008) considered different velocity profiles of granular flows for different basal behaviour and divided the granular flows into four types: a flow with full slip, a flow with zero slip, partial slip with positive velocity at the base and plug flow with no slip. It was suggested erosion rate based on Archard wear equation for all slip cases with sliding velocity, normal pressure and wear coefficient of materials in contact.

Wicklein and Papanicolaou, (2000) suggested an equation for estimating the entrainment rate of material that could potentially be entrained into the flow. In theory, all of this material can be entrained into the flow. Since the flow has a finite carrying capacity for material, excess material would redeposit on the bed. In the model, it is considered that bed shear stress fluctuation is the dominant mode of the sediment entrainment. Cao *et al.*, (2004) presented a theoretical model upon the conservative laws of shallow water hydrodynamics. Entrainment and deposition were considered in the model. Variation of bed channel elevation is defined with sediment entrainment and deposition fluxes across the bottom boundary of flow, and bed sediment porosity.

2.5.2 Physical Models and Field Investigations

To test the entrainment of debris flow, different sizes of flume had been built and used by Iverson *et al.*, (2011), Richard M. Iverson and Ouyang, (2015),Mangeney *et al.*, (2010) and Egashira, Honda and Itoh, (2001). The experimental setup mainly consists of a tank, an erosional zone and a deposition pad. A schematic graph of the flume experiments and summary of the size of the flumes were used by Iverson *et al.*, (2011),Mangeney *et al.*, (2010) and Egashira, Honda and Itoh, (2001) in entrainment studies are shown in Figure 2.2 and table 2.3 respectively.

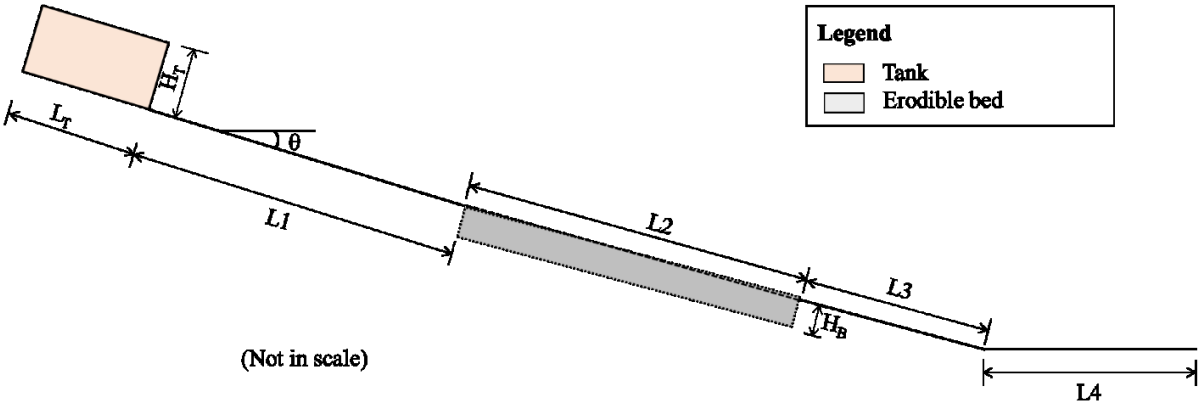

Figure 2.2 Schematic diagram of the flume experiment.

Egashira, Honda and Itoh, (2001) suggested a formula for calculating erosion rate based on the assumption that the channel bed's slope is always adjusted to the angle corresponding to limiting equilibrium conditions. Unsaturated debris in the channel will leave behind material that will reach the limiting equilibrium slope angle.

Table 2.3 Size of the flumes used in experimental study

Authors	H_T (m)	L_T (m)	L_1 (m)	L_2 (m)	H_B (m)	L_3 (m)	Width (m)	θ(°)	L_4 (m)
Iverson *et al.*, (2011)	≈ 1.6	4.7	6	42	≈ 0.12	47	2.0	31	---
Mangeney *et al.*, 2010	0.14	0.2	0	0	0 - 0.006	3	0.1	0 – 30	---
Egashira, Honda and Itoh, (2001)	---	---	4	0	0.1	2	0.1	12	---

Iverson, Logan and Denlinger, (2004) revealed that Despite the fact that small experiments are unlikely to replicate some avalanche behaviour seen at geophysical sizes, they can be used

to test models of ideal granular avalanches by ignoring the effects of intergranular fluid and cohesion. Therefore, Iverson *et al*., (2011) carried out a large scale entrainment experiment in which an erodible bed is formed by discharging SGM abruptly from a head gate then, same material is released from the tank to simulate the debris material. The key variable manipulated is the bed-sediment volumetric water content. The impact of bed-sediment water content on entrainment is analysed by measuring flow-front speed, flow volume and momentum gains at specified locations. Normal stress, pore water pressure and height of debris material are monitored by electronic sensors during the test. The results indicates that pore pressure generated as wet bed sediment is overridden and once gradually entrained by debris can reduce friction.

Bowman *et al.*, (2010) creatively used a geotechnical centrifuge apparatus to study debris flow entrainment under undrained and drained conditions. Both fixed and erodible bases were used in the experiment. It is noted that using the centrifuge apparatus could produce a better approximation of real-scale physical process.

Berger, McArdell and Schlunegger, (2011) designed an erosion sensor to monitor the entrainment process. Though there were drawbacks like the detection limit and presence of a sediment layer covering the sensors, this method offers a new thought to monitor the entrainment during the process of debris flows. McCoy *et al.*, (2013) designed an apparatus using sensors to measure changes in the height of the bed sediment and incision bolts had been used to measure the average incision rate. After the debris flow, the variation of covered length of the bolt can be measured because of which average incision rate in one debris flow event could therefore be estimated.

Table 2.4 Summary of selected list of available entrainment model

S. No	Author	Model	Remarks
1	Wicklein and Papanicolaou, (2000)	$E_i = 0.02\rho * SG_j * A * d_i * (1-p) * p_{Aij} * \frac{F_i}{T_b} * \frac{d_i}{T_b}$	ρ – water density; SG_j - specific gravity; A -bed area; d_i – size of the particle: p - porosity, P_A - percent active layer, F_i - excess shear stress probability density function; T_b - bursting event period
2	Egashira, Honda and Itoh, (2001)	$E\Delta x = Ev\Delta t = c_* v\Delta z$ $E = c^* v \tan(\theta - \theta_e)$	E - erosion rate; v - average velocity of the debris flow; Δx is the distance increment, Δt - time increment; c* - sediment concentration; Δz - erosion depth during
3	McDougall and Hungr, (2005)	$\frac{\partial z}{\partial t} = Ehv$ $\bar{E} = \frac{ln\left(\frac{V_f}{V_o}\right)}{\bar{S}}$	E - Volume growth rate (m^{-1}); $\bar{E}$ - Average volume growth rate; V_0,V_f - estimated volume entering and volume exiting the zone respectively; h - flow depth; v - flow velocity.
4	Chen, Crosta and Lee, (2006)	$E = \alpha \frac{V_{eroded}}{A_{affected} d_{com}}$	V_{eroded} - total eroded volume; α - correction coefficient; $A_{affected}$ - total erosion affected area; d_{com} - travel distance of the centre of mass;

5	Medina, Hürlimann and Bateman, (2008)	$h_{ent} = \frac{\tau_b - \tau_{res}}{\rho_f g(\cos\theta \tan \emptyset_{bed} - \sin\theta)}$	τ_{res} - resistance stress of the material;, τ_b - active force; g - gravity; θ is the slope angle; $\emptyset_{bed}$ - friction angle; ρ ,ρ_f – debris density; v – mean velocity.
6	Medina, Bateman and Hürlimann, (2008).	$\frac{\partial z}{\partial t} = \frac{(\tau_b - c - h\rho_f g \cos\theta \tan \emptyset_{bed})}{\rho v}$	
7	De Blasio, Breien and Elverhøi, (2011)	$\frac{dh}{dt} = c\lvert U\rvert^{y}(\tau_{xy} - \bar{\tau})$ $\frac{dh}{dt} = 0$ for $\tau_{xy} < \bar{\tau}$)	U- Velocity of the debris; $\bar{\tau}$ – critical shear rate for erosion: y and c – constants.
8	Iversion, (2012)	$E = \frac{(\tau_{1bot} - \tau_{2bot})}{\rho(v_{1bot} - v_{2bot})}$	τ_{1bot} , τ_{2bot} - shear stress at the bottom of the first layer and the second layer respectively ; ρ - bulk density of flow and bed material; v_{1bot}, v_{2bot} - velocity at the bottom of first layer and bottom layer respectively;
9	Richard M. Iverson and Ouyang, (2015)	$-\frac{\partial z}{\partial t} = \frac{\tau_{1bot} - \tau_{2bot}}{\bar{\rho}_1 u_1(z_b)} - u_1(z_b)\left[\frac{\sigma_{2top} - \sigma_{1bot}}{(\tau_{1bot} - \tau_{2bot})}\right]$	

10	Kang and Chan (2018)	$E = \frac{2\dot{R} \sin \alpha_{0\iota}}{t_\iota}$	t_i- time taken for one particle to roll another particle; α_{0i}- angle between channel bed and line connecting center of two particles at t_0

Crosta, Imposimato and Roddeman, (2009), Mangeney *et al.*, 2010 and Farin 2014 analysed entrainment by granular column collapse on erodible bed. Granular column collapse mdeodel is a simple approach widely used to study granular flows and has provided meaningful insights into flow behaviour. Granular column collapse is defined as collapse of an initially static column of grains along a horizontal surface. The layout of granular column collapse is shown in Figure 2.3.When the confining gate is opened, the column starts collapsing and the particles fall downwards are followed by progressive sliding and deposition. Since granular column collapse itself encompasses a vast area, previous studies in this topic have been discussed separately in the following section.

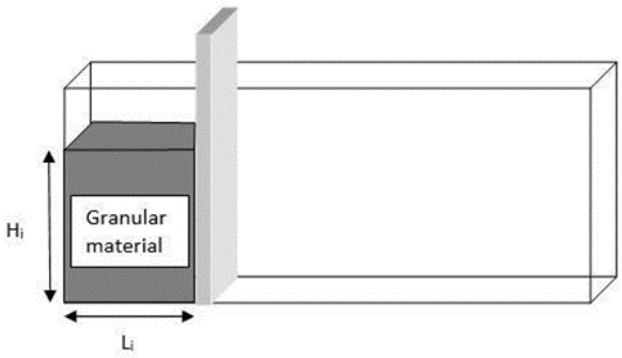

Figure 2.3 Granular column layout

2.6 Studies on Granular Column Collapse Model

Behaviour of granular media as static piles or flows forms the basis of understanding many man-made processes and natural phenomena (Lube *et al.*, 2004). Similarity in behaviour is recognized between solid materials in debris flow and dry granular flows (Iverson, 1997). For example, shear stress is sustained with very slow deformation due to friction in grain contacts and inelastic grain collisions cause shear stress to flow very quickly. As a result, several studies focused on the mechanical behaviour of dry granular flows in simple and limited

model settings. It is envisaged that these conclusions may shed light on the mechanisms of beginning and dissemination of genuine debris flows (Lajeunesse *et al.*, 2005; Lube *et al.*, 2005).

2.6.1 Laboratory Investigation

Experimental investigations have been carried out by collapsing columns comprising granular materials on horizontal plane (Lajeunesse *et al.*, 2005; Lube *et al.*, 2005). Lajeunesse *et al.*, (2005) observed that the final runout distance and flow dynamics are independent of the volume of the material released and depend on the initial aspect ratio. A correlation between final runout distance and aspect ratio of the granular column is established after normalizing the parameters. But the relations were established by conducting 2D unidirectional collapse experiments.

While studying the collapse of granular columns in rectangular channels, Balmforth and Kerswell, (2005) focused on the final deposit shape. At higher aspect ratios, the run-out is well represented by a simple power-law expression that varies with channel width.

Thompson and Hupper, (2007) discovered that, while the column collapses containing water-saturated sand into the water exhibit a different type of flow, the scaling of the final height and final runout distance with aspect ratio is nearly identical for dry and saturated flow. The run-out distance of dry flows is the distance travelled by material originating from the upper third of the initial column's outer surface. The initial geometry is relatively insignificant in determining the shape of the final deposit in dry flow with aspect ratios greater than one.

In laboratory studies, Girolami *et al.*, (2012) discovered that friction dominates the flow over vertical acceleration for smaller aspect ratios and pressure gradients are small in comparison to friction forces. When the aspect ratio is large, the flow is dominated by inertia, such as vertical acceleration, and pressure gradients become significant in comparison to friction forces. Frictional forces balance the inertial force at intermediate aspect ratios.

Experiments on granular column collapse in the presence of an erodible bed conducted by Mangeney *et al.*, (2010) and Farin, Mangeney, and Roche (2014) quantified how well the deposit and dynamics of dry granular flows changes. The runout distance and flow duration

increased significantly as the erodible bed thickness increased. Only flows on slopes greater than a critical angle showed this strong effect of bed entrainment.

Large-scale tests with dry and submerged granular materials were conducted in order to understand the granular flow on inclined planes (Denlinger and Iverson, 2001). The flow is stable and uniform for moderate to small slopes, but it accelerates along the plane for large inclinations. Maximum thickness of deposit was observed for a value of roughness which may correspond to effective friction at the bottom. With decreasing bed thickness, the critical angle controlling flow behaviour tended to increase (Daerr and Douady, 1999).

2.6.2 Analytical and Numerical Investigation

As a matter of fact, almost all numerical studies addressing the granular column related problem fall into one of three categories.: shallow-type models (Mangeney *et al.*, 2010; Balmforth and Kerswell, 2005; Mangeney-Castelnau *et al.*, 2005), viscous-plastic or elasto-plastic models (Crosta, Imposimato and Roddeman, 2009; Ionescu *et al.*, 2015, Lagrée, Staron and Popinet, 2011), Discrete Element Methods (DEM) (Staron and Hinch, 2005; Girolami *et al.*, 2012; Lacaze, Phillips and Kerswell, 2008; Zhao, 2014).

Mangeney *et al.*, (2010) present an analytical solution to the dam break problem, which involves the flow of a frictional material over a sloping plane covered by a thin layer of the same material. The mass and momentum conservation equations describe a simple representation of material flow.

Mangeney-Castelnau *et al.*, (2005) used a depth averaged model based on the long wave approximation to perform numerical simulation. The model's generic solutions are gravity-independent and are determined solely by the initial aspect ratio and effective friction angle. Numerical simulations are in agreement with the experiments for aspect ratio (a) < 1. The findings shed light on the relationship between the area overrun and initial potential energy of the flowing mass.

An elasto-viscoplastic flow law-based hybrid Eulerian–Lagrangian approach was used to investigate the effect of an erodible layer on the collapse of a granular column over a horizontal bed. Crosta, Imposimato and Roddeman, (2009) observed a significant decrease in runout, possibly due to a much thicker erodible layer in their case. Crosta, Imposimato and

Roddeman, (2009) discovered that the friction angle influences run-out behaviour significantly.

Ionescu *et al.*, (2015) propose a first attempt to thoroughly compare the granular flow dynamics simulation of the continuum visco-plastic approach to experimental results. On a horizontal plane, the model successfully anticipated the complete spread of the column, but on an inclined plane, it considerably overestimated the maximum runout distance. By including the friction applied by the lateral walls, the new model proposed by Martin *et al.*, (2017) allows for the quantitative reproduction of column collapses.

The finite element method was used by Lusso *et al.*, (2017) to simulate a 2D viscoplastic flow and they came to the conclusion that studying flows over an erodible bed requires a pressure and rate-dependent viscosity.

Granular flow through inclined plane exhibits transient behaviour. The change in the height of flowing granular mass does not affect the velocity profiles or flow behaviours, but varying the inclination of the plane (Soundararajan, 2015). Constitutive laws based on plastic theories relating the microstructure to the macroscopic behaviour provide insight into the granular flow mechanism (Roux and Combe, 2002). They are limited to initiation of deformation at present but prediction of quasi-static flow is not involved. Granular flow simulation down an inclined plane by material point method captures the flow behaviour in initial stages and shows inconsistent behaviour when the flow ceases (Bandara, 2013).

Energy dissipation along rough surfaces can be predicted using rheology models based on coulomb friction. In larger scale simulation using rheology models, grains on the flow surface had higher inertial number due to low mean pressure, whereas those that in the main flow had lower value of inertial number due to high mean pressure and model is less effective in large scale problems.

Despite a considerable number of research on the granular flow behaviour, a constitutive equation describing the behaviour of granular flow is lacking. Depth averaged equations of continuum modelling have been employed in modelling geophysical problems and it has two shortcomings (Iverson, 2003; Lajeunesse *et al.*, 2005). One is the viability of depth-averaged approach only when the flowing layer thickness is considerably thin than the lateral dimension. Other is the deduction of empirical laws from experiments under steady flow conditions. Conventional numerical methods like FEM and FDM are macro-scale and grid

based approaches which lacks the capability of capturing the microstructure phenomenon in soils (Yang and Wang, 2012). They play a limited role in enabling one to understand the circumstances in which landslides may occur. DEM, being a Lagrangian approach, tracks material behaviour by the use of a set of discrete particles thereby avoiding mesh distortion in large deformation problems. Large movements of granular assemblies can be simulated by Discrete Element Method (DEM). As stated by Cundall and Strack, (1979), interaction of many small elements with each other can be used in modelling debris flow. Following section deals the applications of DEM and numerical modelling of granular column collapse by DEM.

2.6.3 Discrete Element Method

Discrete Element Method enables us to examine quantities that are not accessible experimentally and providing valuable insight into flow dynamics. Zhu *et al.*, (2008) provided various examples where DEM is applied and these comprise drums, mills, mixers and hoppers, pipeline flow, industrial processes like examining breakage rates, mixing and wear rates. Phenomena like dispersion, segregation, particle packing and densification of bed are described by DEM models. Though constitutive models are not largely available for particulate processes, certain operations like coupling equations are based on fundamental understanding of empirical parameters that are function of equipment and other material properties are well characterized. Formulations of DEM were based on molecular dynamics concepts and brought into use on the assumption of rigid bodies and deformable contacts (Cundall, 1971).

DEM is the best choice for dealing with problems at the grain scale, such as miniature penetrometers. By adjusting certain parameters in DEM, we were able to achieve qualitative agreement between numerical and experimental results (Lin and Wu, 2012). The ability of DEM to directly capture particle scale interactions distinguishes it from other continuum models such as depth-averaged models, Material Point Method and Smooth Particle Hydrodynamics (Kesseler, Heller and Turnbull, 2018). To extract macro-scale information from DEMs for comparison to continuum-based models, averaging procedures can be used (Zhu *et al.,* 2008). Extended DEM (XDEM) methodology comprises of Lagrangian- Eulerian approach where particulate phase is coupled with gas phase through void space of a packed

bed reactor. The thermodynamic state of each particle is determined by considering the mass and heat transfer between the surrounding gas phase and particle surface.

There are two main goals for using DEM in geomechanics (O'Sullivan, 2011). Firstly, it simulates large deformation problems more effectively in boundary value problems than in continuum-based analysis. The second application is for measuring material behaviour on a wider level than a sophisticated laboratory examination. DEM simulation reveals the hidden information in a conventional experiment. Hence DEM simulation can be used to study the flow transition behaviour effectively.

Zenit, (2005) pointed out that the use of DEM in landslide simulations is very powerful because all numerical data are accessible at any stage of the test, including data that cannot be obtained directly from laboratory experiments, such as interaction forces and individual particle trajectories.

Staron and Hinch, (2005) investigated the collapse of a granular assembly onto a horizontal floor using a 2D discrete element model. At large aspect ratios, the collapse was primarily caused by the free fall of granular materials, whereas the free fall process was not visible when the aspect ratio is small. This finding implies that the initial aspect ratio of granular materials determines the depositional morphology.

Though the 2D DEM simulations identified the critical effect of initial geometry on granular flow mechanism, the procured results do not quantitatively match the results of physical ones because of the particle shape effect is not taken into account.

Cleary and Frank, (2006) investigated the axisymmetric collapse of a spherical particle assembly using 3D DEM analyses. The rolling resistant moment is used in the model to analyse the particle shape effect. Although the obtained results qualitatively matched the laboratory model test results, they did not explain the mechanism guiding the higher runout of debris materials.

Staron and Lajeunesse, (2009) investigated the interlinked roles of volume and topography in landslides using a 3D DEM model and demonstrates that the sliding and spreading of debris material is strongly influenced by granular volume. In the DEM model, a representative elementary volume (REV) must be chosen so that the size of the granular column or the number of grains present has no effect on the numerical results obtained (Modenese, Utili and

Houlsby, 2012). The effects of aspect ratio, internal friction angle and characteristic strain on runout distance and deposit height was investigated. They have calculated the effect of model size ratio [S] on the normalised runout distance, where [S] should be greater than 40 and shown in Figure 2.4.

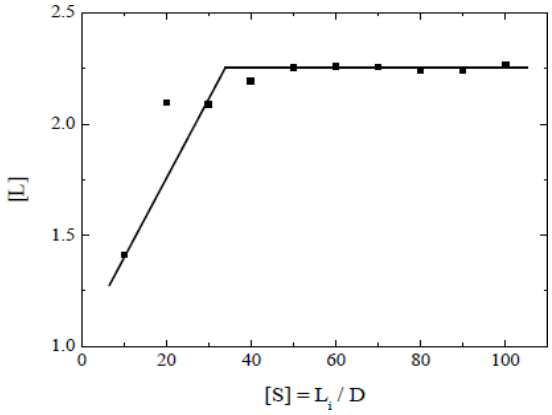

Figure 2.4 Influence of model size ratio

Utili, Zhao and Houlsby, (2015) showed that different depositional morphologies were obtained with respect to different aspect ratios. Since the flow profiles and final deposit depend on the initial aspect ratio which is a dimensionless quantity, the profiles are presented in dimensionless form as shown in the Figure 2.5.

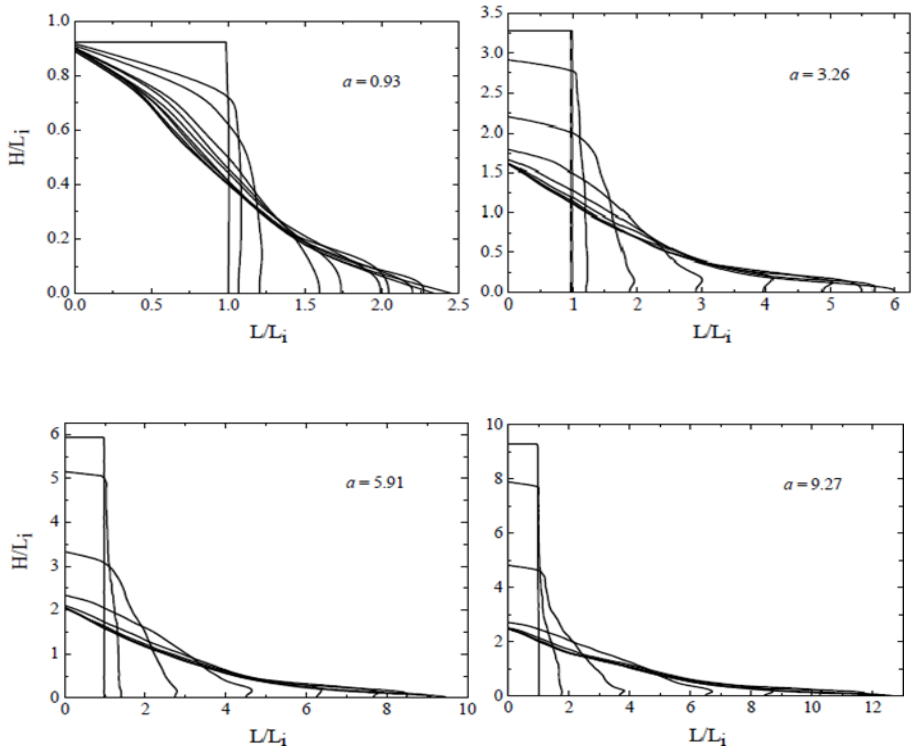

Figure 2.5 Depositional profile evolution (Utili, Zhao and Houlsby, 2015)

2.7 Summary of the Literature Survey

A detailed literature survey was conducted on landslides and runout models. The summary of literature review is listed below.

• Runout is very sensitive to the topography and the resolution of the computational domain (Quan Luna, 2012).

• Runout model need to be computationally efficient (Quan Luna, 2012).

• Momentum based formulation in continuum models is still the most reliable approach (Beguería *et al.*, 2009).

• Eulerian and Lagrangian approach have their advantage and disadvantage but usable and promising (Hungr and Evans, 2004; Crosta, Imposimato and Roddeman, 2009).

• Existing runout models work well in backward analysis but give highly diverging values in forward analysis (Beguería *et al.*, 2009).

• Reliable guidance needs to be worked out for selecting rheological models and their parameters (Quan, 2012).

• More research is needed in defining the mechanism of entrainment (Iversion, 2012; Mangeney *et al.*, 2010).

2.8 Need for the Study

Based on a comprehensive literature survey, the need for the study has been identified as follow:

• Entrainment plays a vital role in the run-out of a debris flow, since the entrainment mechanisms significantly change the mobility of the flow (Iverson, 1997).

• The entrained volume may increase several times in volume of the initially mobilized mass (VanDine and Bovis, 2002).

• The acceleration or deceleration of the moving mass as a result of entrained material, depend on the characteristics of the erodible material, the topography and the dynamics of the flow (Mangeney *et al.*, 2010).

• Erosion impacts the motion by a decrease in bed friction force per unit mass, and generation of a resistive force. The resistive force is generated due to a momentum transfer between the moving mass and the soil cover. The soil mobilizes and accelerates to flow velocity. This is why entrainment mechanism should be included in continuum models (Issler and Johannesson, 2011)

• Models using a constant volume were not able to accurately forecast debris flow characteristics (Chen, Crosta and Lee, 2006).

2.9 Objectives

Based on the research gaps identified from the literature review, the main objectives of the present research are

i. To study the entrainment phenomena of soil particles by modelling granular column collapse on an erodible bed using discrete element method.

ii. To incorporate the equation of entrainment in a continuum model to perform a more realistic runout modelling

iii. To quantify the uncertainties involved in the material parameters of continuum runout model and validate the model using case studies at two sites (Peringalam and Kaipalli in Kerala state, India)

Chapter 3

Influence of Erodible Layer on Granular Column Collapse Using Discrete Element Analysis

In this chapter, Granular column collapse over an erodible bed is analysed with 3D Discrete Element Method for different aspect ratios. The effect of entrainment on the granular flow is examined for different aspect ratios of columns, and parameters such as flow velocity, bulk coordination number, and kinetic energy are analysed and discussed

3.1 Discrete Element Method (DEM)

The Discrete Element Method (DEM) is a numerical method for modelling the dynamics of soil particles that interact at discrete contact points (Zhao, 2014). According to Zhu *et al.*, (2008) the numerical techniques in DEM are divided into two categories: *i) Hard sphere model ii) Soft sphere model.* The primary distinction between these two models is the particle penetration at contacts. Both the models are time dependent and hence the evolution of the particle domain is examined at distinct time intervals.

The **hard sphere model** is called ‘collisional’ or ‘event driven’ (ED) model. In this model, the interaction force between particles is impulsive. Particles exchange only momentum and

particle contact forces are not considered. There is an absence of interpenetration or particle deformation during impact. During collision, energy is dissipated in the form of heat and by plastic deformation. Coefficient of elastic restitution characterizes the resultant loss of momentum. Its algorithms analyse events in the order of occurrence, which means that in the analysis, only one collision can occur at a time. During the simulation, the time increment varies which is equally spaced between every two collisions. Also, between collisions particles follow uniform trajectory. It is computationally cheaper but fails in simulating the dense materials having multiple particle contacts which makes the simulation non-physical. Since the real mechanism of force transfer involves deformation at contacts, this model is not widely used in geotechnical engineering.

The **Soft sphere model** solves the discrete time increments and the governing equations of linear and rotational dynamic equilibrium of the particles that collides and those coming into contact. The rigid particles are allowed to overlap to represent some deformation at the contacts. Evaluation of normal and tangential forces is done when the normal and tangential overlaps takes place. Friction and elastic restitution comes into effect only when particle penetration occurs. The nature of this approach makes multiple simultaneous contacts possible. Similarity of algorithm exists between DEM and soft sphere approach. It allows for small overlaps which is useful in calculating forces acting on the particles. Hence, this is the most suitable method. This research follows the soft sphere approach.

In reality, soil particles possess irregular shape which can be taken as polygonal. Such shapes pose difficulty in modelling and contact detection. If irregular shape is adopted, two particles may contact at multiple points which also increases the computational time. Considering one of the assumptions made in the particle based simulations by Potyondy and Cundall, (2004) i.e., each contact involves only two particles, the shape of particle is chosen to be spherical. It makes the contact detection simpler and also reduces the computational time. Particle shape is an inherent soil characteristic that plays a major role in mechanical behaviour of soils (Mitchell and Soga, 2005). To study the realistic mechanical behaviour, rolling friction can be applied to soil particles which arises due to the shape of the particle. In this study, no such rolling resistance is considered for easier understanding of the particle behaviour.

The first and foremost step in DEM simulation is Contact detection. Once the particles are inserted into the domain, the particles come into contact. Number of contacts that a particle possesses depends on the size and shape of the particles. Smaller particle has fewer contacts than a larger one. A contact is detected for spherical particles when the distance between two

particles is less than the sum of their radii. As a result, contact detection entails measuring the distance between all the particles in the system. This process is computationally expensive because it consumes roughly 90% of the computational time. The schematic representation of contact detection of particles is shown in the Figure 3.1. The steps involved in contact detection are:

i. Discretization of the calculation domain into three-dimensional cells. The size of the grid is determined by particle size distribution and a grid size of 3 to 5 times the smallest particle radius is usually optimal.

ii. Immediately following discretization, the cells containing particles are marked active and checked for contacts.

iii. The forces exerted by each colliding particle are computed.

iv. Elements are repositioned and active cells are identified once more.

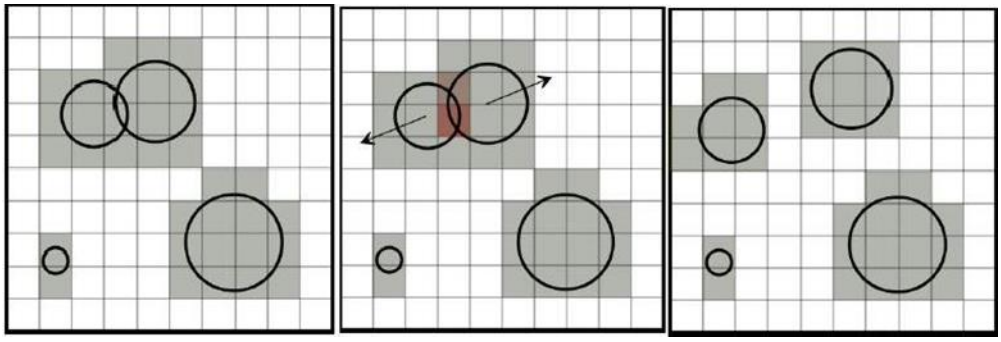

Figure 3.1 Contact detection of particles (Hiuhu *et al.*, 2015)

Once contact detection is complete, a contact model is used to calculate the inter-particle forces caused by particle deformation at the contacts. Particle deformation during collisions is modelled as overlap. To calculate the magnitude of forces, contact models use the amount of normal and tangential overlap between two particles. The calculations make use of material properties such as Young's modulus, restitution, and friction coefficients. The contact models are mostly developed for spherical contacts and are based on contact mechanics theories. Depending on the requirements, various contact models exist, such as Hertz Mindlin contact model, DMT model, Van der Waals model, JKR model, the Liquid Bridge models, and so on. Contact models can simulate elastic or plastic collisions between cohesive and non-cohesive materials. Working of contact model is shown in Figure 3.2.

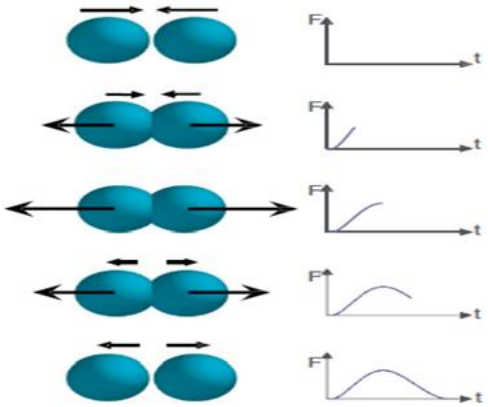

Figure 3.2 Contact force model (Hiuhu *et al.*, 2015)

The contact models employed performs the force calculation at the inter-particle contacts. Non-contact forces would generally be capillary forces in unsaturated soil from a geomechanics perspective. Forces resulting from particle collisions are not the only ones used in DEM. The effects of particle body forces like gravity or non-contact forces like electrostatics or Van der Waals forces can also be simulated here. Cundall and Strack, (1979) substituted contact points with springs (normal or shear, also normal or shear dashpots). The normal force has two terms, a spring force and a damping force. The tangential force also has two terms: a shear force and a damping force. A particulate DEM model generates an ideal system of rigid particles that can move and are linked by rigid springs that simulate contact interactions. When particles move apart, the contacts are broken, and the springs are removed. Similarly, the formation of new contacts introduces new springs. During the simulation, particles come into contact, loose contact, slide over each other making the stiffness of the overall system vary. Thus the analysis is non-linear. It is called geometrical non- linearity when the packing geometry of the particles vary during the simulation. An analogy exists between the particles in a DEM model and the nodes in a finite element analysis (O'Sullivan, 2011). With this analogy, the overall governing equation 3.1 of the system can be expressed as that of the dynamic analysis in structures by finite element method.

$$\mathbf{M}\frac{\mathbf{d^2u}}{\mathbf{dt^2}} + \mathbf{C}\frac{\mathbf{du}}{\mathbf{dt}} + \mathbf{Ku} = \Delta\mathbf{F} \qquad 3.1$$

Where M is the inertia mass matrix, C is a damping matrix, u is incremental displacement vector and ΔF is an incremental force vector including moments. The global stiffness matrix K is affected by the particles with which it comes into contact. By considering the equilibrium of individual particles rather than solving the entire system simultaneously, the global system of equations is avoided.

In 2D DEM analysis, particles have three degrees of freedom (two translational and one rotational), whereas in 3D DEM analysis, particles have six degrees of freedom (three translational, three rotational). Rotational motion analysis is more difficult than translational motion analysis. Newton's second law governs the motion of bodies under the influence of different forces. It calculates translational and rotational accelerations, which are then time integrated to update particle velocities and displacements. The rotational motion of particles is calculated using the equation 3.2 below.

$$\mathbf{I}\frac{\mathbf{d\omega}}{\mathbf{dt}} = \mathbf{M} \qquad 3.2$$

Where I is the moment of inertia, M is the resultant contact torque acting on the particle, ω is the angular velocity and t is time. The translation motion is determined by the following equation 3.3. The forces acting on 2D discrete particle is shown in Figure 3.3

$$\mathbf{m}\frac{\mathbf{dv}}{\mathbf{dt}} = \mathbf{F_g} + \mathbf{F_c} + \mathbf{F_{nc}} \qquad 3.3$$

Where v is the translational velocity of the particle, m is the mass of the particle, F_g is the resultant gravitational force acting on the particle, F_c and F_{nc} are the resultant contact and non-contact forces between the particle and surrounding particles or walls. The applied forces and torques are assumed to be known and therefore it is manipulated with the above equations to give particle translational and rotational accelerations. Equilibrium equations generate two sets of ordinary differential equations for each particle.

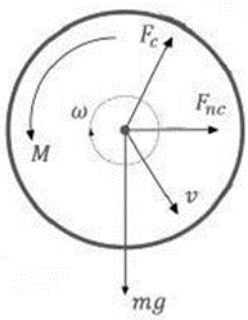

Figure 3.3 Forces acting on a 2D discrete particle (Hiuhu *et al.*, 2015)

Updating Particle Positions

With the resultant forces acting on the particles known, the particle's acceleration can be calculated using the particle's equilibrium equation 3.4. The particle's translational motion is given by

$$\mathbf{m_p a_p^t = F_p^t} \quad 3.4$$

Where m_p denotes the moment of inertia matrix, a_p denotes the acceleration vector at time t, and F_p denotes the resultant force vector. In three dimensions, the vectors have three components. The three-dimensional case mass (inertia) matrix is given by

$$m_p = \begin{bmatrix} m_p & 0 & 0 \\ 0 & m_p & 0 \\ 0 & 0 & m_p \end{bmatrix}$$

Because a mass of particles behaves normally, the diagonal elements of the mass matrix are equal to m_p and the non-diagonal elements are equal to 0. The idea is to use these acceleration values to calculate incremental displacements and update particle positions. The time integration method refers to the numerical analysis of updating parameters with the first and second derivatives of time.

For time integration with a time increment t, the central difference method is used in most DEM codes. The following equations 3.5 and 3.6 describes the relationship between acceleration and velocity vectors:

$$\boldsymbol{v_p^{t+\frac{\Delta t}{2}} = v_p^{t-\frac{\Delta t}{2}} + \Delta t a_p^t} \quad 3.5$$

$$\boldsymbol{x_p^{t+\Delta t} = x_p^t + \Delta t v_p^{t+\frac{\Delta t}{2}}} \quad 3.6$$

With a time lag of t/2, velocities and displacements are calculated. Particle rotational velocity is calculated using the dynamic rotational equilibrium equation 3.7.

$$\mathbf{I_{p,z}\left(\frac{d\omega}{dt}\right)_{p,z} = M_{p,z}} \quad 3.7$$

The tangential component of contact force is calculated using angular velocity. The central difference time integration method for calculating angular velocity is given by equation 3.8

$$\boldsymbol{\omega_{p,z}^{t+\frac{\Delta t}{2}} = \omega_{p,z}^{t-\frac{\Delta t}{2}} + \Delta t \frac{M_{p,z}^t}{I_{p,z}}} \quad 3.8$$

Time Integration

The time integration scheme proposed by Cundall and Strack, (1979) is only conditionally stable, requiring the use of smaller timesteps. A particle's movement within the granular flow

is influenced not just by contact with its immediate neighbours, but also by disturbance transmitted by from particles far away. In DEM simulation, the time increment selected should be small enough to affect only the particles directly adjacent to it. To maintain numerical stability, single time step disturbances must not propagate from a disc further than its nearest neighbours. It is also recommended that the total energy of the system be monitored to check numerical stability. The strain energy stored in the contact springs and the kinetic energy of the particles are components of the total energy.

When solving a system of differential equations, two types of errors occur. The first is the approximation error produced when the equation is numerically solved. The second error is the result of approximations made while calculating incremental displacements from calculated accelerations. This is known as a truncation error. For any numerical model that simulates dynamic system response, truncation errors will be introduced at each timestep by equation 3.9.

$$\mathbf{x_p^{t+\Delta t} = x_p^t + \Delta t\left(\frac{dx_p}{dt}\right)^t + \frac{\Delta t^2}{2!}\left(\frac{d^2x_p}{dt^2}\right)^t + \frac{\Delta t^n}{n!}\left(\frac{d^nx_p}{dt^n}\right)^t + O(\Delta t^{n+1})} \quad 3.9$$

The truncation error is $O(\Delta t^{n+1})$. This truncation error is proportional to Δtn+1, where n is the derivative order. When the timestep is small, the higher the value of n, the smaller the error. As a result, a smaller timestep also aids in the pursuit of accuracy. Figure 3.4 below provides an overview of the DEM calculation cycle.

In DEM simulation, a finite number of particles is used which gives a hint of mass conservation. Conservation of momentum is achieved through Newton's equations of motion. It is important to consider the energy balance in a DEM simulation to avoid problems with numerical stability. Tracing the energy components in detail will give insight into the material response from a geomechanics perspective.

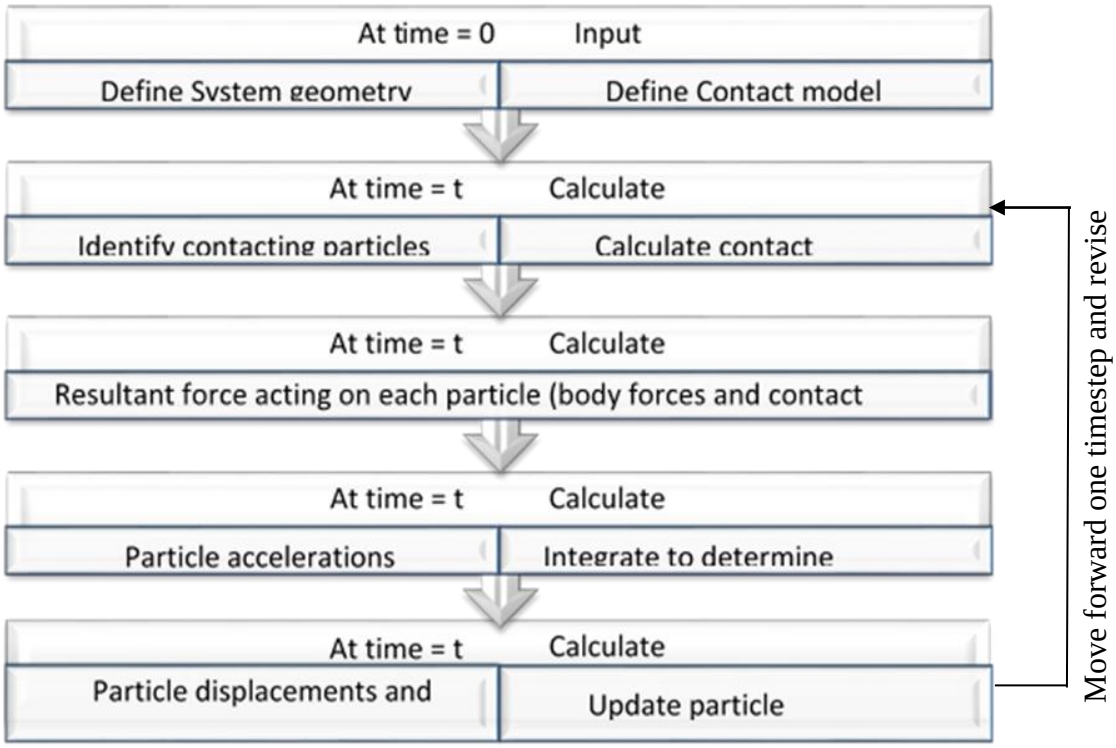

Figure 3.4 Flowchart representing sequence of calculation in DEM (O'Sullivan, 2011)

During the simulation, input energy is through boundary force or body forces and dissipation of energy is through frictional sliding and rupture of contact springs. There exists a continuous transfer or conversion of strain energy to kinetic energy and vice versa. The internal energy of the system is contributed by the strain energy and frictional energy at the contact. The external energy is contributed by the body forces, externally applied forces and boundary forces that arise due to interaction with the rigid wall boundaries. Summary of DEM calculation is shown in Figure 3.5 below.

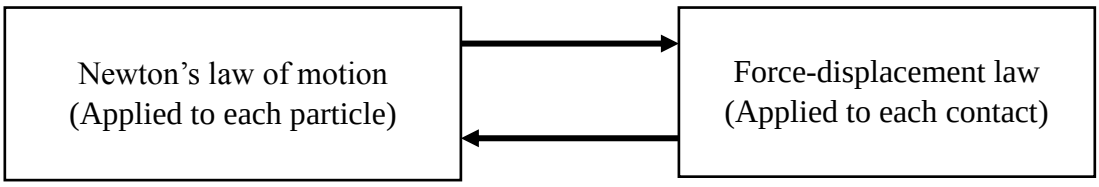

Figure 3.5 Summary of DEM calculation

3.2 LIGGGHTS

LIGGGHTS is an Open Source Discrete Element Method particle simulation software developed by DCS Computing GmbH. LIGGGHTS stands for LAMMPS Improved General Granular and Granular Heat Transfer Simulations. LAMMPS is a molecular dynamics software generally used in the field of molecular dynamics. With the physical and algorithmic analogies, LAMMPS is improved to study DEM simulations with a granular package. The aim of LIGGGHTS development is to apply it for industrial applications.

Large Scale Atomic/Molecular Massively Parallel Simulator Improved General Granular and Granular Heat Transfer Simulations (LIGGGHTS), open source software, was used to solve three dimensional discrete element method (DEM) simulations in the study (LIGGGHTS 2016). DEM involves a Lagrangian approach which keeps track of the particle-particle interaction forces, particle velocities (both rotational and linear), displacements and position (O'Sullivan, 2011;Padrós, 2014).

The LIGGGHTS code is written in C++ and can be run on a single processor or multiple processors. The primary code invokes the main script, features, and libraries. LIGGGHTS is an open source code implying that it is widely available for free. It is available for download from their website, along with the complete LIGGGHTS package, which includes all of the libraries, examples, benchmark problems, and files related to the code.

The LIGGGHTS website provides a post-processing tool called Paraview for visualising simulation results and animation. It is an open source data analysis tool for viewing particle simulation results such as force, velocity, and particle positions. At each timestep, the LIGGGHTS code dumps output in the form of a text file in VTK format containing details about each particle in the simulation. If the output text file is in a format other than VTK, it is converted to VTK using a special conversion tool called lpp (LIGGGHTS Post- Processing tool).

LIGGGHTS input file

The input script should be properly organised with commands to include logical information such as the size of the simulation box, atom type used, defining material properties, and particle insertion but also how the particles are inserted. The output-related commands should be placed at the end of the file. In general, any input script consists of four steps: *Initialization*

– define the parameters that must be defined before creating particles. *Set up* – specify particles, geometry, material properties and particle generation. *Settings*- speed, memory utilization, output options, etc. *Running a simulation*.

Running LIGGGHTS

Running of LIGGGHTS is performed soon after the input file is completely defined. Then the code has to be called with predefined command which includes the name of the input file. It has to be performed in the directory where the related input files are located. Once it has been started, the command prompt can be used to view information about the evolution the analysis. Following are the things that are shown in the command prompt while the code is running

- Simulation box size and the processor grid for parallel computation.
- Information regarding the insertion of particles and memory usage per processor.
- "Thermo" info about timestep, number of particles in the domain, translator and rotational energy and total simulation box volume. It shows the statistics of the time needed for the individual parts of algorithms, particle distribution and neighbour distribution among the processors.

The command prompt will display the state of insertion, including number of particles inserted, mass and timestep, if the particles are successfully inserted. Errors or warning messages can be visited in the documentation to have an idea of that and could be rectified. Sometimes input script might run with warning messages. The computation process ends when it completes the specified number of timesteps mentioned in the input code. At the end, information about the mass of the particle inserted, number of particles inserted, timesteps, and time required to complete the simulation are displayed, along with the total number of neighbours created.

Post processing in LIGGGHTS

Each timestep's output files are saved in the directory defined in the input script. All the data about atoms like forces, radius, and velocities are to be visualised in Paraview which is an open source data visualisation and analysis tool. . Different particle characteristics are viewed such as velocity, forces, radius, atom types, and temperature. It manages to visualize the

parameters at any time with greater precision. All the results obtained in the study related to DEM are obtained using Paraview.

3.3 Granular Column Collapse

Granular column collapse model is used in the present study to gain more insights into the entrainment phenomenon during the flow of granular mass. 3D DEM is used to model the flow after the collapse of granular columns with different aspect ratios. An erodible layer is spread over the horizontal surface upon which the column of granular particles collapses. The erodible layer is comprised of particles possessing similar properties to that of those in the granular column. In the presence of erodible bed, changes in run-out behaviour due to particle entrainment from the erodible layer is studied. Simulations were carried out with granular columns of different aspect ratios and run-out distances were measured along the direction of flow in both rigid and erodible bed.

To avoid complexity and to reduce computational time, the particle shape is chosen to be spherical due to which a single contact is established between two particles. The process starts with the contact detection (particle-particle and particle-wall) in which, each and every contact is formed by rigid contact springs which simulates contact interactions (normal stiffness, k_n and tangential stiffness, k_t). The contact springs are removed once the particles move apart and establish loose contact with the neighbouring particles. With the continuous introduction and elimination of contact springs, there exists a change in the overall stiffness of the system, which makes the analysis non-linear. Hence, Non-linear Hertz-Mindlin contact model (Hertz, 1882) was used in the current study to calculate the particle interaction forces.

3.3.1 Validation of the Model

The granular column collapse model used in this study is validated using the granular column collapse experiment conducted by Shi, Zhang and Zhang, (2018) which is shown Figure 3.6. A sand column of dimension 50mm x 50mm x 90mm with the properties mentioned in Table 1 is generated in DEM numerical domain. The space enclosed by the removable gate and the nearest wall is packed with granular materials.

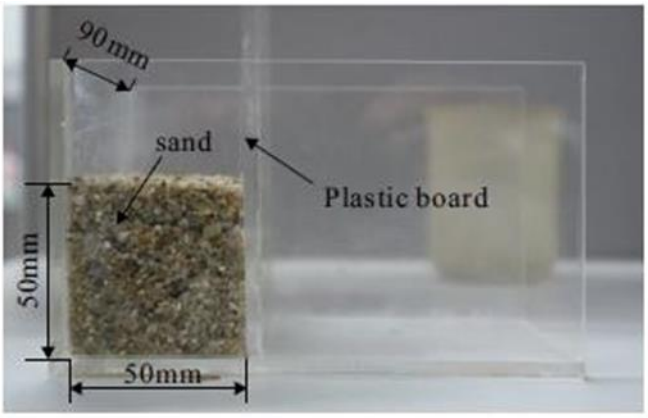

Figure 3.6 Experimental configuration Shi, Zhang and Zhang, (2018)

Table 3.1 Parameters considered for simulation of experimental work by Shi, Zhang and Zhang, (2018).

Parameters	**Value**
Particle Density (kg/m^3)	1450
Mean grain diameter (m)	0.0021
Young's modulus (MPa)	2.6
Poisson's ratio	0.31
Internal friction angle (deg)	35
Cohesion (MPa)	0

A loose granular column is generated with an initial column height (Hi) and initial column width (Li) as shown in Figure 3.6. The friction coefficient of the wall surfaces is kept constant and same as that of the particles. By this way, every particles experience the same amount of friction. After the generation of the particles with specified size, gravity is applied to the particles which make the particles to settle down by gravity and form a dense granular column similar to the natural deposit. Once the particles settle down properly and attain a static state, the gate is released immediately to initiate the column of granular particles collapses over a

rigid horizontal surface. The effect of resistance imposed by the lateral walls on the granular flow are reported as very small by Mangeney *et al.*, (2010). When the particles come to rest, the final run-out distance (Lf) covered by the granular deposit and final granular height (Hf) is found. As proposed by Zenit, (2005), the outermost edge of the deposit is the point where majority of the flowing materials are in contact with each other. This idea neglects the position of loose materials that are jumping out of the flow. The configuration of numerical model used in this research is based on a granular column collapse model as proposed by Lube *et al.*, (2005). The particles fall downwards followed by progressive sliding and deposition after reaching a static state. The run-out distance is measured along the x-direction.

Figure 3.7 gives the validation of the model used in this study with rigid bed using the experimental results of Shi, Zhang and Zhang, (2018). It shows the run-out distance covered by the failed granular mass at specific time intervals of 40ms, 80ms, 160ms and 320ms respectively. The values obtained through numerical simulations using DEM are in close agreement with the experimental results. The relation between normalized run-out lengths and aspect ratios is shown in Figure 3.8 in which the results presented by different researchers on the granular column collapse model on erodible bed are plotted along with the numerical results obtained from the present study. The solid line represents the numerical results of the present study. It is found that the results obtained in this study were in near agreement with the experimental observation of Lube *et al.* (2005), numerical analysis using 2D finite element method by Crosta, Imposimato and Roddeman, (2009) and 3D DEM analysis of Zhao, (2014).

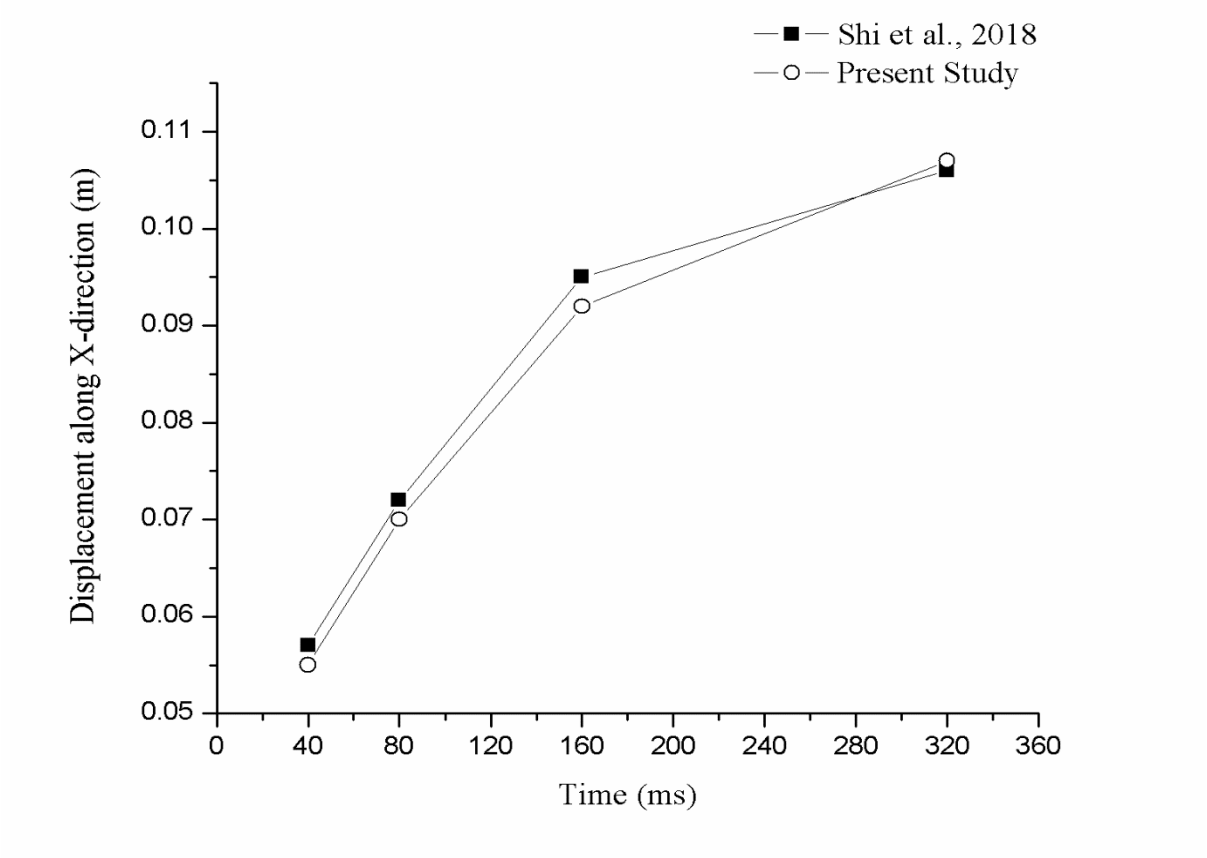

Figure 3.7 Validation graph comparing the experimental results by Shi *et al.* 2018 and numerical results obtained through simulations in DEM.

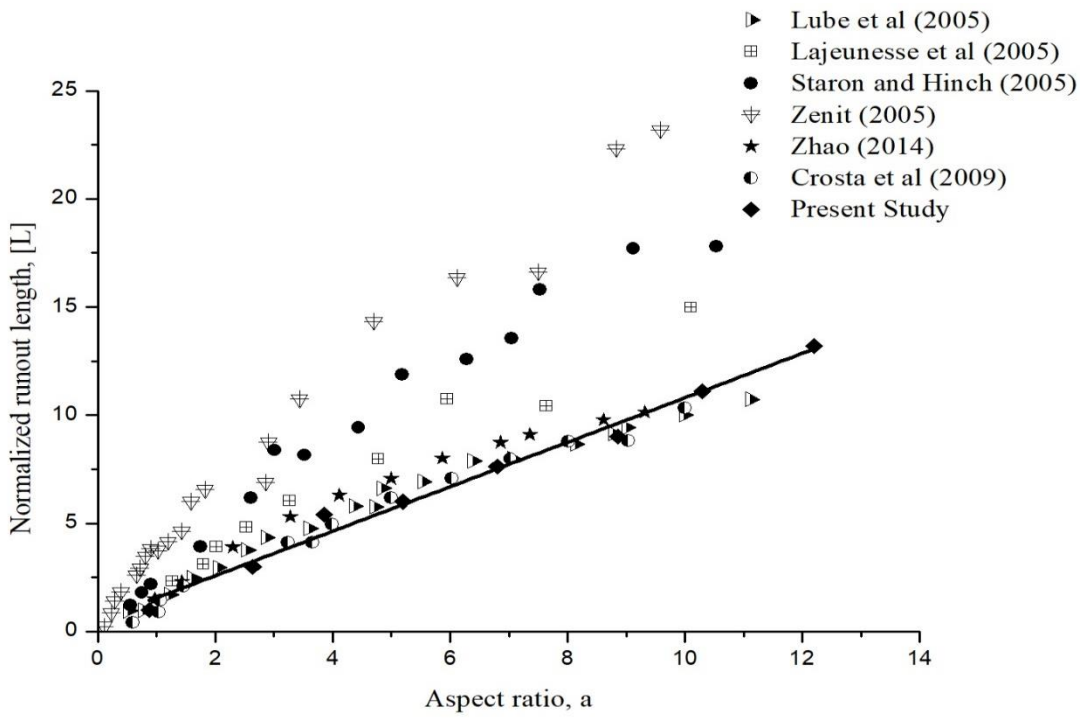

Figure 3.8 Relationship between aspect ratio and normalized run-out length.

3.3.2 Granular Column Collapse with Erodible Layer

The granular column model used in the present study is shown in Figure 3.9. Particles are modelled as spheres with six degrees of freedom and with a particle density of 2650 kg/m3. Particles are allowed to settle down by gravity to form a granular column which is bounded at one side by a confining gate. Spherical particles of diameter 3 mm are randomly distributed inside the prismatic granular column. As soon as the granular particles attain a static state after settling down, the confining gate is released immediately causing the granular column to collapse under gravity and the granular mass flows till it attains a state of rest. Ionescu et al (2015) have reported that the velocity at which the gate is opened can affect the spreading of the flow, but has no effect on the final deposit. In the present work, the effect of gate opening is not considered and the gate is completely opened at once in all the simulations. The flow pattern is initiated by the vertical fall of the particles followed by lateral spreading over the erodible bed and terminates by deceleration and attaining a state of rest. Simulations were carried out with rigid (non-erodible) bed also for comparison. The rigid bed is made smooth by eliminating the friction effects of the boundary.

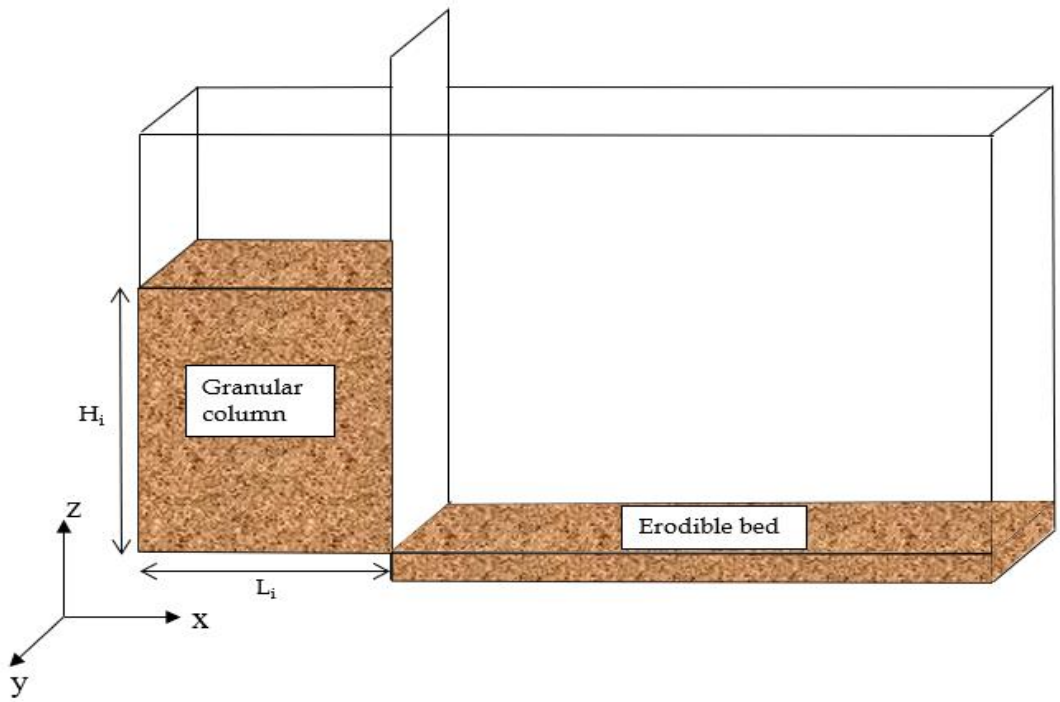

Figure 3.9 Granular column collapse model with erodible bed as its horizontal spreading surface.

The input parameters used in the granular column collapse model are given in Table 3.2. Particles in the erodible bed have similar properties as those present in the granular column. In this study, rolling friction is not considered to achieve maximum run-out distance possible. Mangeney *et al.*, (2010) employed an erodible bed of 300 cm length, 10 cm width and 1.4 mm to 6.5 mm thickness for horizontal bed. The erodible bed used by Farin *et al.* (2014) was 8 mm thick for a channel width of 10 cm and 1mm - 6 mm thick for a channel width of 20 cm with the bed slope varying from 24.4° to 31°. The erodible bed taken in this study was 20 cm in length, 10 mm thick and 3 cm wide. Two different regions were created in the model for different values of material properties required to be assigned for the boundary wall and the bed. The neighbour list was created such that the interaction force at the contact between the particles does not influence the particles present farther from the contact. The time-step size in the simulation was taken as 10-5 sec which was sufficiently small to eliminate the truncation error due to integration and greater than the critical value required to maintain the stability of the system. The magnitude and direction of gravity were given in such a way that the granular column collapses by gravity. The output from LIGGGHTS was processed using the visualization software Paraview V5.0 (Ayachit, 2015).

Table 3.2 Input parameters used in the present study

Sl. No.	**Parameters**	**Values**
1.	Initial column height (H_i), m	Varies
2.	Initial column length (L_i), m	0.5
3.	Aspect ratio ($a = H_i/L_i$)	Varies
4.	Young's modulus (E), N/m^2	5×10^7
5.	Poisson ratio	0.4
6.	Friction coefficient	0.6

7.	Particle diameter (D), mm	3
8.	Packing porosity (n)	0.43
9.	Particle density (ρ), kg/m^3	2650
10.	Gravity (g), m/s^2	-9.81
11.	Timestep interval, s	10^{-5}

3.4 Results and Discussions

Analysis of run-out distance in granular column collapse is one of the important parameters of interest as it is related to the extent of area affected by the granular flow. Granular columns of four different aspect ratios were considered in the study (0.88, 2.64, 5.2 and 8.86). Figure 3.10 presents the simulation results pertaining to the evolution of particle flow velocity of granular column of aspect ratio 5.2 at different normalized time [T]. Normalized time interval is given by $[T] = \frac{t}{\sqrt{H_i/g}}$ (where t = flow duration; H_i = initial column height; g = acceleration due to gravity). The evolution begins with initial wedge failure followed by horizontal spreading and ends with deposition, in a similar manner as obtained by other researchers like Lube *et al.*, 2005, Lajeunesse *et al.*, 2005, Crosta, Imposimato and Roddeman, 2009).

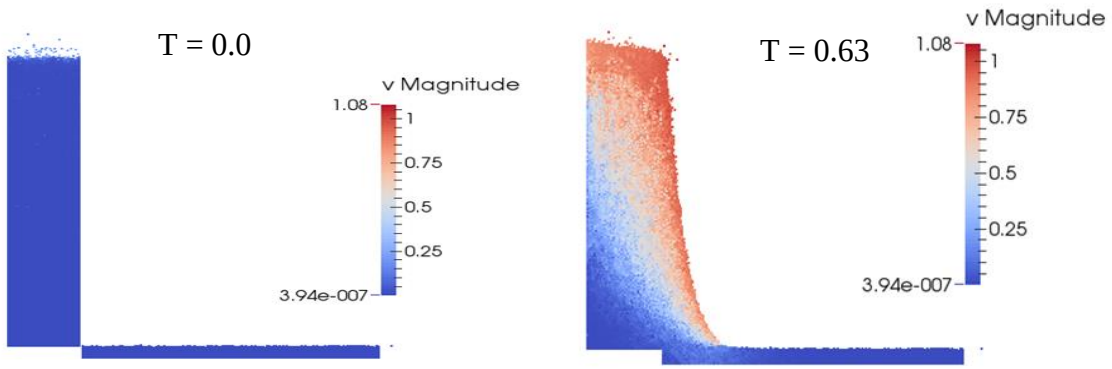

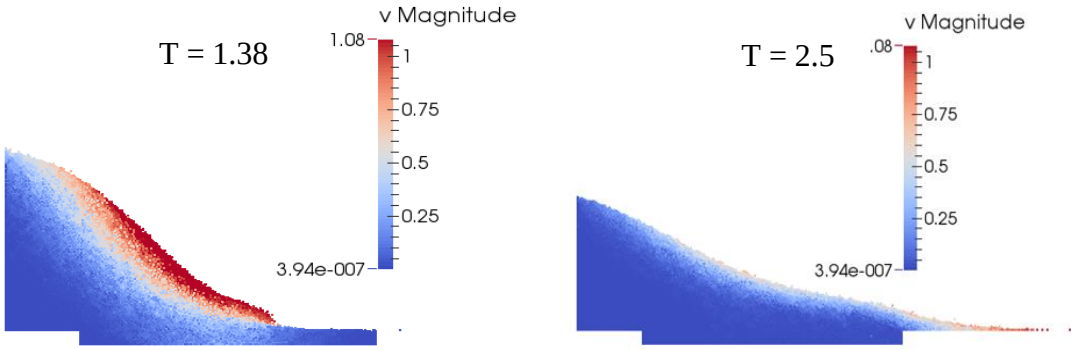

Figure 3.10 Evolution of particle flow velocity (in m/s) at different normalized time [T] throughout the simulation for the aspect ratio = 5.2.

Figure 3.11 shows the variation of run-out length with different aspect ratios for both cases with rigid bed and with erodible bed. For a specific width of granular column, increase in the aspect ratio is found to increase the final run-out length of the failure mass (Crosta *et al.*, 2009). Numerical simulation of CEL by Crosta, Imposimato and Roddeman, (2009) and Multilayer Shallow Model (MSM) by Fernández-Nieto *et al.*, (2016) showed a decrease in run-out distance in the presence of an erodible bed. On the other hand, in accordance with Sovilla, Burlando and Bartelt, (2006) entrainment can decrease or increase the run-out length of the failure mass depending on the amount of material entrained. Figure 3.11 shows that for smaller aspect ratios (less than 3), the change in the run-out distance with erodible layer is not very significant but there is a significant increase in the run-out distance as compared to rigid bed for larger aspect ratios (greater than 3).

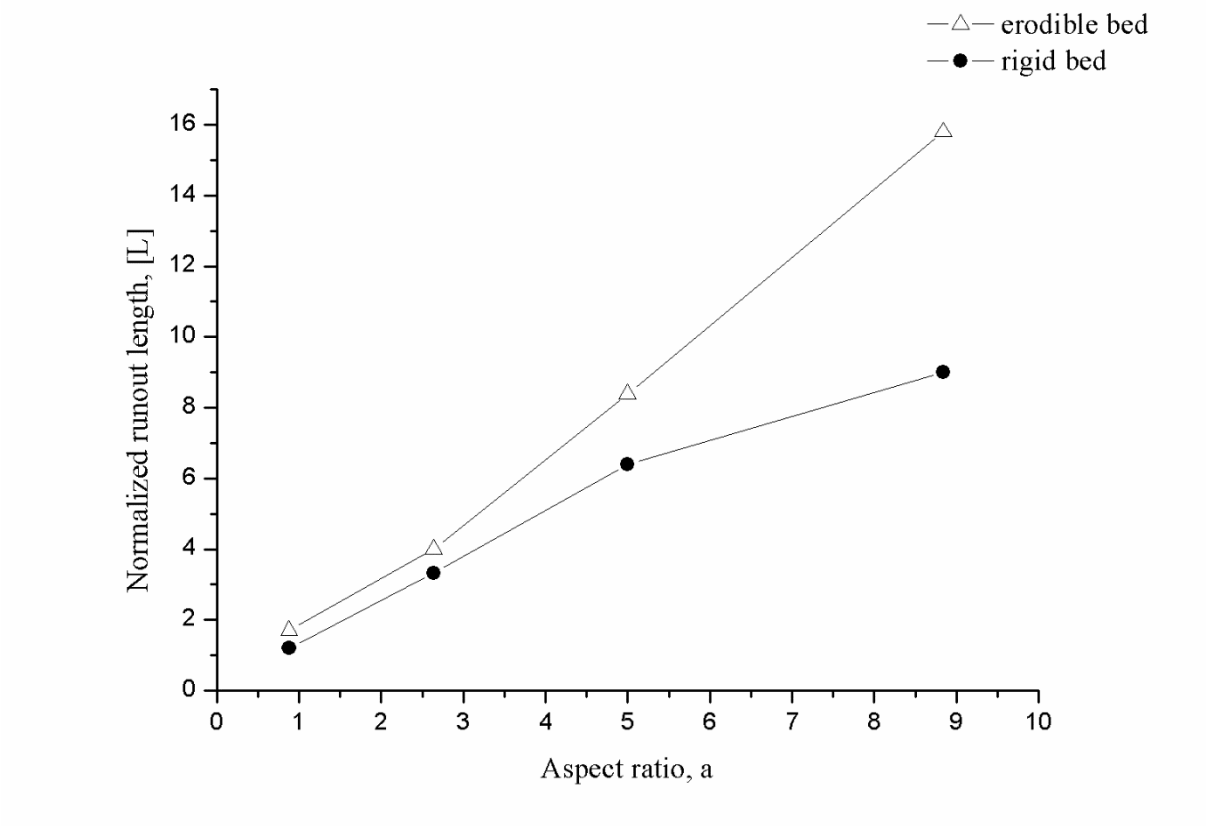

Figure 3.11 Run-out length variation for different aspect ratios in erodible and rigid bed condition.

The coordination number has been recognised as an important variable to study soil failure (Thornton 2000). The coordination number of a particle is the number of contacts established with neighbouring particles. It is given by $\bar{C} = \frac{1}{N_p}\sum_{i=1}^{N_p} C_i$ (C_i = number of contacts for a single particle; N_p = number of particles). It is possible to identify the distribution of particles during the flow by tracking the coordination number. Figures 3.12.a and 3.12.b show the evolution of bulk coordination number of granular columns of four different aspect ratios (0.88, 2.64, 5.2 and 8.86) at every normalized time interval of [T] = 0.5, with and without erodible bed respectively. At T = 0, the granular particles are in contact with each other with the prescribed initial packing density, which is symbolised by the bulk coordination number prior to the collapse of granular columns. As soon as the confining gate is opened, the coordination number of the granular system reduces to a minimum value, at which time the particles are barely in contact with each other and then the coordination number gradually increases with time. The entrained particles increase the density of the failure mass, which is shown by increase in overall coordination number of the system.

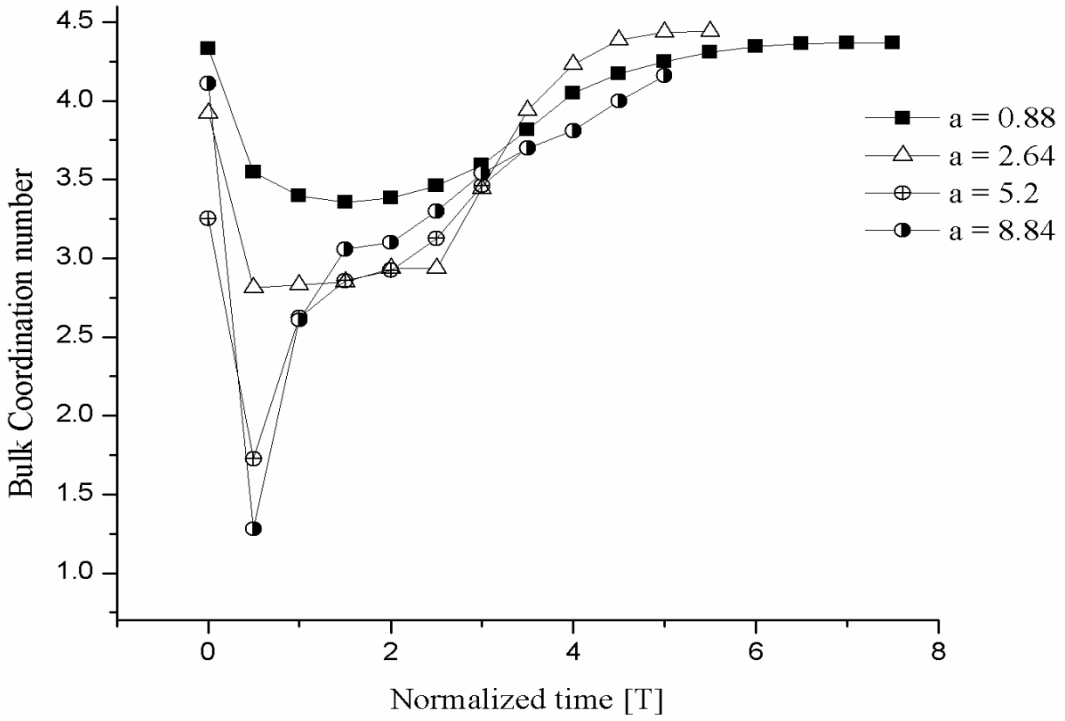

(a) With erodible bed.

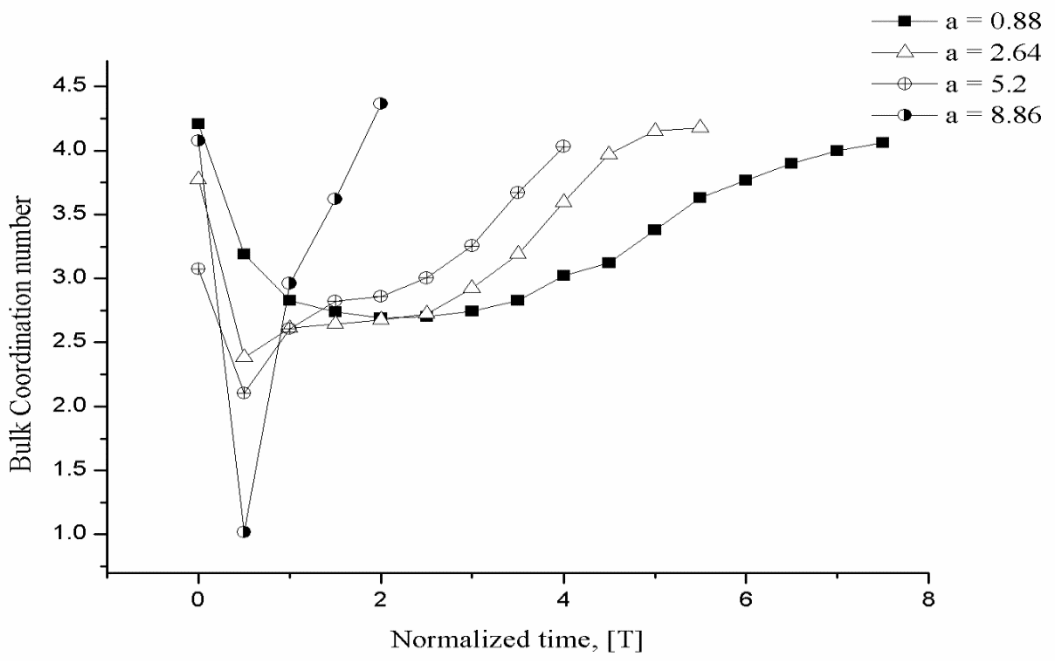

(b) With rigid bed

Figure 3.12 Variation of coordination number of the system at normalized time interval

Evolution of the coordination number during the collapse of granular column is also related to the kinetic energy of the system (Zhao, 2014). After the release of the confining gate, the granular column collapses and the particles fall under gravity undergoing a gradual dynamic motion to reach a static state. With an increase in the aspect ratio, there exists acceleration in the dynamic movement of the particles before attaining a static granular deposit. This is manifested by the gradually varying coordination number for columns of smaller aspect ratio whereas it takes sharp turns for larger aspect ratios. It is due to the fact that the kinetic energy is released gradually at a gentle rate in the case of lower aspect ratios, while there is rapid release in the case of granular columns with large aspect ratios. It is evident that the minimum coordination number attained by the system is comparatively lower in erodible bed condition than in rigid bed. The point showing the minimum value of bulk coordination number of the system represents the occurrence of maximum kinetic energy of the system. Hence, the system with erodible bed witnesses the maximum value of kinetic energy than the one with rigid bed. Soon after the incidence of maximum kinetic energy of the system, the granular flow gradually slows down reaching a relatively denser state at a coordination number of around 4. Therefore, it can be inferred that the collapse of a granular column on an erodible bed results in thicker final deposits.

Figure 3.13 shows the comparison of bulk coordination number evolution for both erodible and rigid bed conditions. Granular flow comprises collision, rolling and sliding. The mechanism of collision is predominant in the case of columns of larger aspect ratios (greater than 3) which is evident with the occurrence of maximum kinetic energy. For smaller aspect ratios (fewer than 3), rolling and sliding mechanism is predominant which is shown by gradual variation in curves. The variation is quite rapid for larger aspect ratios. It can be seen that the curve showing the bulk coordination number of the granular system with erodible bed always stays above the one with rigid bed due to the entrainment of particles from the erodible bed into the granular flow. Since the bulk coordination number represents the density of the system, it is inferred that particle entrainment into the granular flow increases the density of the final flow deposits. Irrespective of the presence of erodible layer, the curves follow similar pattern of evolution for a specific aspect ratio.

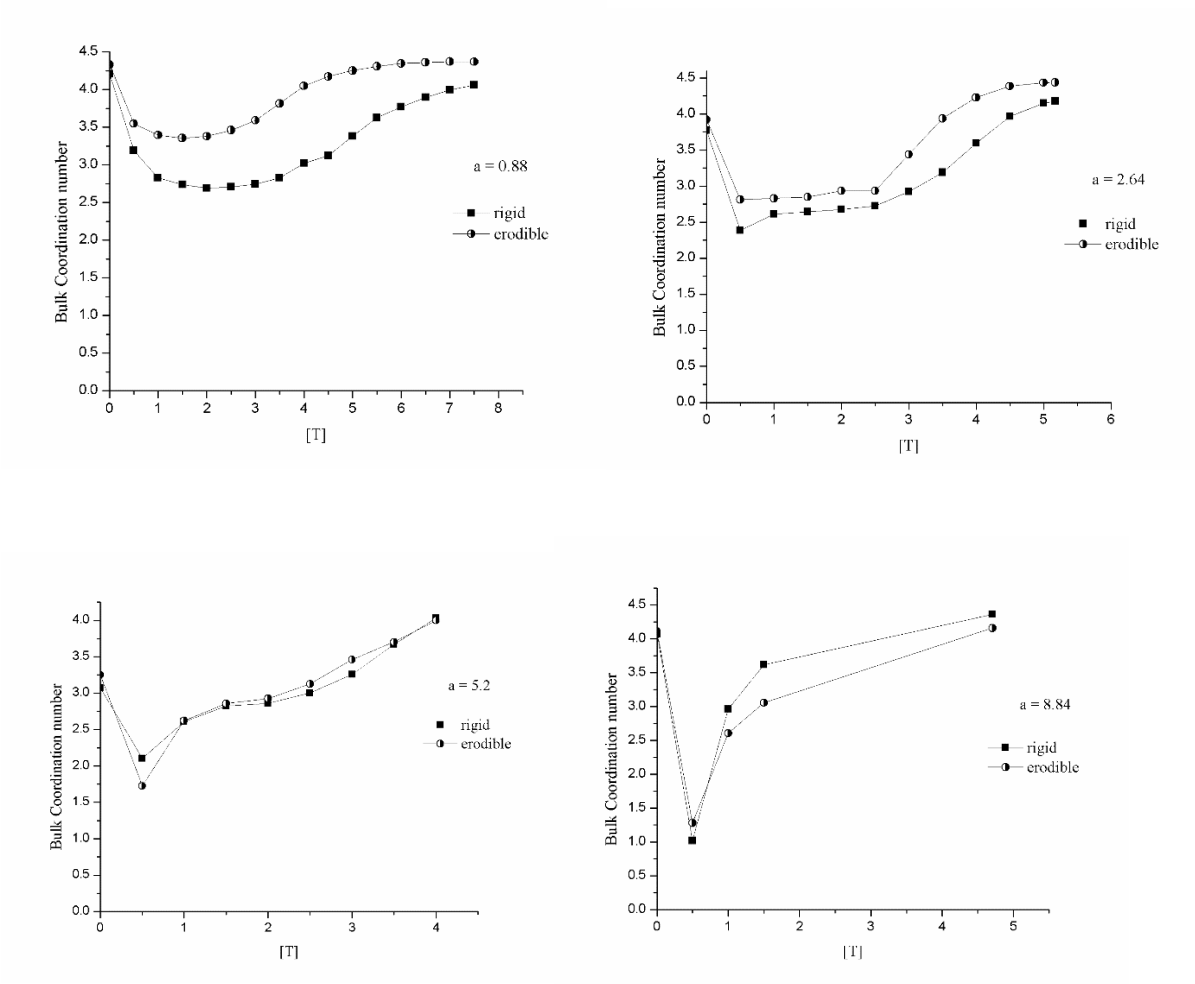

Figure 3.13 Comparison of bulk coordination number for granular column of same aspect ratio with erodible bed and with rigid bed.

In three-dimensional space, the particles undergo both translation and rotation. By taking into account both translational and rotational velocity, the kinetic energy of the granular system is expressed as $E_{k=}\frac{1}{2}\sum(m_i v_i^2 + I_i \omega_i^2)$, where *i* denotes the number of particles included in the system, m_i is the mass of an individual particle, v_i and ω_i are the translational and rotational velocity of a particle with I_i as its moment of inertia respectively $I = \frac{2}{5}mR^2$. The potential energy of the static granular pile is given as: $E_p = \sum m_i gH_i$ where *g* is the acceleration due to gravity and H_i is the height of individual particle in the domain. When the column of particles begins to collapse, the potential energy is converted into kinetic energy and some energy is dissipated. By the law of conservation of momentum, energy dissipation is calculated as $E_{diss}= E_0- E_p- E_k$ where E_0 is the total energy of the granular system, which equals the potential energy of the granular assembly at [T] = 0. In the granular column collapse model with erodible bed, maximum kinetic energy is reached by the column of aspect ratio 8.86 at around [T] = 1. The kinetic energy peak shifts to a higher value due to the presence of loose deposits in the spreading surface of failure mass with a comparatively lower

value under rigid bed condition. From Figures 3.14.a and 3.14.b, it is evident that the intensity of kinetic energy is more in the model with erodible bed and also the kinetic energy increases with increase in the aspect ratio.

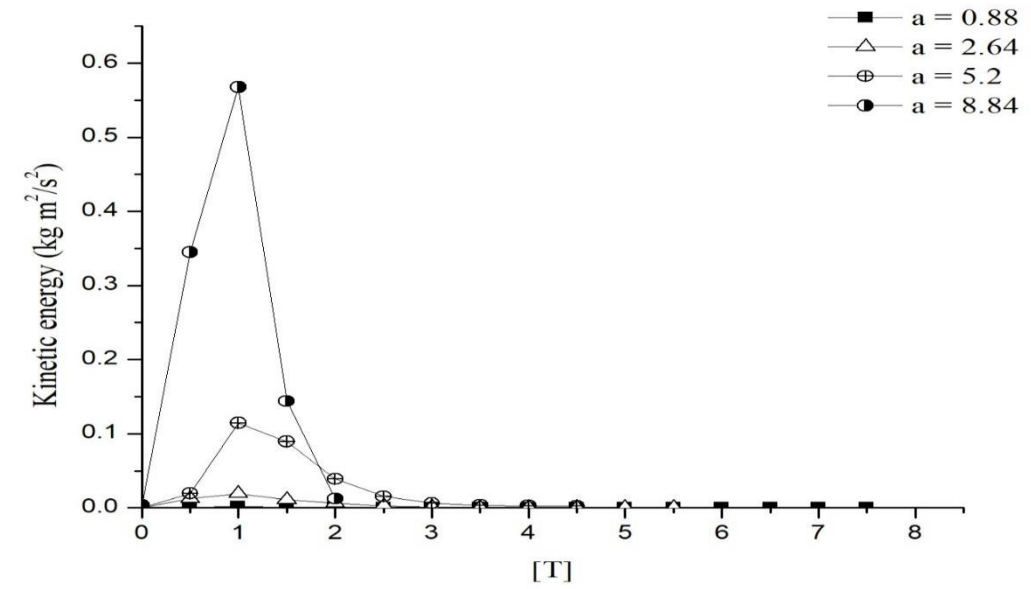

a. with erodible bed as the spreading surface

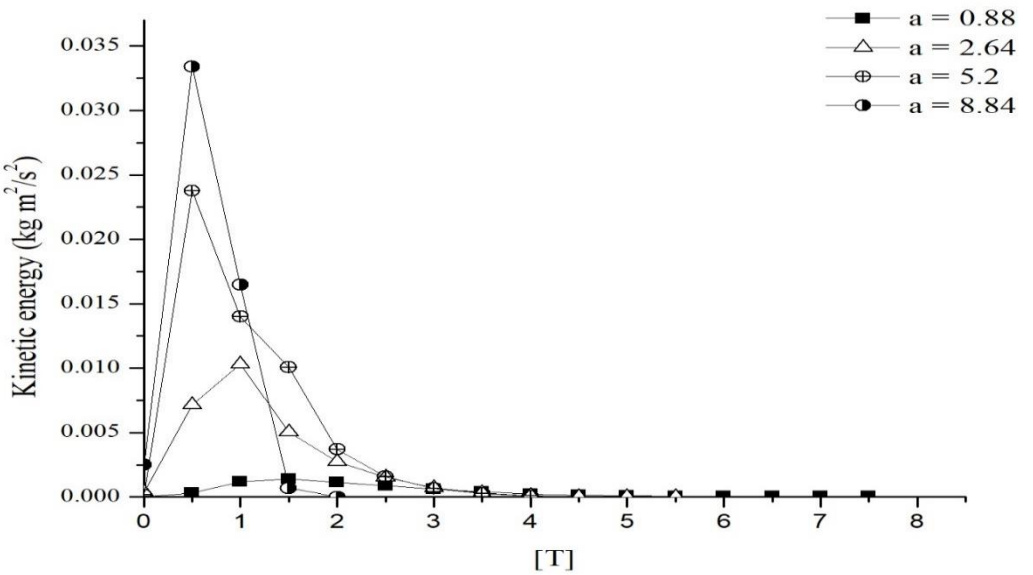

b. with rigid bed as the spreading surface

Figure 3.14 Evolution of kinetic energy during the collapse of column at a normalised time interval of 0.5

Figures 3.15.a to 3.15.d shows the energy curves normalized by the total energy of the system at time interval [T] = 0.5. The potential energy curve is found to shift upwards with an increase in aspect ratio with the dissipation curve getting shifted towards the bottom. The peak point of the kinetic energy curve normalized by the total energy is found to be moving upwards in a progressive manner. These curves show the evolution of energy in the system from the beginning of the simulation when all the particles in the system are at rest at T = 0 till the granular flow deposits hinder the motion. At T = 0, the potential energy of the system is at its maximum with kinetic and dissipated energy around zero. When the gate confining the granular particles is released, the potential energy of the system starts decreasing, converting some of its form into kinetic energy and dissipating the rest. During granular flow, the energy dissipation at particle level is primarily due to particle friction. It can be inferred that the potential energy of the granular system is higher for higher aspect ratios since the magnitude of vertical position of the particles increases accordingly. This simultaneously increases the dissipation as well as kinetic energy which is higher than that of kinetic energy in rigid bed condition. This rise in kinetic energy influences the final run-out length and flow duration time, thereby justifying the increased run-out length in comparison with that of the rigid bed condition.

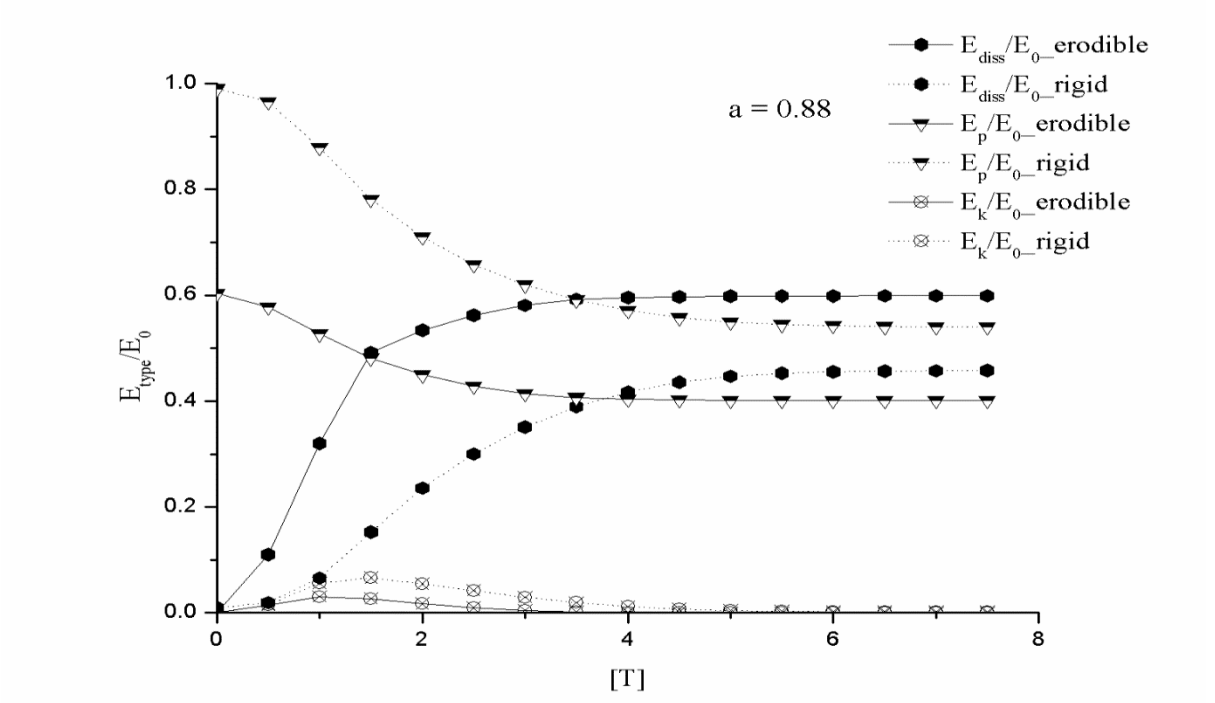

a

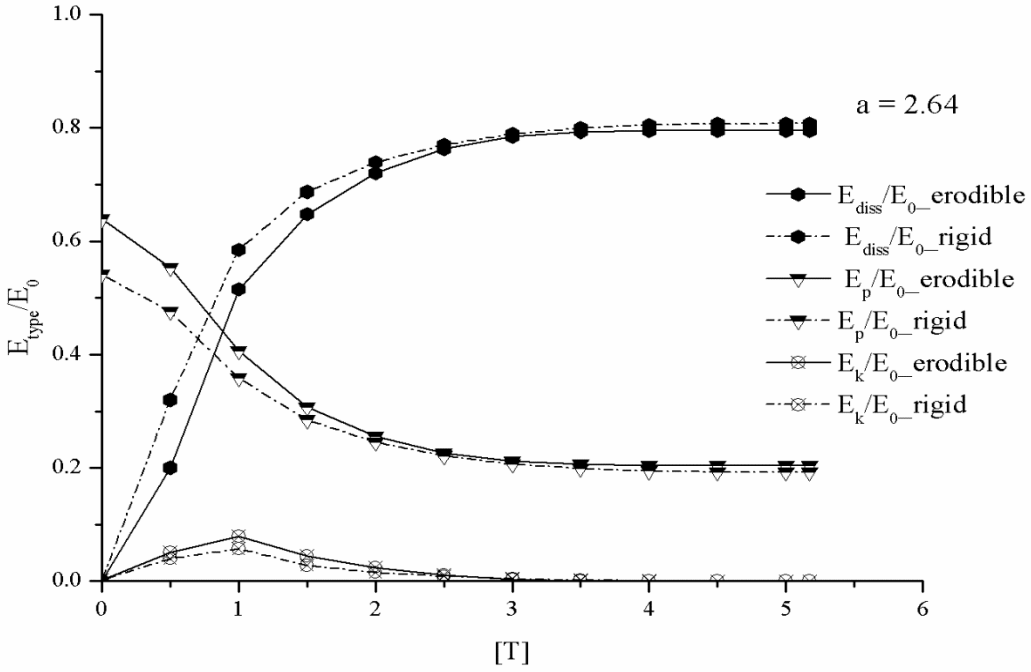
a = 2.64
E_{diss}/E_{0-}_erodible
E_{diss}/E_{0-}_rigid
E_p/E_{0-}_erodible
E_p/E_{0-}_rigid
E_k/E_{0-}_erodible
E_k/E_{0-}_rigid
E_{type}/E_0
[T]

b

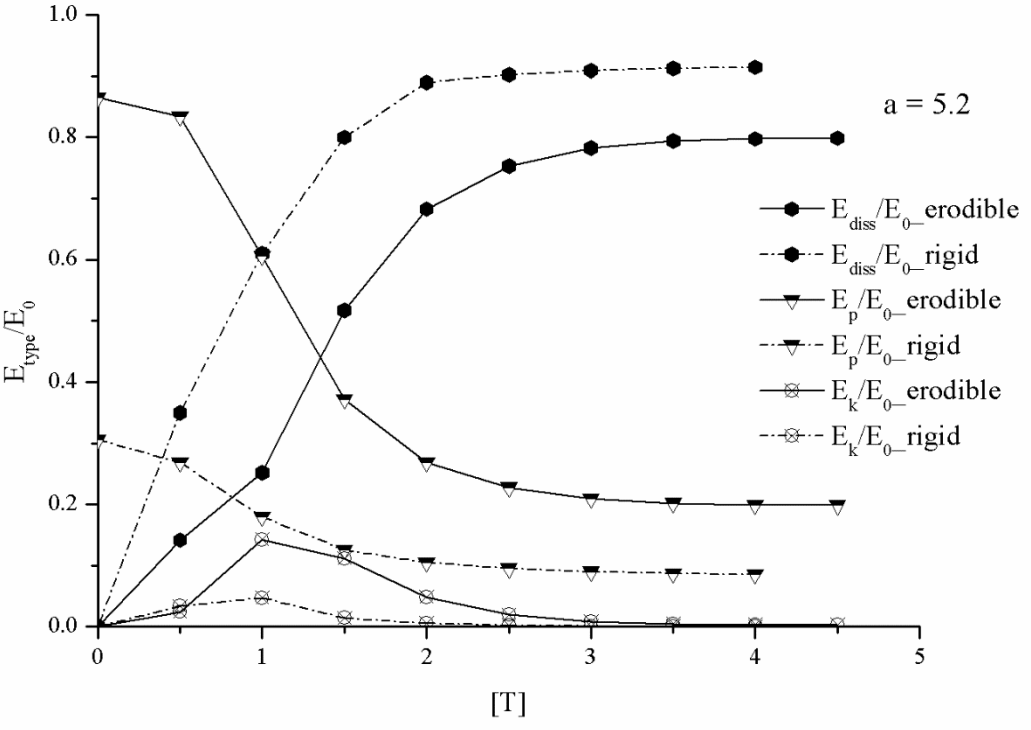
a = 5.2
E_{diss}/E_{0-}_erodible
E_{diss}/E_{0-}_rigid
E_p/E_{0-}_erodible
E_p/E_{0-}_rigid
E_k/E_{0-}_erodible
E_k/E_{0-}_rigid
E_{type}/E_0
[T]

c

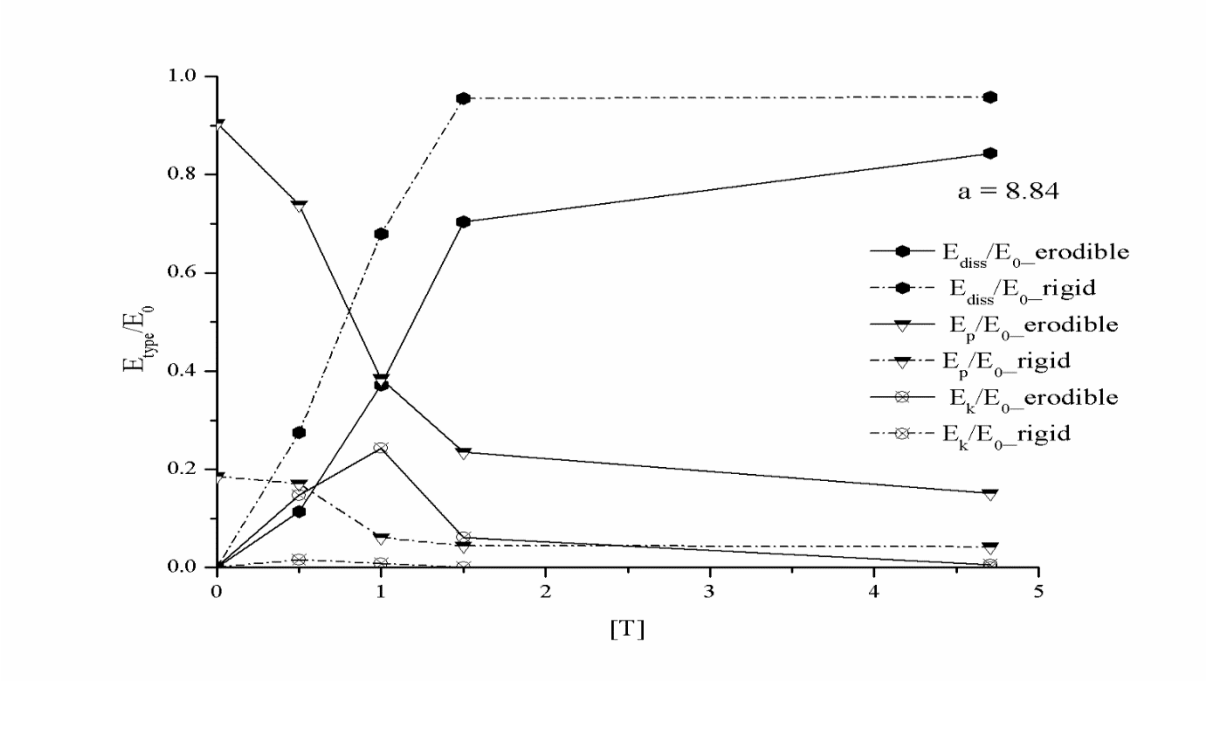

d

Figure 3.15 Evolution of energy components during the column collapse with erodible bed and rigid bed for (a) a = 0.88, (b) a = 2.64, (c) a = 5.2, (d) a = 8.84

Figure 3.16 gives a comparison of dissipated energy normalized with the total energy for the cases of flow through rigid and erodible bed, for columns with different aspect ratios. From the results observed, it is observed that dissipation energy of granular flow increases with aspect ratio. In the presence of erodible layer, the conversion of potential energy to kinetic energy increased rather than getting dissipated. Similar results are also reported by previous researcher like Utili, Zhao and Houlsby, (2015).

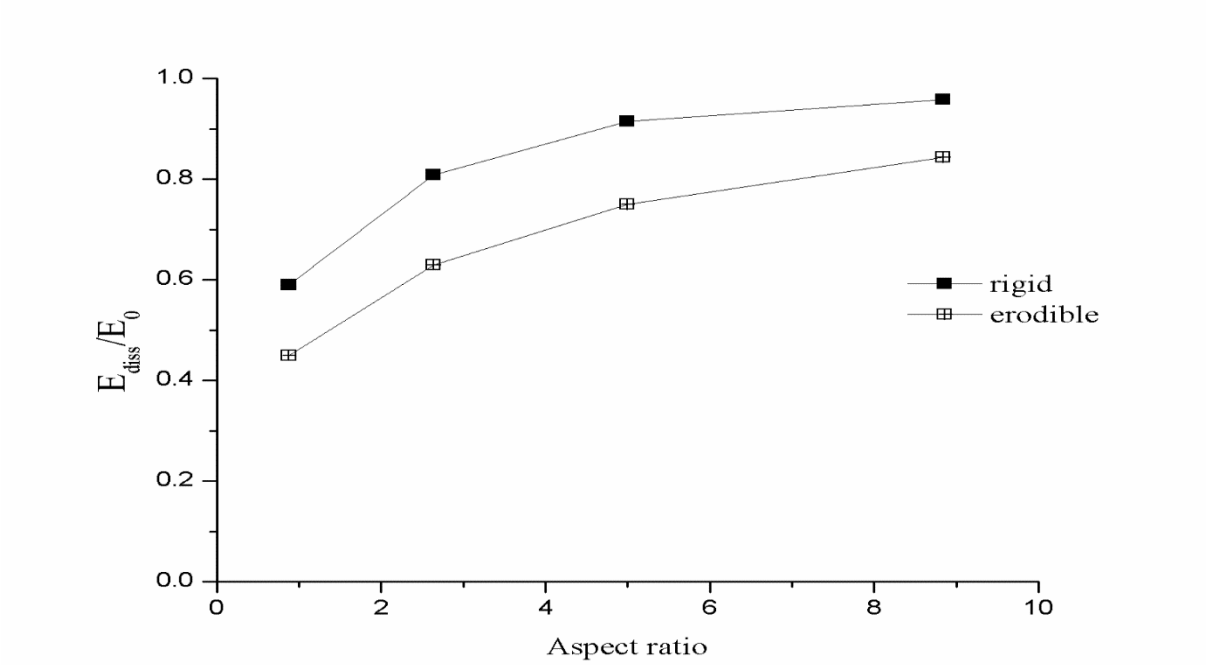

Figure 3.16 Total energy dissipated at the end of column collapse for different aspect ratios and comparison with no erodible condition.

The evolution of normalized mean flow velocity is given by $[V] = \frac{V}{\sqrt{gH_i}}$ (where V is flow velocity; g = acceleration due to gravity; H_i = initial column height) is shown in the Figure 3.17.a and Figure 3.17.b for different aspect ratios in both erodible and no erodible bed cases. Increase in aspect ratio of the granular column leads to remarkable increase in the flow velocity of the granular particles. For aspect ratios of 0.88 and 2.64, greater velocities were experienced by the particles in rigid bed condition than the ones in erodible bed condition. This denotes that the columns of smaller aspect ratios suffer a hindrance in velocity due to the presence of erodible layer. For the granular columns of larger aspect ratios (5.2 and 8.86), particles experience lower velocity in rigid bed condition with comparatively higher velocity in erodible bed condition. The force of impact given by the higher aspect ratio columns causes frontal ploughing thereby making the granular particles in the erodible bed get entrained in the granular flow, leading to greater flow velocity with increased run-out distance and flow duration time. Figure 3.18 shows the comparison of particle flow velocity with and without erodible bed for different aspect ratios (0.88, 2.64, 5.2 and 8.84). The model with erodible bed witnesses comparatively higher velocity and kinetic energy due to the mechanism of collision prevailing during the flow of failure mass.

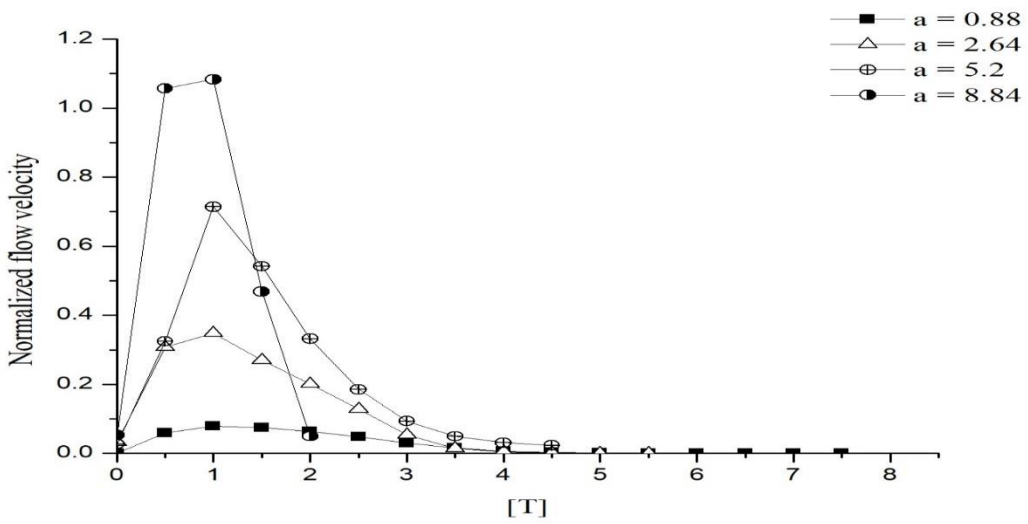

a. with loose particles present along the flow path.

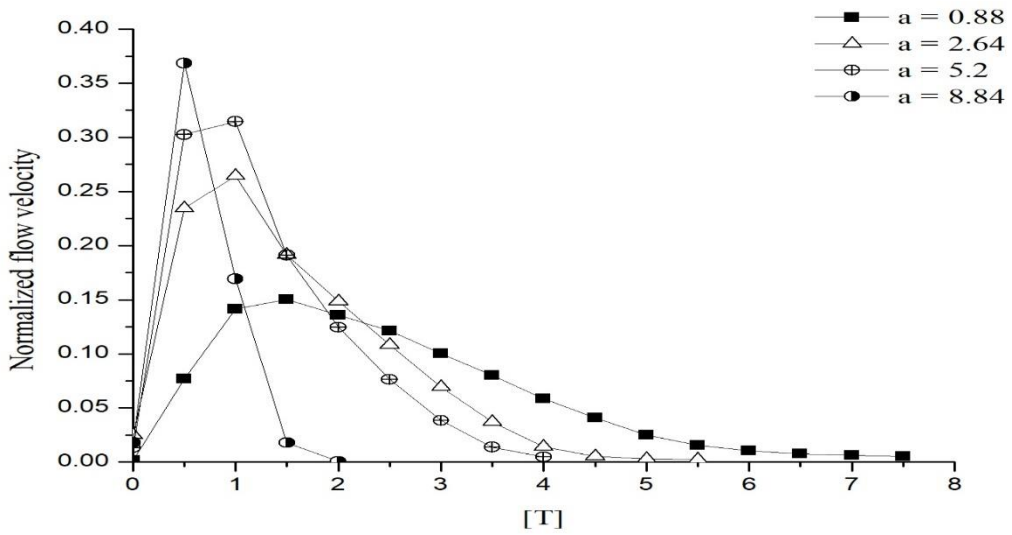

b with rigid bed present along the flow path.

Figure 3.17 Evolution of particle flow velocity throughout the simulation at a normalized time interval [T] = 0.5

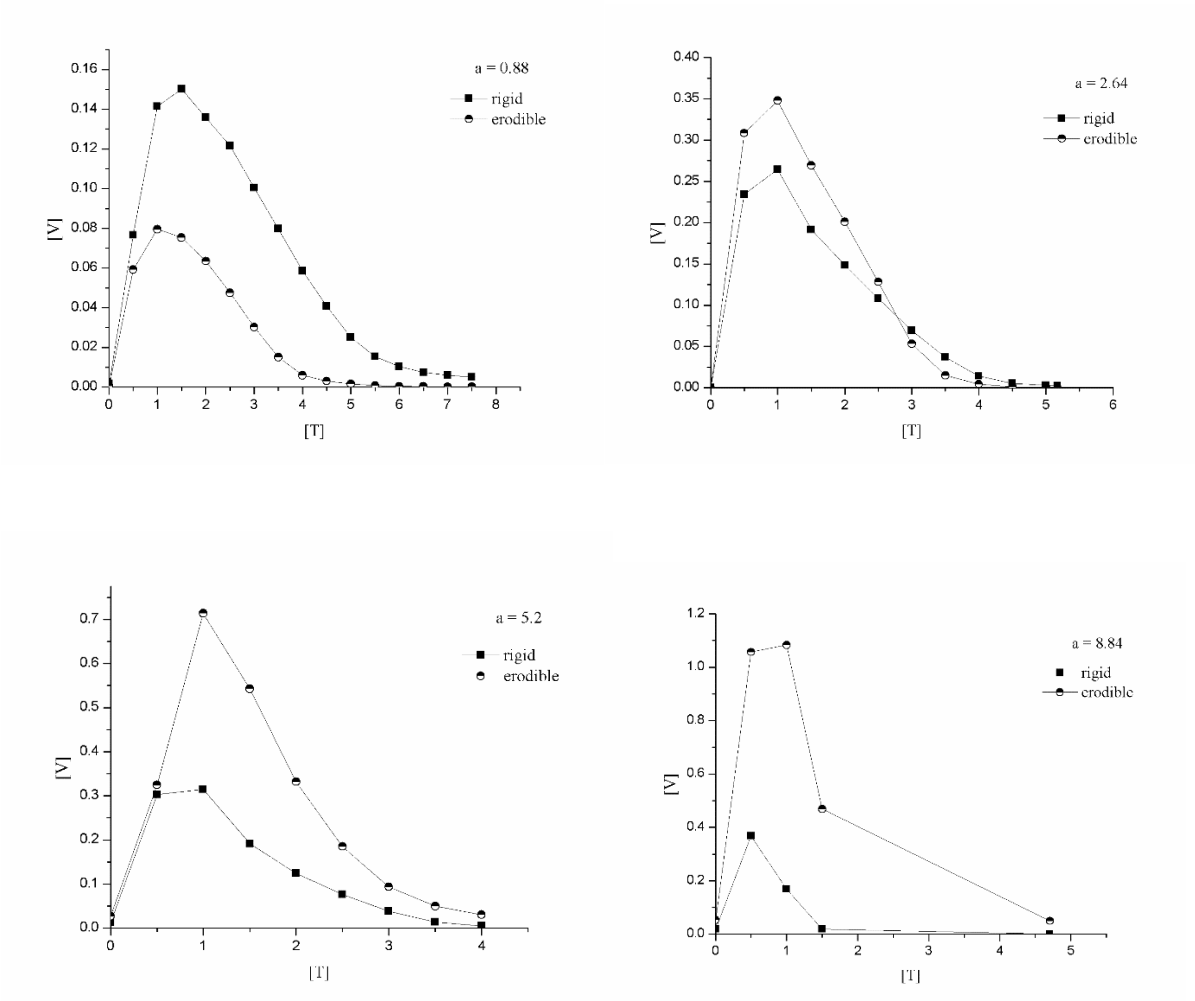

Figure 3.18 Evolution of particle flow velocity throughout the simulation with erodible bed and rigid bed

Chapter 4

Dynamic Modelling of Landslide Runout with Entrainment

This section, focusses on landslide initiation and propagation. The initiation and propagation phase of the landslide are dealt with separately. The combined hydrological and slope stability model is used to analyse transient pore water pressure and slope failure. The propagation phase is analysed with a dynamic runout model with entrainment for landslide case studies in Peringalam and Kaipalli.

4.1 Infiltration Model for Unsaturated Soil Slope Stability Analysis

Analysis of initiation of landslides is critical to identify the instabilities, risks and to propose suitable mitigation measures. A slope stability analysis typical to the region of study, ie. Western Ghats of Kerala, India is explored. First, the hydrological model is established, which provides pore pressure variations with depth and time, and then the slope stability model is implemented. Output obtained from hydrological model is given as input to stability model and thereby a combined model which gives Factor of Safety is obtained.

The physical process of rainfall infiltration and slope stability are investigated with couple analysis of Seep/w and Slope/w. If flow condition changes with time, then the flow is transient flow. Infiltration of rain water into unsaturated soil involves transient flow analysis. This transient flow of rainwater into the slope highly depends on soil water characteristic curve SWCC and hydraulic conductivity function. Seep/w uses Darcy's law for flow of water through unsaturated soil as well as saturated soil. The seepage in the slope is expressed with through the following partial differential water flow equation 4.1.

$$\frac{\partial}{\partial x}\left(k_x \frac{\partial H}{\partial x}\right)+\frac{\partial}{\partial y}\left(k_y \frac{\partial H}{\partial y}\right)+Q=\frac{\partial \theta}{\partial t} \qquad 4.1$$

Change in pore water pressure is related to change in volumetric water content. SWCC, saturated hydraulic conductivity, compressibility and saturated water content determined from laboratory test.

The deterministic analysis was performed to understand the effects of unsaturated soil properties, rainfall intensities, slope angle and duration in the stability of the slope. The study area was located in Vellathooval (N9.897036, E77.180949), Idukki district of Kerala. Historically this place recieves rainfall from June to August and October to November. The slope angles in that area varies from 30^o to 40^o and in certain places it was more than 40^o. S-valavu, in Vellathooval, Adimali area witnessed major landslides in 2018 Kerala flood. Seven people were killed with road network and buildings damaged severely. The infinite slope model used in this study is depicted in Figure 4.1. Field observation and laboratory test, soil properties and topographical data used in this analysis are listed in table 4.1

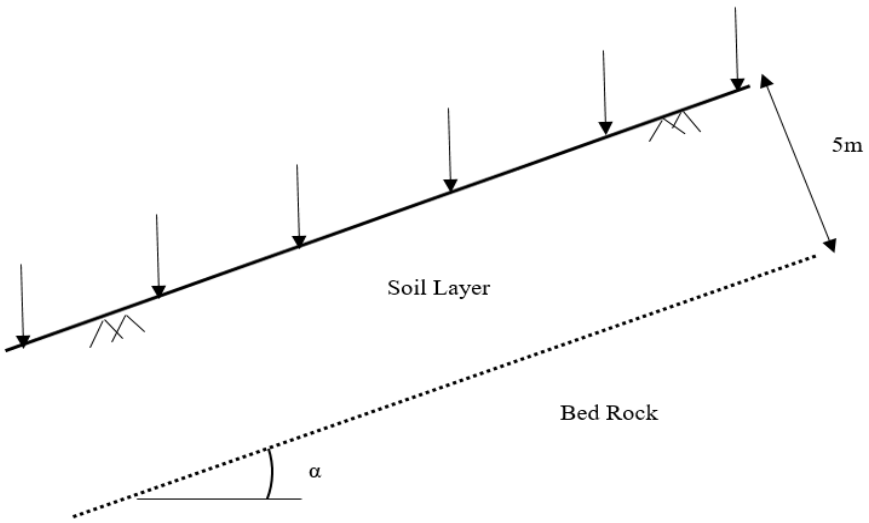

Figure 4.1 Infinite slope model

As shown in Figure 4.2, soil samples were taken from the site after which laboratory tests were carried out to measure the matric suction and the corresponding volumetric water content. SWCC for the study area is prepared with WP4 dew-point potentiometer which is commonly used in unsaturated soil. The basic principle of dew-point potentiometer is CMH (Chilled Mirror Hygrometer). The soil specimen is placed in the sensing sealed chamber and brought to vapor pressure equilibrium prior to cooling. The instrument is provided with an internal fan in the sample chamber to reduce the equilibrium time. Thermoelectric cooler controls the mirror temperature. The soil sample temperature in degree Celsius and water potential in kPa are automatically displayed on the screen. Figure 4.3 shows the suction measurement of the specimen using Dew point potentiometer. From experimental results, Fredlund and Xing (1994) model was used to fit the SWCC. For this purpose, SWRC-fit is used (Seki, 2007). SWCC used in this study is shown in Figure 4.4.

Figure 4.2 Field investigation and sample preparation for SWCC at Vellathooval, Idukki district of Kerala

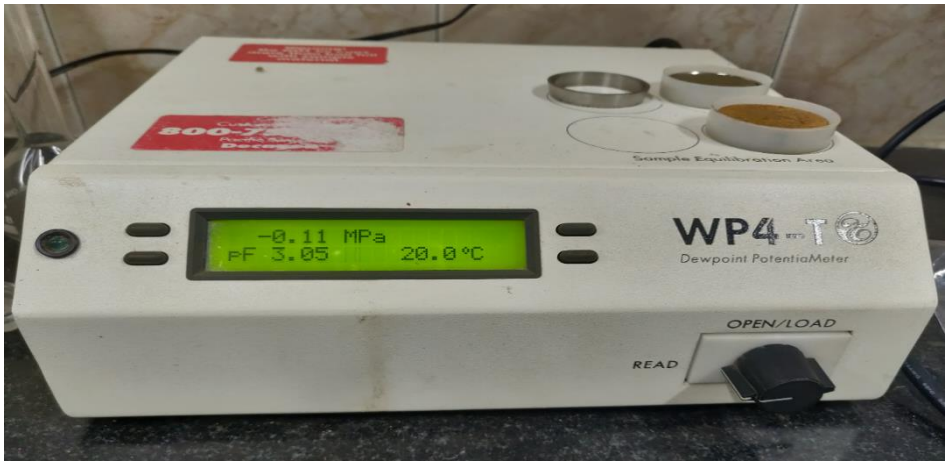

Figure 4.3 Suction measurement of the specimen using dew point potentiometer

Hydraulic conductivity function which reflects the ability to conduct water depends on the volumetric water content function. It is related to an amount of water in the soil and saturated hydraulic conductivity. If suction increases in soil, more pores will be filled with air and it makes difficult for the rainwater to infiltrate. This leads to decrease in hydraulic conductivity. Hydraulic conductivity function used in the present analysis is shown in Figure 4.5.

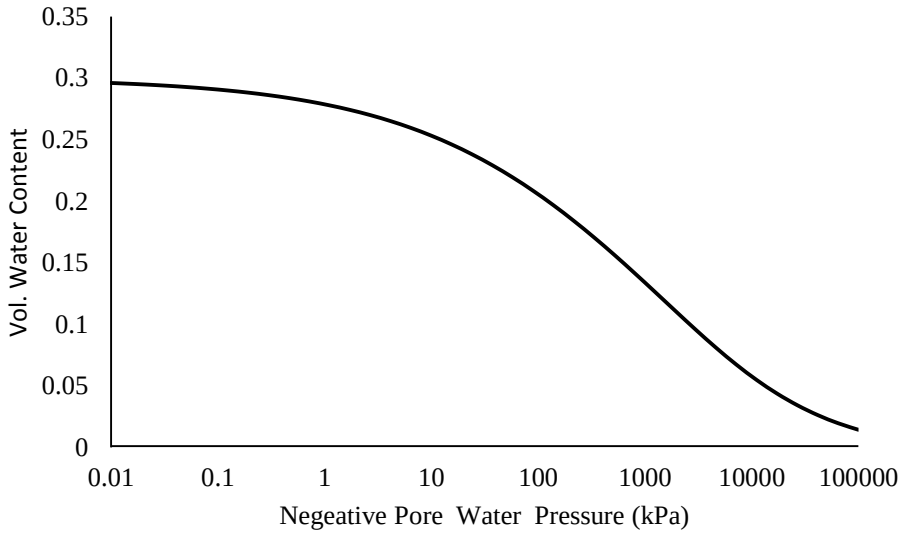

Figure 4.4 Soil Water Characteristic Curve used in seepage modelling

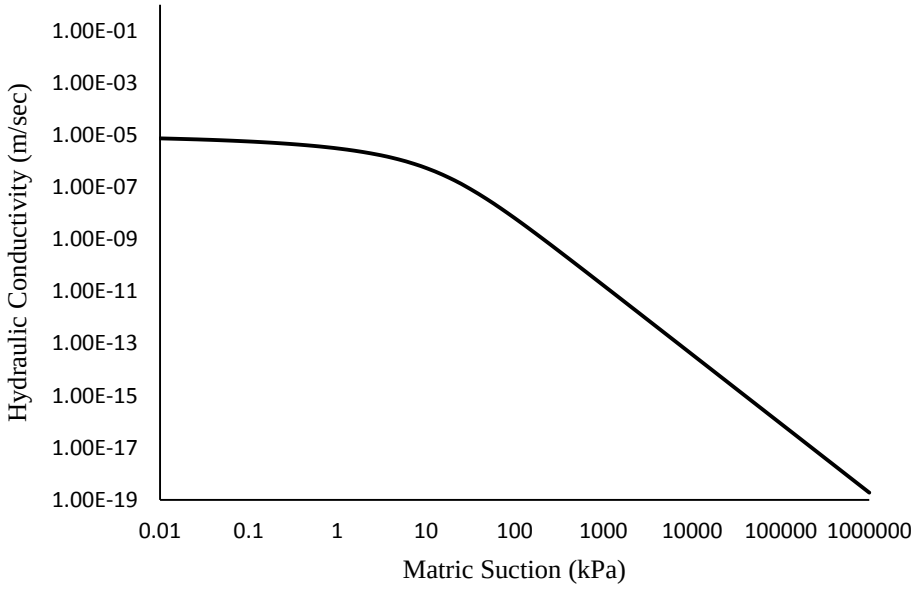

Figure 4.5 Hydraulic conductivity function used in seepage modelling

The ratio of intensity of rainfall to saturated hydraulic conductivity (k_{sat}) affects the wet front and degree of saturation. The rainfall intensity of 0.2 k_{sat}, 0.4 k_{sat} and 0.6k_{sat} was considered in the analysis. As mentioned earlier, rainfall intensity less than 0.2ksat was not enough to vanish the suction in the slope. Rainfall intensity of more than 0.6ksat, rainwater turns into runoff. So rainfall intensity of sensitive range 0.2k_{sat} to 0.6k_{sat} was considered in this analysis. Infiltration flux with potential seepage face is applied over the slope and null flux boundary is applied between the soil layer and bedrock. Variation of pore water pressure for a given rainfall intensities are evaluated against rainfall duration.

Pore water pressure profile obtained from Seep/w analysis is utilized to evaluate factor of safety for the slopes in Slope/w. Mohr-coulomb model and Bishop method (Bishop, 1959) are used to calculate stability by factor of safety. To overcome the uncertainties involved in the deterministic analysis, reliability analysis is performed to find probability of failure with respect to rainfall intensity and duration on the slopes. Reliability analysis will be useful to come over the limitations in deterministic analysis by Monto-Carlo simulation (Eckhardt, 1987; Fishman, 2013; Whitman, 2000).

4.2 Transient Pore Pressure Response and Slope stability Analysis

The variation of pore water pressure on the slopes, typical rainfall intensities of 0.2 k_{sat}, 0.4 k_{sat} and 0.6k_{sat} are applied on the slope sections of inclination 35^o, 40^o, and 45^o. The parameters used in the analysis are mentioned in Table 4.1.

Table 4.1 Results of laboratory and field investigation

Properties	**Value**
Unit density	16 kN/m^3
Cohesion	3 kPa
Angle of internal friction	27^o
Saturated hydraulic conductivity k_{sat}	1e-05 m/s
Compressibility	1e-05
Soil layer thickness	5 m
Slope angle, α	35^o,40^o, 45^o
Length of slope	90 m

By applying different rainfall intensities i.e. 0.2 k_{sat}, 0.4 k_{sat}, 0.6 k_{sat} on the slopes, variation of suction is observed at different sections of the slope namely X-X at crest, Y-Y at middle, and Z-Z at toe. These variation of pore water pressure along the depth of the slope is plotted for 35 ^{o}, 40 ^{o}, and 45 ^{o} at three sections X-X, Y-Y and Z-Z for rainfall duration. Change in factor of safety to the rainfall duration is plotted for varying rainfall intensity on the slopes.

4.2.1 Pore Water Pressure

Figure 4.6.a to Figure 4.6.i shows an evolution of pore water pressure of slope 35^o with respect to the rainfall along the depths of the slope for various rainfall intensities in different sections. At t=0, it is observed that pore water pressure is -750kpa at the crest. With increase in rainfall duration, pore water pressure also increases. It leads to decrease in effective shearing resistance and reduction in frictional forces between soil particles. The rate of dissipation of pore water pressure at the crest for various rainfall intensities is very low and negligible. Almost in all the cases, negative pore water pressure got disappeared after 14 days.

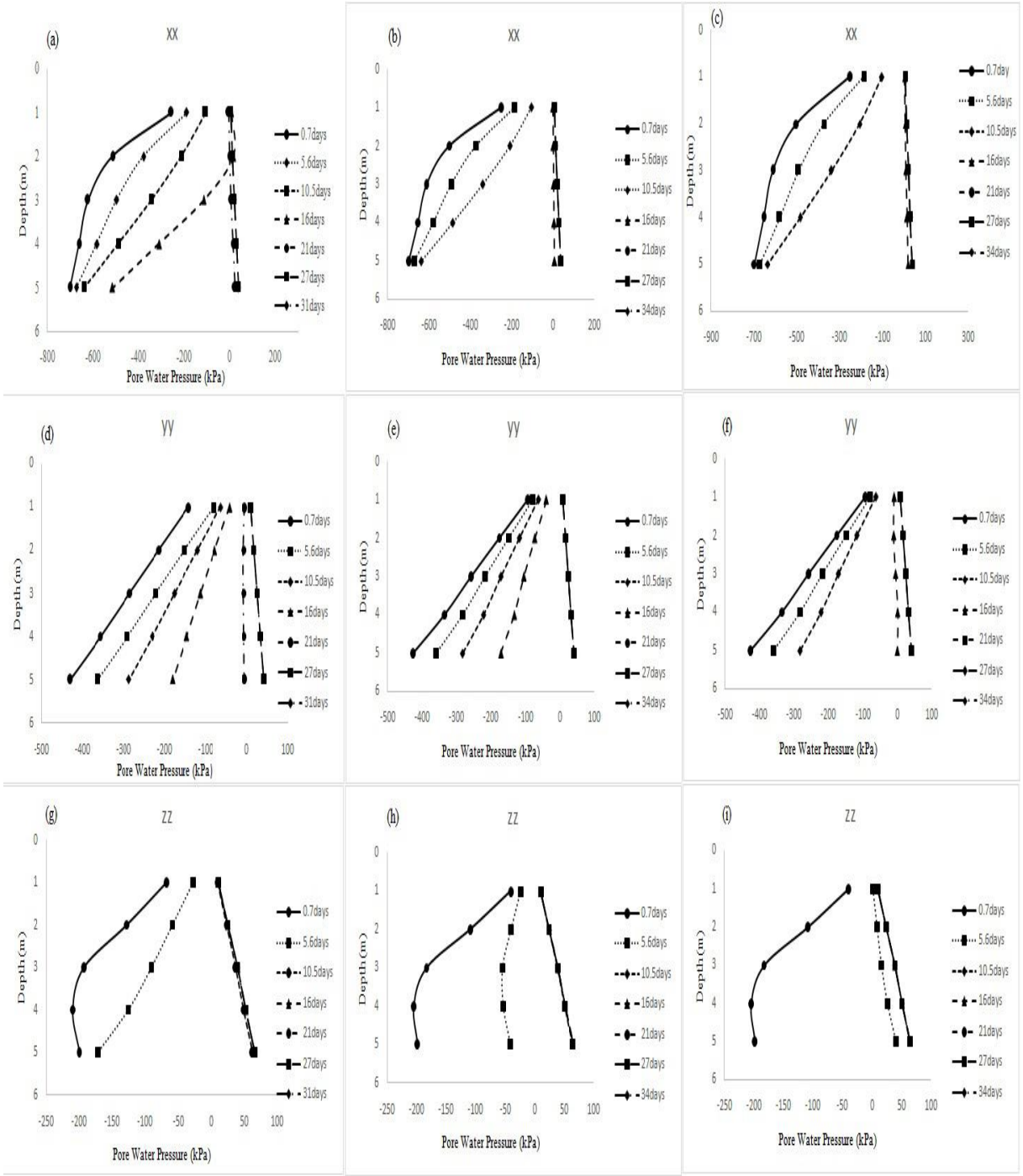

Figure 4.6 Variation of pore water pressure for slope angle of 35°

At section Y-Y, the rate of increase in pore water pressure with respect to rainfall intensities is comparatively higher to section X-X. Initial suction at the depth of 3m in section Y-Y is -459kpa. The suction fully vanished and cross zero at 3m depth for rainfall intensities of 0.2 k_{sat}, 0.4 k_{sat} and 0.6 k_{sat} are 22, 18 and 17 days respectively. At Z-Z section, suction vanished quickly with respect to rainfall intensities. At 1m depth of the Z-Z section, pore water pressure is -252kpa. It crosses zero 9, 7 and 5 days respectively for the rainfall intensities of 0.2 k_{sat}, 0.4 k_{sat}, and 0.6 k_{sat}.

The variation of suction at sections X-X, Y-Y and Z-Z with respect to rainfall intensities and duration for slope angle of 40 º and 45 º is shown in Figures 4.7 and 4.8.

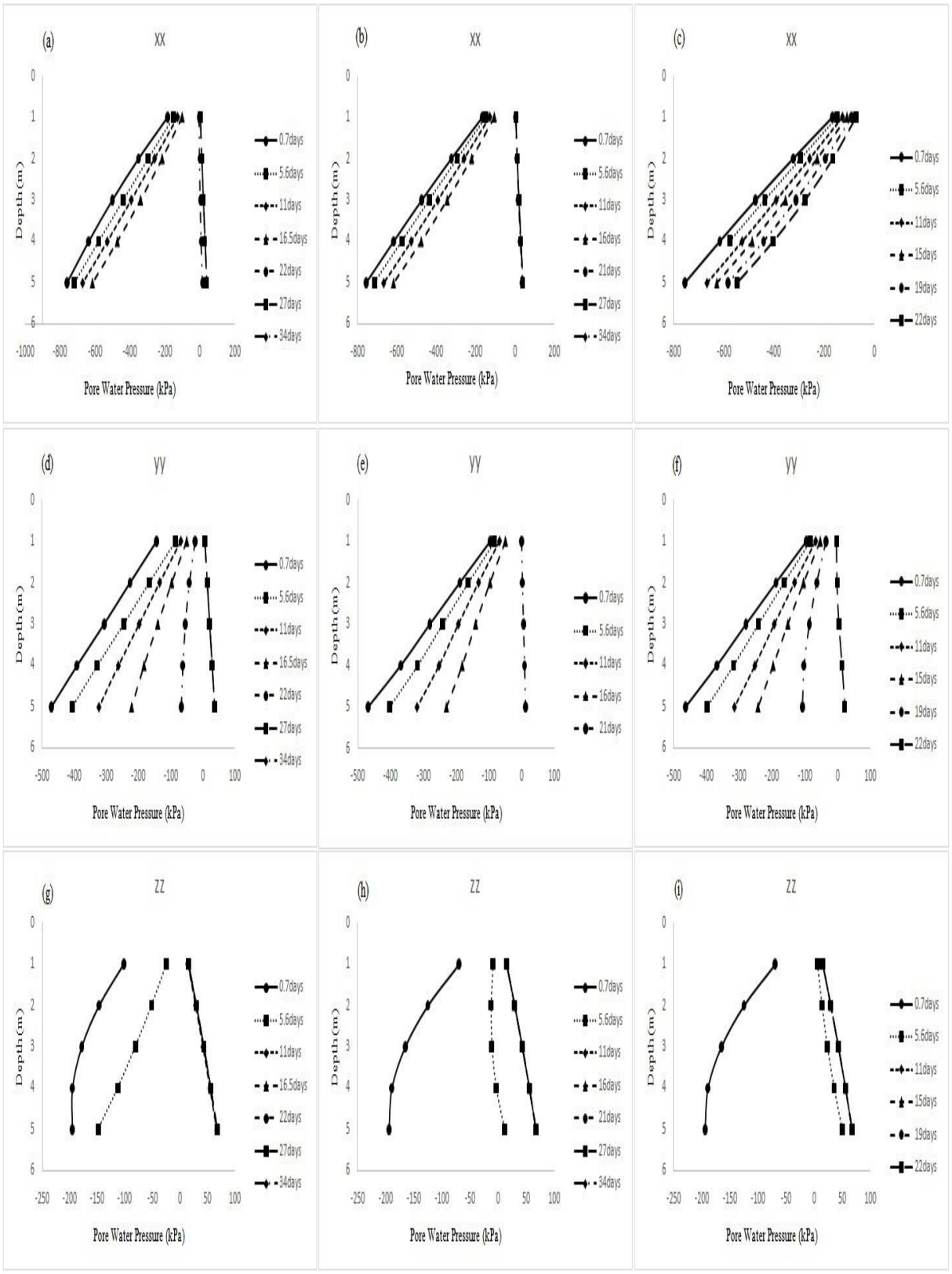

Figure 4.7 Variation of pore water pressure for slope angle of 40º

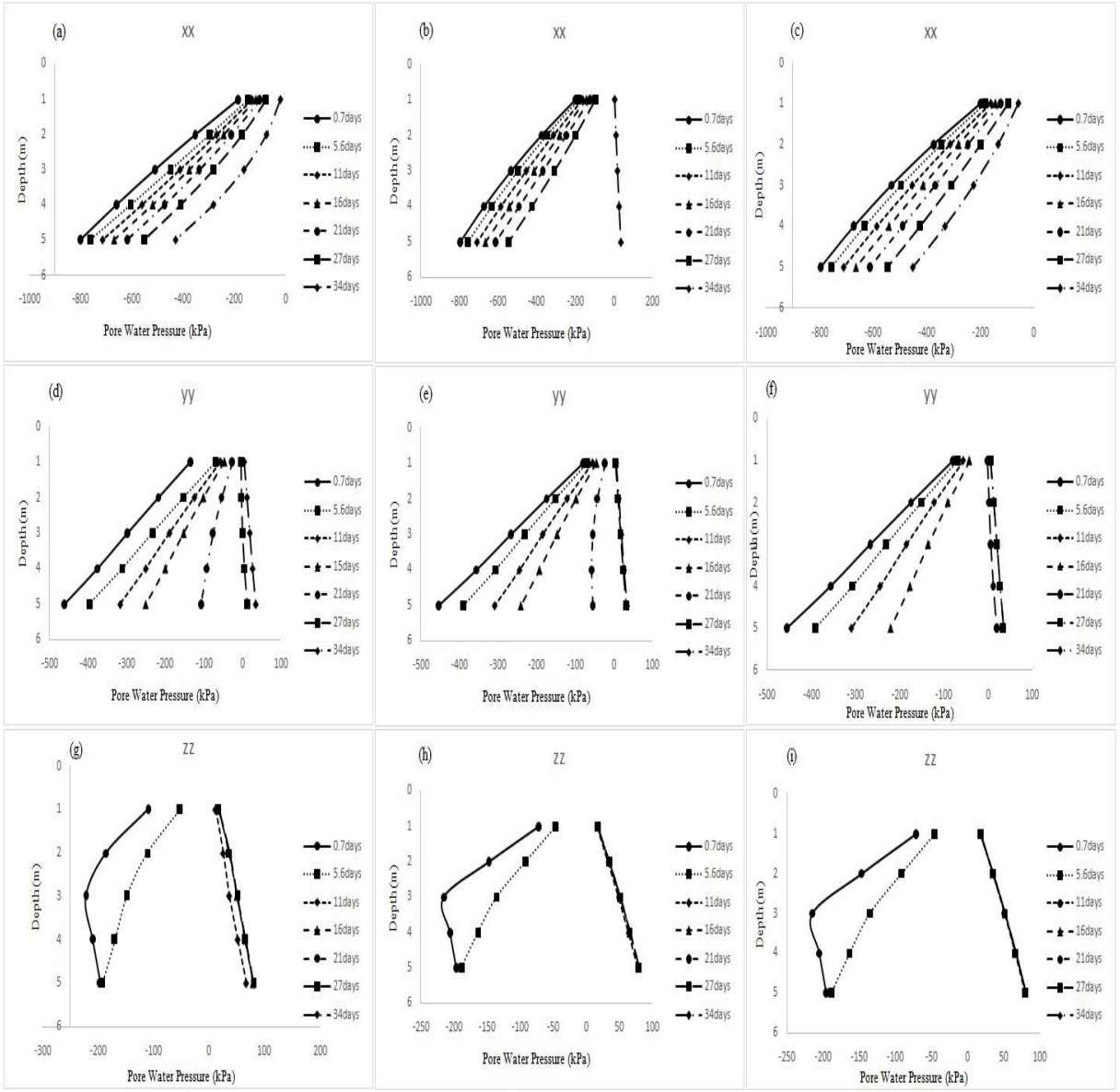

Figure 4.8 Variation of pore water pressure for slope angle of 45^o

It is noticed that change in pore water pressure at various section for different rainfall intensities of the slopes of 40^o and 45^o are similar to 35^o. The rate of increase of pore water pressure increased with increase in duration and rainfall intensities.

4.2.2 Effect of Rainfall Intensity and Duration on the Stability of Slope

Variation of safety factor with respect to rainfall duration of 0.2 k_{sat}, 0.4 k_{sat} and 0.6 k_{sat} rainfall intensities is shown in Figure 4.9, 4.10 and 4.11. With increase in rainfall intensity, factor of safety value gets decreased. For a rainfall intensity of 0.2 k_{sat}, it takes more than 21

days to reduce the factor of safety less than 1 in all three slopes subjected to analysis. But duration got reduced with increase in rainfall intensities. Factor of safety also decreased with increase in slope inclination. After applying 0.4 k_{sat} rainfall intensity for 7 days in slopes of 35°, 40°, 45°, and then factor of safety values were 2.1, 1.916 and 1.72 respectively.

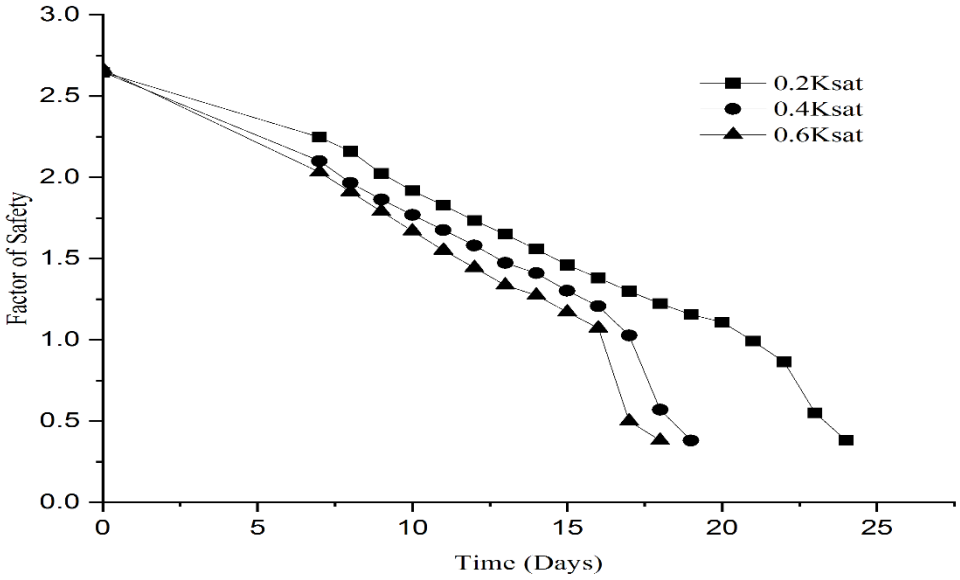

Figure 4.9 Variation of factor of safety with rainfall duration for slope 35°

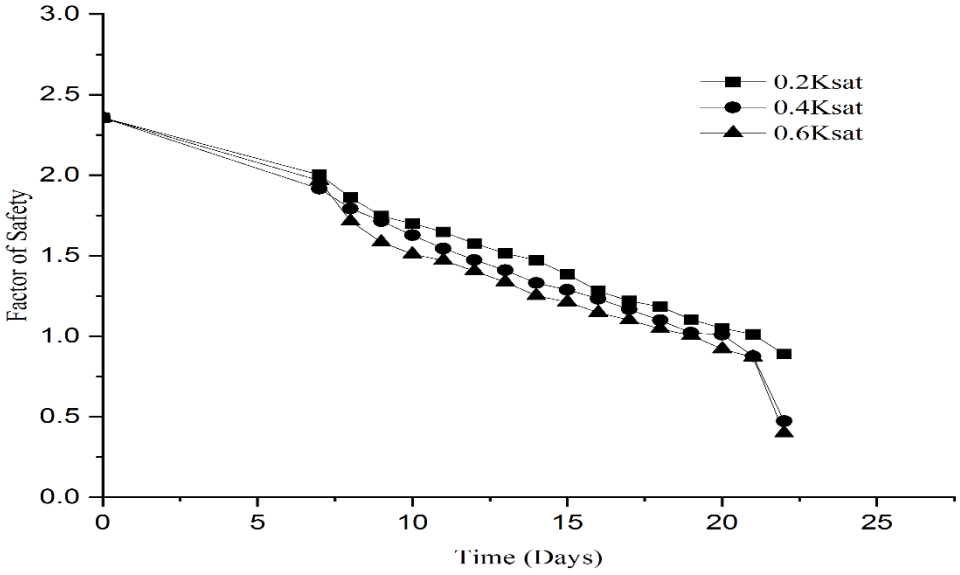

Figure 4.10 Variation of factor of safety with rainfall duration for slope 40°

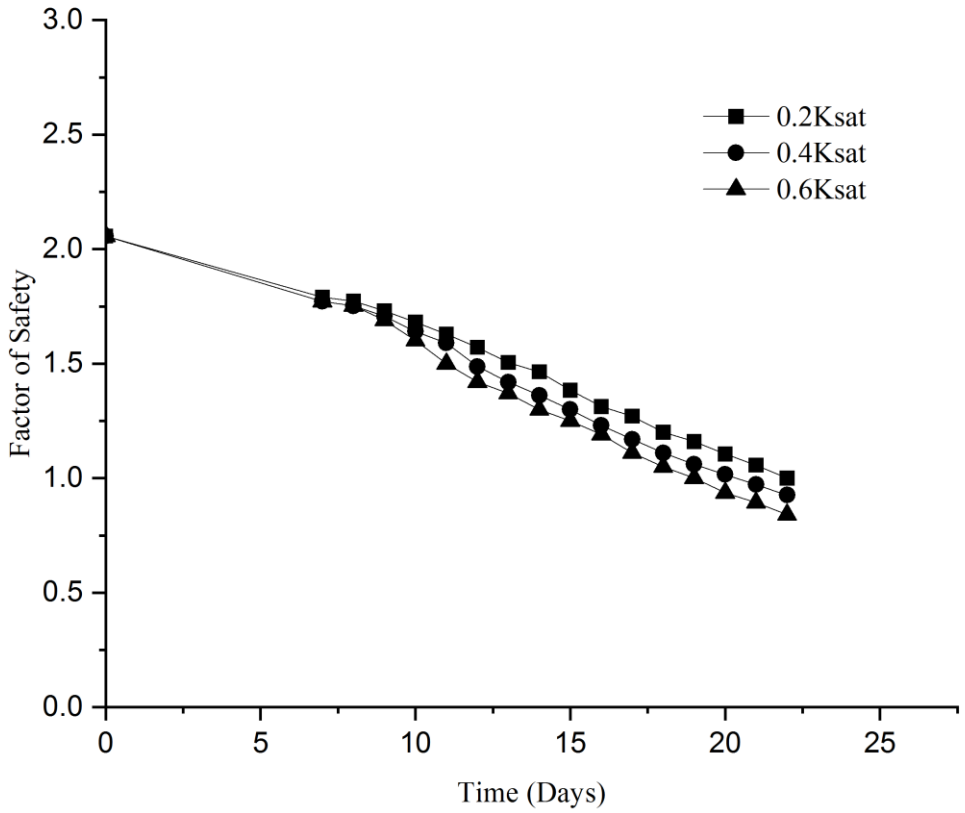

Figure 4.11 Variation of factor of safety with rainfall duration for slope 45^{o}

4.3 Probability of Failure

The risk of slope failure is quantified by probability of failure. Variation of probability of failure with respect to rainfall duration and intensity for different slope angles shown in Figures 4.12, 4.13 and 4.14. The mean and coefficient of variance value are -60kPa and 30%. It is observed that probability of failure is very low for the rainfall intensity of 0.2 k_{sat}. This indicates that suction exits in the slope which is sufficient to keep the slope stable. With higher slope angle and increase in rainfall intensity, probability of failure also increases. In all three slopes, after 3 weeks' probability of failure crosses more than 50% for rainfall intensity of 0.4 k_{sat}. As the slope angle increases, vulnerability to failure also increases during high intensity rainfall.

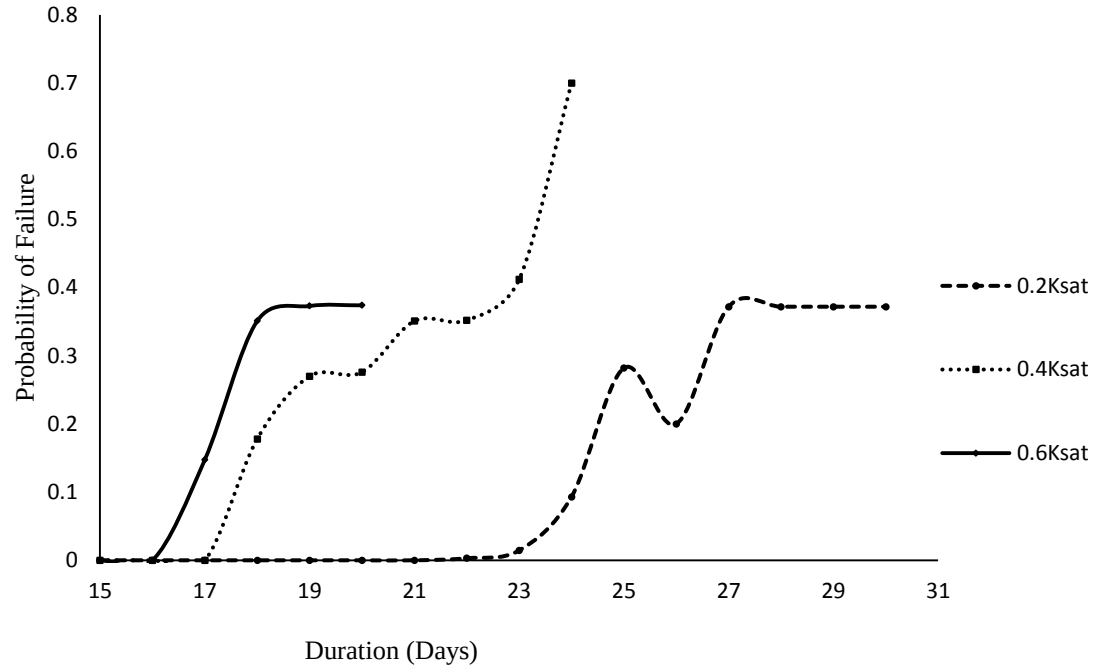

Figure 4.12 Variation of probability of failure with rainfall duration for slope 35^{o}

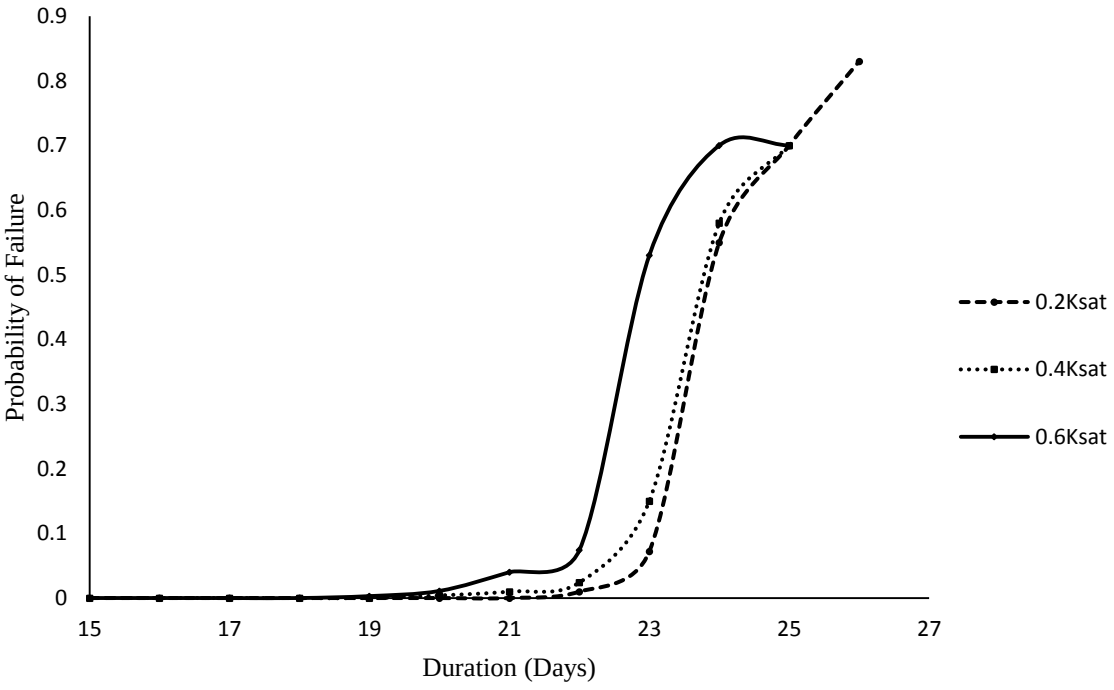

Figure 4.13 Variation of probability of failure with rainfall duration for slope 40^{o}

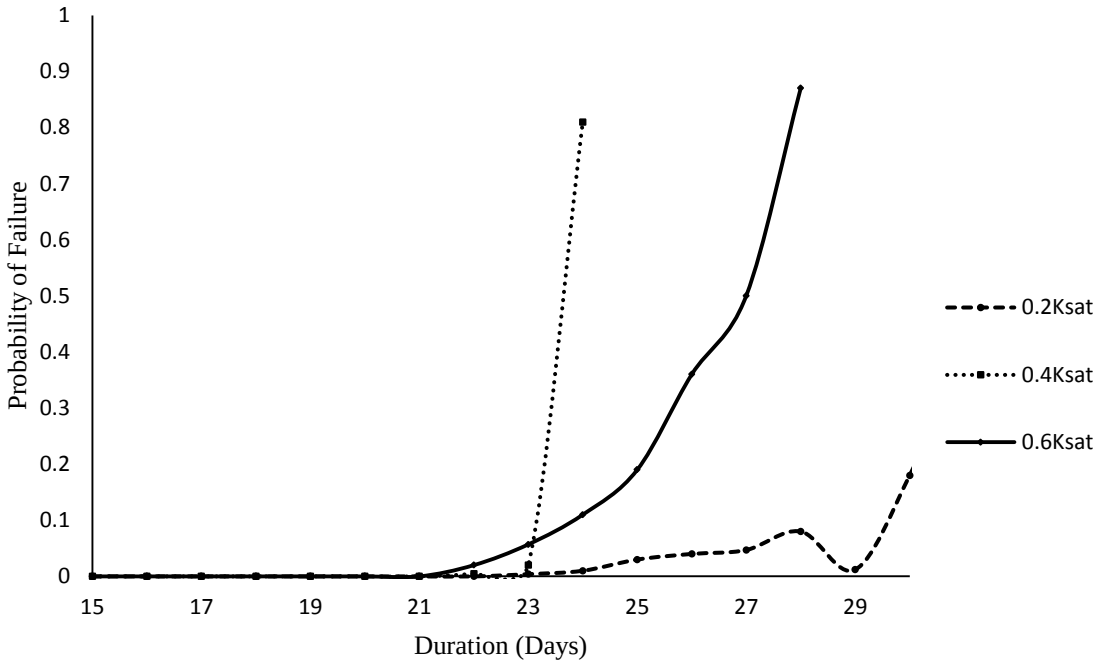

Figure 4.14 Variation of probability of failure with rainfall duration for slope 45^{o}

Some researchers have tried to use a single mathematical model to describe the entire process of landslide initiation and propagation (Bandara, Ferrari and Laloui, 2016). However, in cases where the landslide evolves into flow type phenomena, the modelling of transitioning from solid-like to fluid-like behaviour presents significant challenges. As a result, we will deal with each phase separately, taking different approaches.

The post-failure quantitative assessment of distance, material spreading, and velocity with respect to the initial condition is important in assessing landslide risk. The main goal is to predict or reproduce the debris flow as precisely as possible. It is necessary to emphasise the post-failure runout hazard rather than the initiation of landslides, which can have a direct impact on the overall loss of human lives.

4.4 Numerical Modelling of Landslide Runout

4.4.1 Entrainment Model

To quantify the effects of soil entrainment into the flow of runout, there is a requirement to include appropriate entrainment phenomena in runout model. The existing models in the literature were diversified for different flows. But most of the models were designed to include entrainment as a function of flow height, velocity and shear forces acting on the system. The selected list of currently available entrainment model is provided in Table 2.4. These models can be separated into groups as analytical and empirical approaches based on the approach and how one calculates the entrainment rate. Analytical approaches have two methods, namely, Static analysis and Dynamic analysis which are based on the study of physical phenomenon that cause entrainment. Static analysis calculates the entrainment depth based on the concepts of basic soil mechanics that failure of the erodible layer will occur when shear stress of the flow exceeds the strength of the erodible layer. On the other hand, dynamic analysis calculate the rate of erosion based on the net shear stress acting at the interface of the flow layer and erodible layer.

In this work, dynamic approach is used to account the entrainment phenomena and it is shown in the equation 4.3. The quantity of newly entrained mass is depends on the availability of momentum (Fraccarollo and Capart, 2002; Medina, Hürlimann and Bateman, 2008; Richard M. Iverson and Ouyang, 2015). Entrainment rate depends mainly on the bed shear force and basal resistance force. Basal resistance force of the flow is calculated based on the rheology of the flow.

$$E_r = -\frac{\partial z}{\partial t} \tag{4.2}$$

$$\frac{\partial z}{\partial t} = \frac{1}{\rho V}\left(\tau_b - \tau_{res}\right) \tag{4.3}$$

E_r - entrainment rate (m/s); τ_b - bed shear force; τ_{res} basal resistance force; V - the mean velocity of the flow.

4.4.2 Model Description

Under the assumptions that flow depth is small compared to the length of the flow, flowing mass is incompressible, flowing mass is considered as an equivalent fluid and free surface top, the flow dynamics can be simulated in Eulerian frame. Entrainment rate and depth averaged velocity of the flow can be modelled in Eulerian frame with the governing equations for flow

$$\frac{\partial h}{\partial t} + \frac{\partial (hu)}{\partial x} + \frac{\partial (hv)}{\partial y} = E_r \quad 4.4$$

$$\frac{\partial u}{\partial t} + u\frac{\partial u}{\partial x} + v\frac{\partial u}{\partial y} = -g(s_x + k\frac{\partial h}{\partial x} + s_f q_x) - \frac{uE_r}{h} \quad 4.5$$

$$\frac{\partial v}{\partial t} + u\frac{\partial v}{\partial x} + v\frac{\partial v}{\partial y} = -g(s_y + k\frac{\partial h}{\partial y} + s_f q_y) - \frac{vE_r}{h} \quad 4.6$$

$$\mathbf{q_x} = \frac{-\mathbf{u}}{\sqrt{\mathbf{u^2}+\mathbf{v^2}}} \; ; \boldsymbol{q_y} = \frac{-v}{\sqrt{\boldsymbol{u^2}+\boldsymbol{v^2}}}; \; \mathbf{s_x} = \mathbf{tan}(\boldsymbol{\alpha_x}); \mathbf{s_y} = \mathbf{tan}(\boldsymbol{\alpha_y})$$

Where h is the thickness of the flow, u and v are depth averaged velocity, s_x and s_y are slopes in the direction of x and y respectively, q_x and q_y are directional coefficient. s_f is the resistance to the flow which is calculated with rheology of the flow.

The most commonly used rheology model to measure flow resistance at the interface of the flowing mass and bed are Frictional, Voellmy and Bingham model. Frictional model will be used when it is assumed that flow resistance is due to effective stress and not on velocity. Voellmy model is used for granular cohesionless material and Bingham model is main applicable for a material which is high in plastic clay. Those models are shown in Table 2.1. Voellmy model is used in this present study because it is observed that both case studies have granular cohesionless material.

The core part of the present model is built from raster based model Massmov 2D. Massmov 2D has been implemented using a GIS, open source scripting language, PC Raster. Explicit finite difference mesh is used and central difference forward scheme is implemented to solve it numerically.

4.5 Case Studies

The model described was applied and evaluated for well documented past debris flow event of Peringalam, Kerala, India because of the availability data from the past research in that region and the same was applied to another case study in Kaipalli, where not all landslide inventory data are available. The Peringalam event occurred on 14th October of 2004. It caused damage to agriculture field and road which connects Peringalam and nearest town Poonjar. Both case studies, Peringalam and Kaipalli are shown in the Figure 4.15 and 4.16. To solve the governing equations 4.4 to 4.6, 2D finite difference method is implemented in PCRaster GIS open source software with Digital Elevation Module (DEM), soil depth map and rheological parameters (Kuriakose *et al.*, 2009) as inputs. Landslide inventory data are provided in Table 4.2. The density of the soil and internal friction angle for Peringalam case was taken from the past research work in this region, while it was calculated using back study for Kaipalli case. Voellmy model was used in the case studies to find the frictional resistance between the flowing mass and bed layer (Kuriakose *et al.*, 2009; Kuriakose, 2010). Turbulent coefficient and basal friction angle of Voellmy models were calibrated by matching with the values observed on the field and it is mentioned in the Table 4.2 along with landslide inventory data. Debris flows induced by landslides have turbulent coefficient and basal friction angle in the range of 100 to 600 m/s^2 (Hungr and Evans, 1996) and 0 to 40^o.

Figure 4.15 Peringalam, Kottayam, Kerala (Photographed in 2007) (Kuriakose, 2010)

Figure 4.16 Kaipalli, Menachi river basin, Kerala (Vijith *et al.*, 2014)

Table 4.2 Landslide characteristics and parameters used to simulate the flow

Parameters	**Peringalam**	**Kaipalli**
Initial volume	437 m^3	2276.25 m^3
Deposit volume	1533 m^3	-
Deposited depth at D point in deposition zone	5.2 m	-
Maximum depth observed	6.4 m	-
Density of the failed mass in initiation zone	2000 kg/m^3	1650 kg/m^3
Density of the erodible layer	2000 kg/m^3	2000 kg/m^3
Angle of internal friction	35^o	33^o
Basal friction angle	34^o	29^o
Turbulent coefficient	250 m/sec^2	275 m/sec^2

4.6 Probabilistic Analysis of Runout

Deciding the turbulent coefficient and the basal friction angle or range is indeed a tedious and difficult process. As a result, the uncertainties associated with the runout model need to be discussed. In this work, the model is applied and the mean values of rheological parameters are fitted according to field observed data and then random variable are generated for turbulent coefficient and basal friction angle to simulate various possible runouts. The application of Monte-Carlo simulation in runout modelling offers further insight into risk management by offering a framework to predict potentially expected runout behaviour (Gauer

and Issler, 2004; Meunier and Ancey, 2004). Latin hypercube sampling technique was used to generate 2000 random variables of Basal Friction and Turbulent Coefficient. In case of Peringalam, random variables were generated for a Mean of 250 m/s^2, Standard Deviation 15 of Turbulent Coefficient and Mean 34^o and Standard Deviation 4^o of Basal friction angle. For Kaipalli, random variables generated were for a Mean of 275 m/s^2, Standard Deviation 5 of Turbulent Coefficient and Mean 29^o, Standard Deviation 2 of Basal friction angle. The variables generated for Turbulent Coefficient and basal friction angle are shown in Figures 4.17 and 4.18 for Peringalam and Kaipalli case respectively.

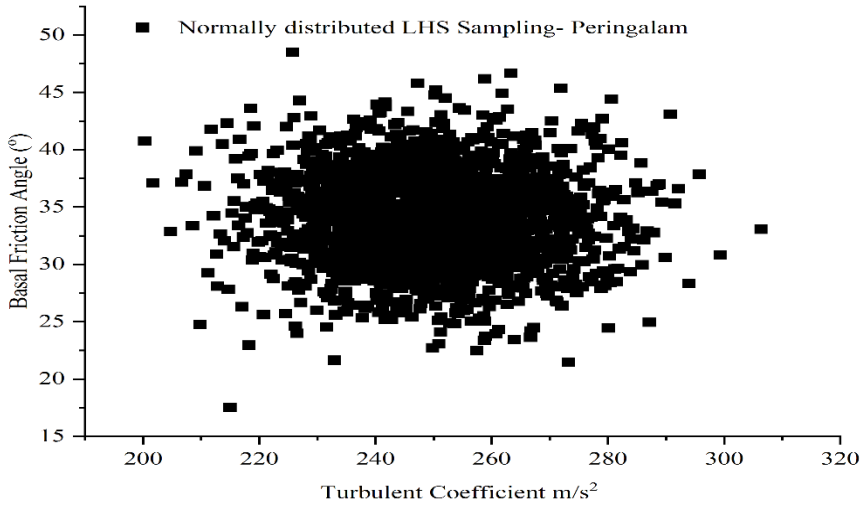

Figure 4.17 The generated variables of turbulent coefficient and basal friction angle for Peringalam

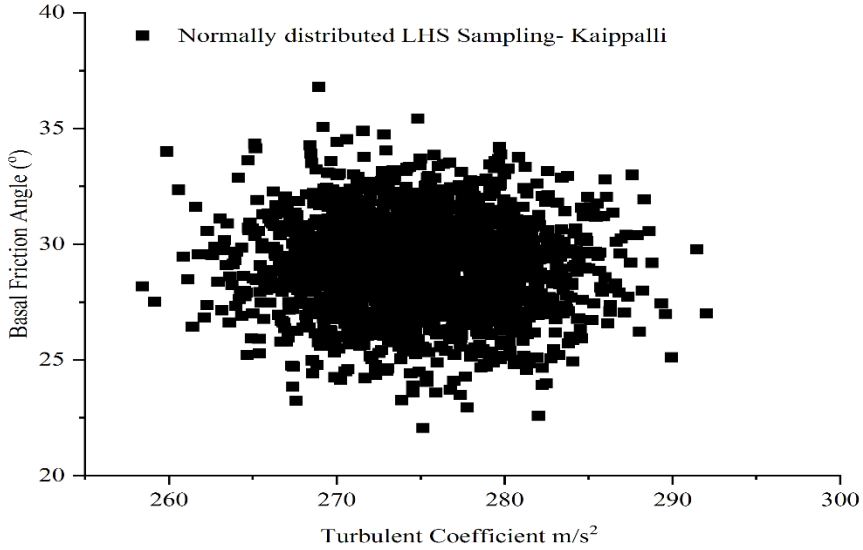

Figure 4.18 The generated variables of turbulent coefficient and basal friction angle for Kaipalli

4.7 Results and Discussion

4.7.1 Case study 1: Peringalam

Figure 4.19 shows the depth of deposit at transition zone (R point) and deposition zone (D point) in Peringalam case and the values mentioned are the measured depths at the respective locations in 2007 (Kuriakose *et al.*, 2009; Kuriakose, 2010). The explicit finite difference mesh in the present study helps to trace the flow depth and velocity at particular point. The simulated runout for the calibrated input are compared with the observed data in Figure 4.19. Figure 4.20.a shows the landslide parts which are divided into initiation zone, scouring area, deposition zone and outside the area. Figure 4.20.b is the observed deposit map. Figure 4.20.a and 4.20.b were prepared based on the field work and digital elevation model. Figure 4.20.c shows the scoured depth in transportation zone simulated by model and in Figure 4.20.d where the maximum depth in simulated output is 6.6 m which is very close to the observed value of 6.4 m.

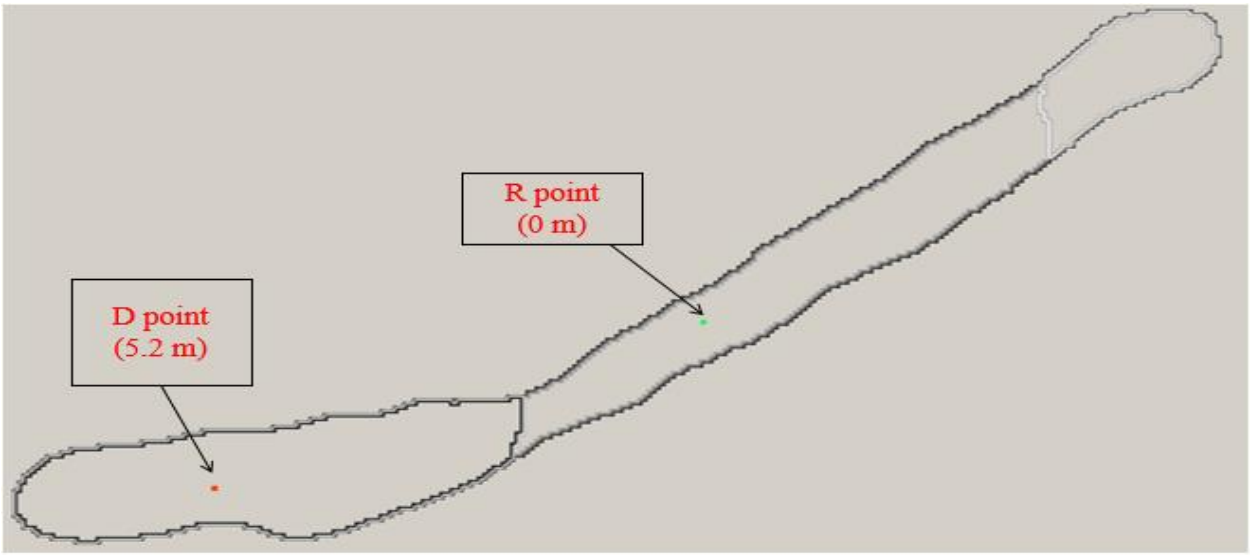

Figure 4.19 Schematic diagram of Peringalam 2004 debris flow event

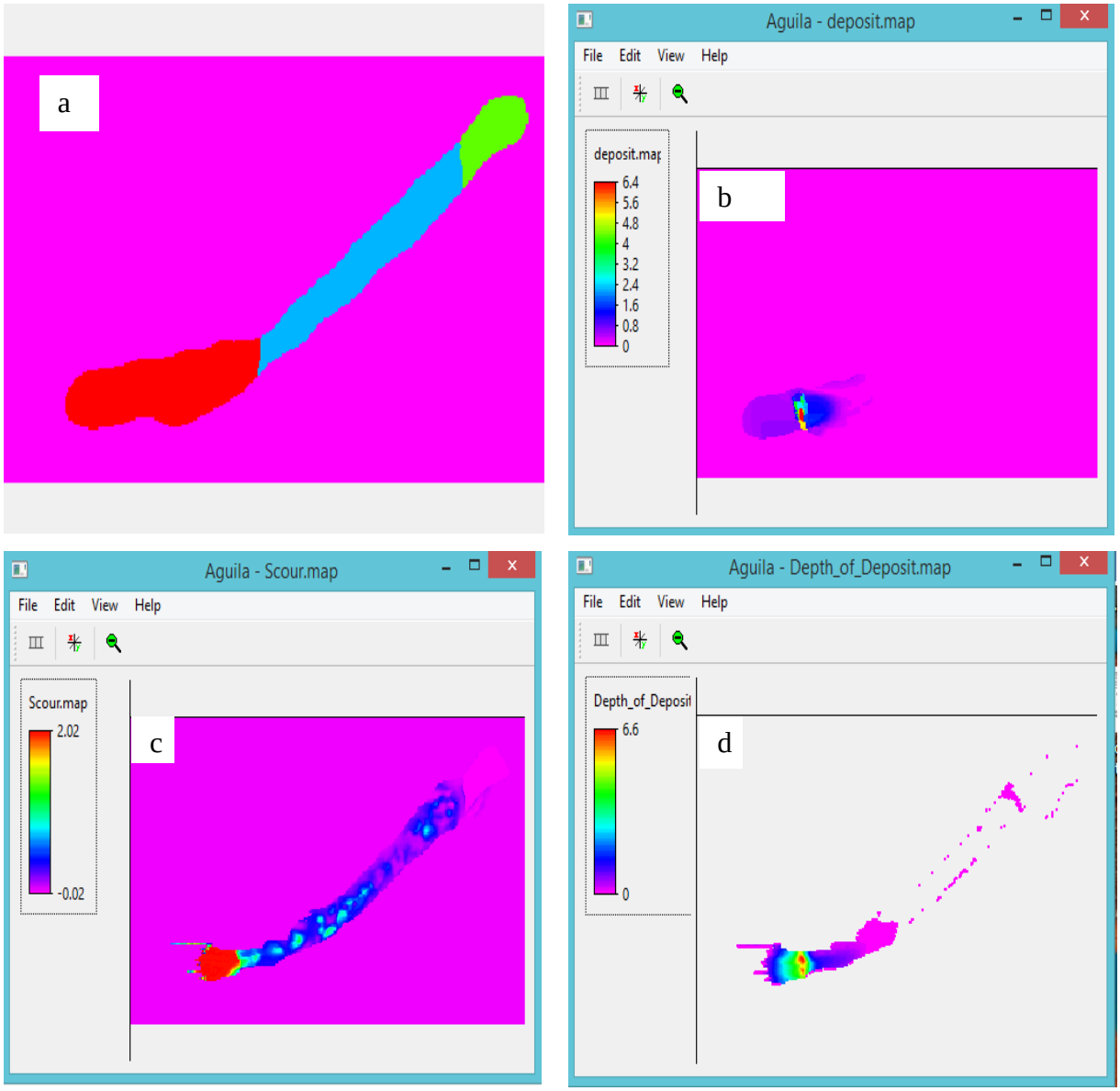

Figure 4.20 Comparison of simulated outputs of Peringalam 2004 event with observed data a). Slide Part b). Observed Depth c). Scour Depth d). Simulated Depth of Deposit

A simple probabilistic approach was employed to quantify the uncertainties in the occurrence of the runout. The probability of every point in runout path was calculated by number of runouts reached at that point divided by the total number of occurrence (2000) in this case. Current model shows that central part of the deposit area has the highest probability of getting runout and it reduced as moved away from the centre part. Figure 4.21 shows that 42 percentage of deposition area had a probability of runout of 80 to 100 percentage. Each pixel in Figure 4.22.a to 4.22.d shows the probability that a runout with depth 0-2m, 2-4m and 4-6m would reach respectively. Figure 4.22.b shown that 28% deposition area in Peringalam event have 80 to 100% probability of runout deposit of depth 0 m to 2 m. From the Figure 4.22.d it

is observed that less than 1% of deposition area in Peringalam event had a probability of deposit of depth above 6m.

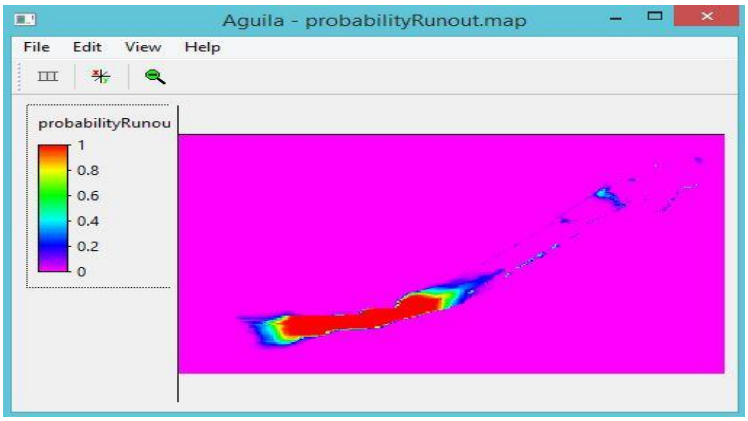

Figure 4.21 Prediction of the Probability of Runout in Deposition Zone Of Peringalam 2004 Event

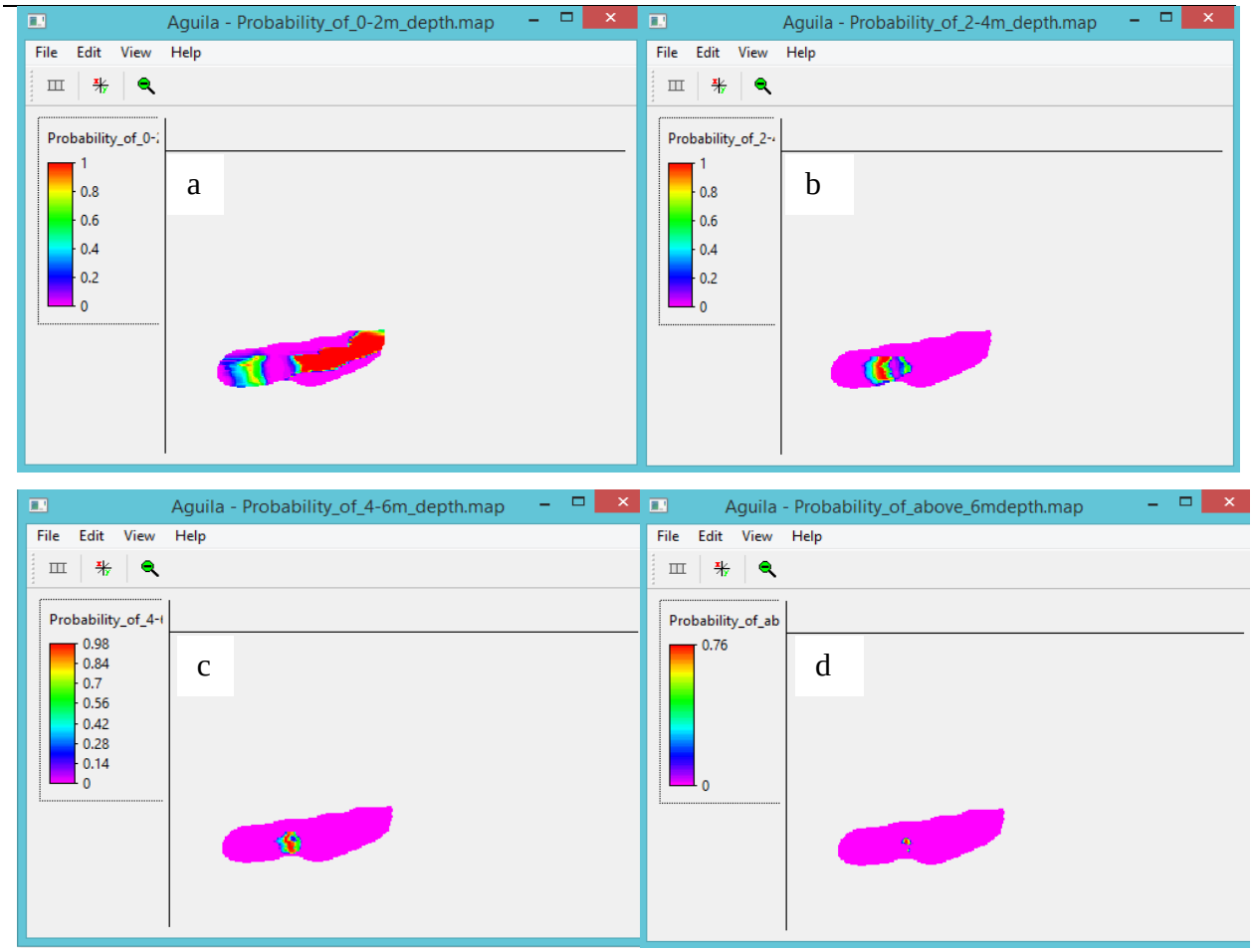

Figure 4.22 Probability of runout of (a) Depth 0 m - 2m (b) Depth 2m – 4m (c) Depth 4m – 6m (d) Depth Above 6m For Peringalam 2004 event

For each of the 2000 simulations, the maximum flow height and maximum flow velocity for the point D and R were reported along with volume of material deposited in deposition zone.

The normal distribution was fitted to the simulated outputs and shown in the Figures 4.23 to 4.29. The mean for maximum flow depth and mean of maximum flow depth at point D were 6.403 m and 5.39 m respectively. The observed depth at point D is 5.2 and simulated mean depth at point D is 5.39 m with standard deviation of 0.48654 but in case of the point R observed depth is 0 and the mean flow depth at point R is 1.37 m. The mean maximum flow velocity is measured as 26.494 m/s. the mean velocity measured in D and R point are 5.245 m/s and 13.678 m/s respectively. D point have lower velocity than R point which is showing that the runout have higher velocity in transportation scouring zone than the deposition zone. The observed volume of material deposited in deposition zone is 1533 m^3, volume of material deposited measured with current entrainment model gave a mean volume of 1885 m^3 with standard deviation of 197.68 m^3.

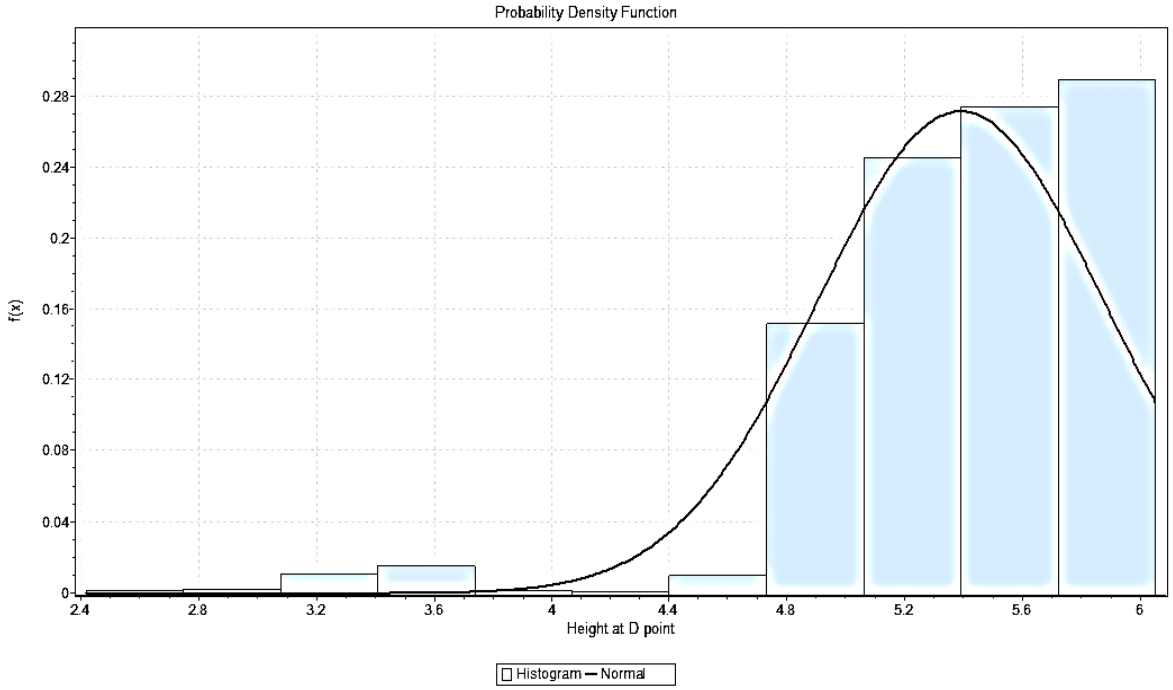

Figure 4.23 Normal distribution fitted to maximum height at D point Peringalam 2004 event

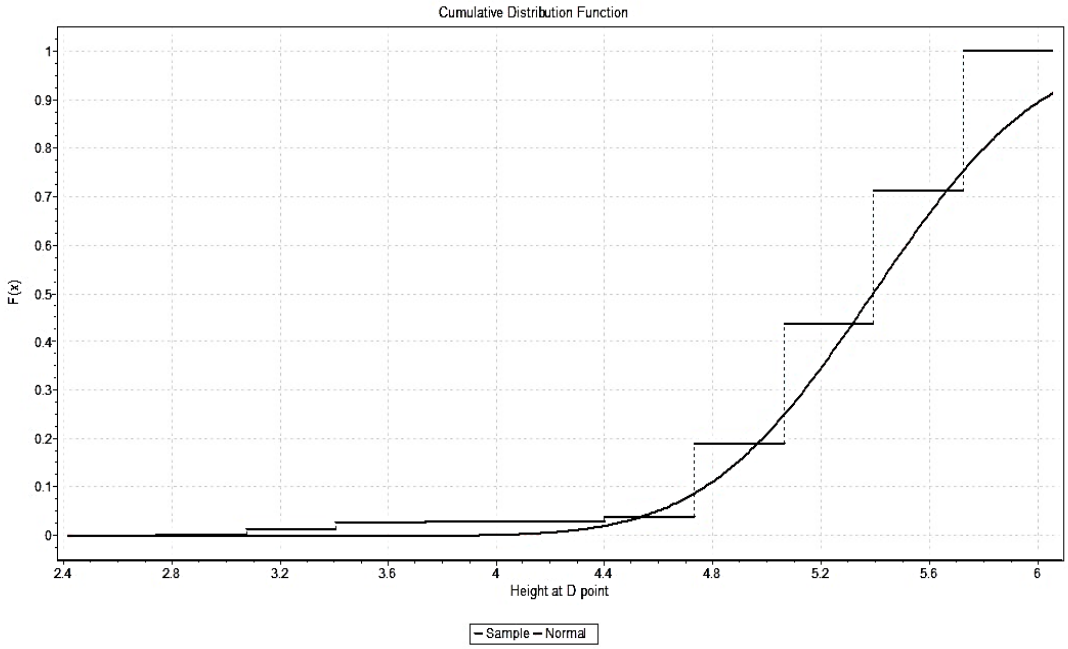

Figure 4.24 Cumulative probability plot of normal distribution as function of maximum height at D point of Peringalam 2004 event

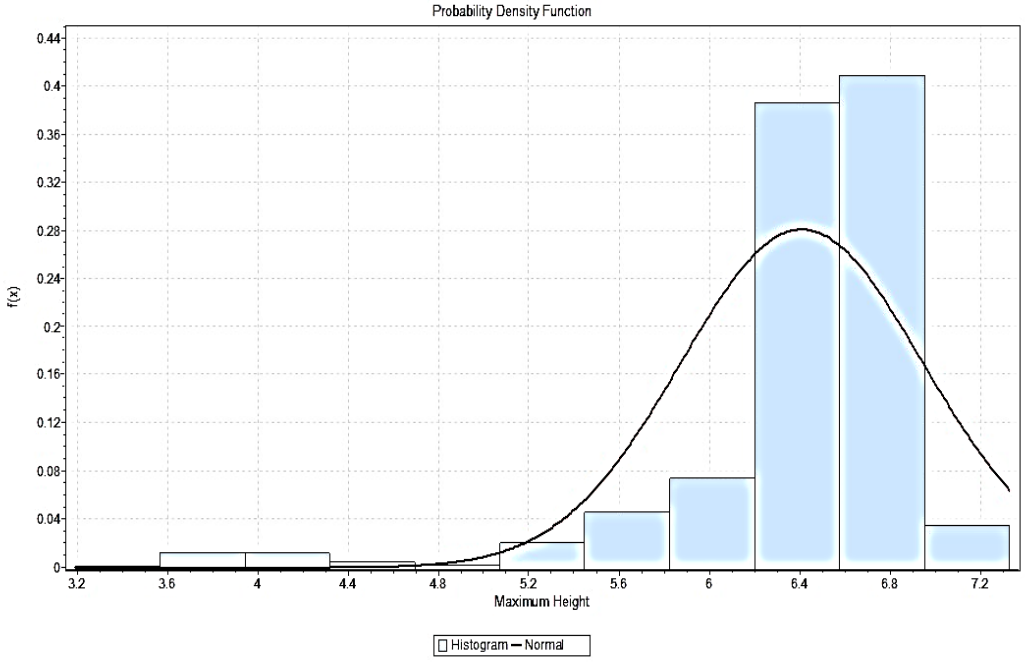

Figure 4.25 Normal distribution fitted to maximum height of the flow of Peringalam 2004 event

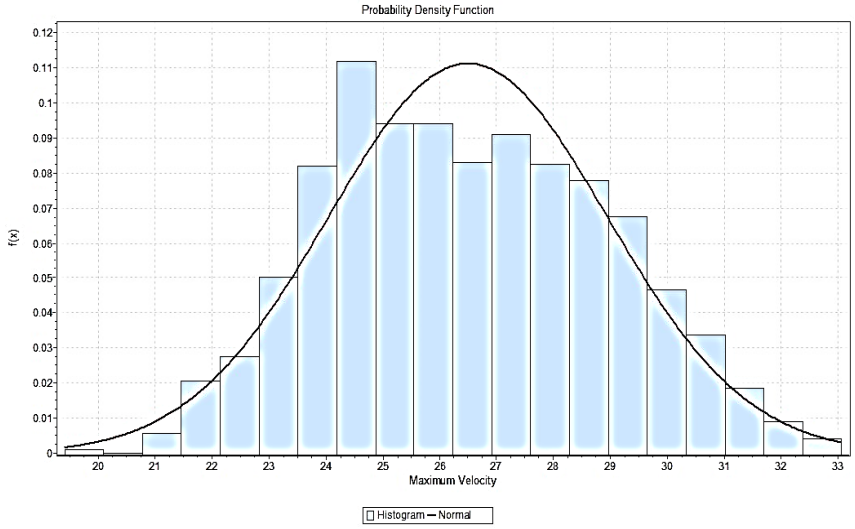

Figure 4.26 Normal distribution fitted to maximum velocity of the flow of Peringalam 2004 event

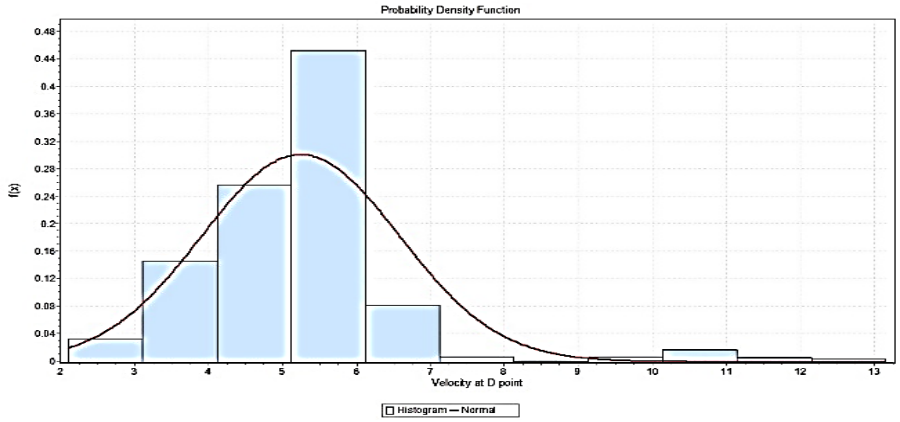

Figure 4.27 Normal distribution fitted to maximum velocity at D point of Peringalam 2004 event

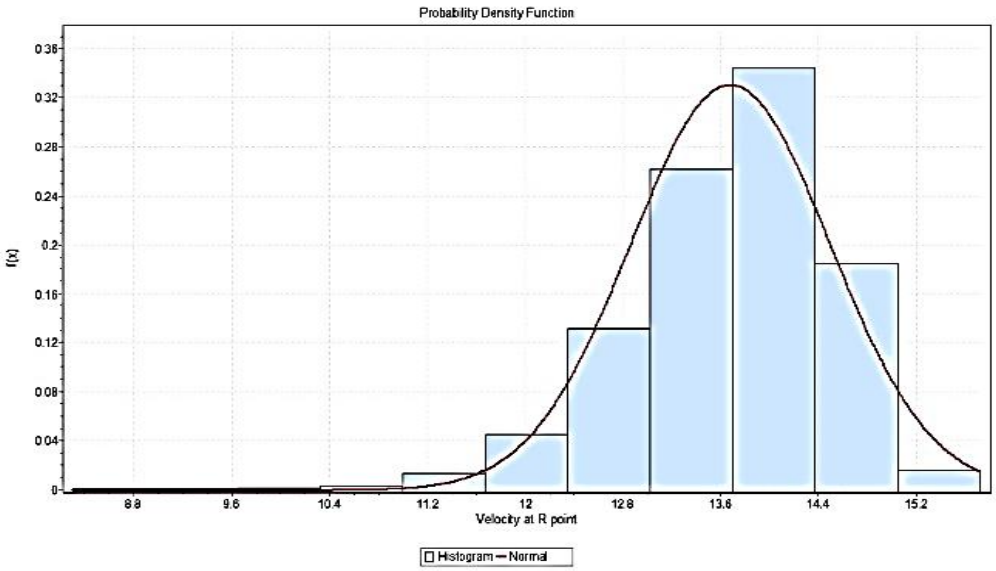

Figure 4.28 Normal distribution fitted to maximum velocity at R point of Peringalam 2004 event

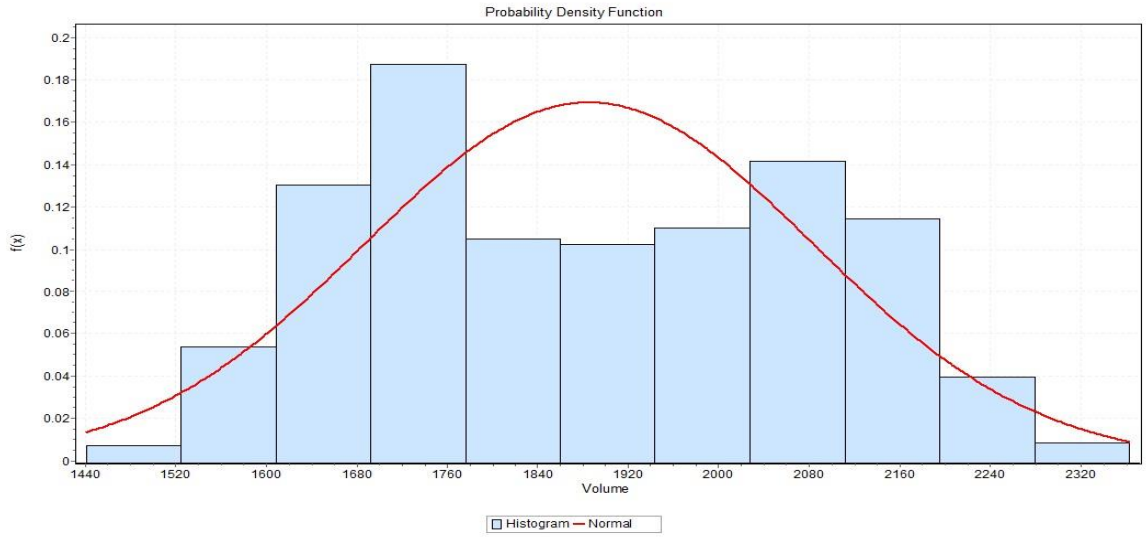

Figure 4.29 Normal distribution fitted to volume in deposition zone of Peringalam 2004 event

4.7.2 Case study 2: Kaipalli

The simulated runout for the calibrated input are compared with the observed data in figure. Figure 4.30.a shows the landslide parts which differentiates the initiation zone, scouring area, deposition zone and outside the area. Figure 4.30.b is the observed deposit map. Figure 4.30a and Figure 4.30.b are prepared based on parameters obtained by back calculation from field observations. Figure 4.30.c shows the scoured depth in the flow path and in Figure 4.30.d maximum depth in simulated output is 6.44 m which is very close to the observed value of 6.7 m.

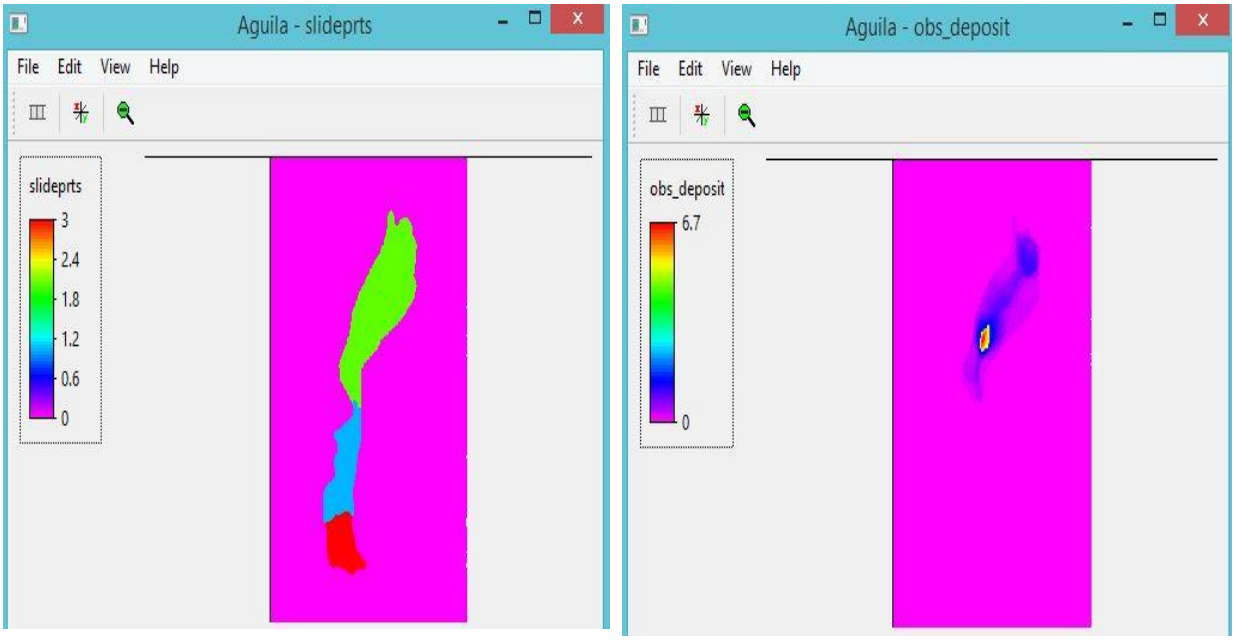

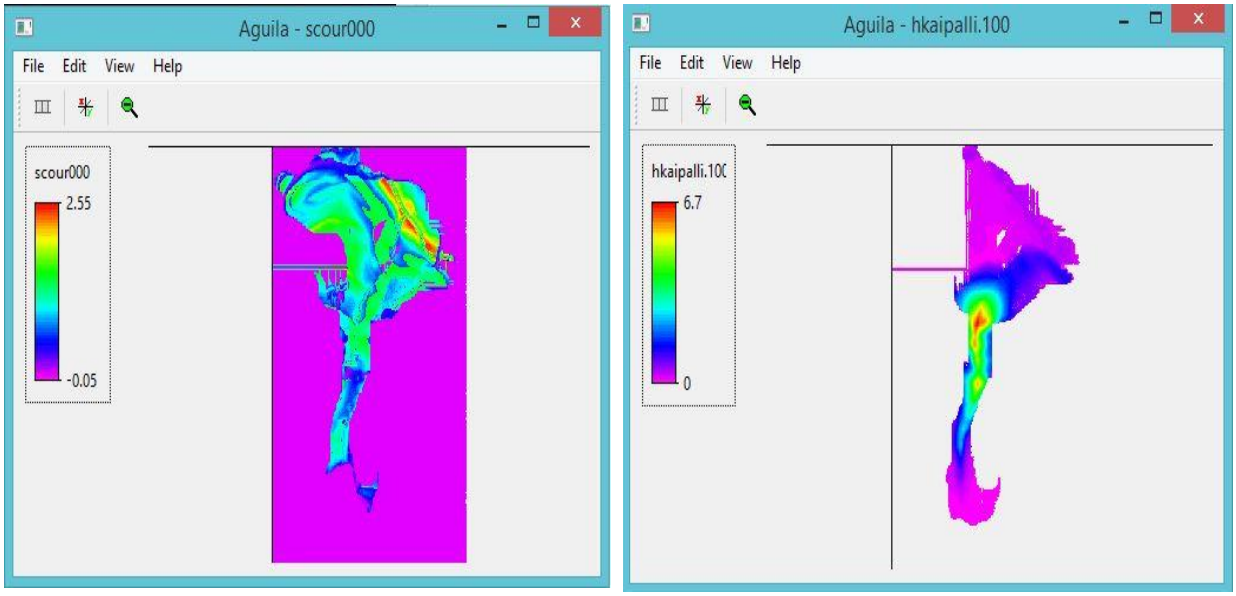

Figure 4.30 Comparison of simulated outputs of Kaipalli event with observed data a). Slide part b). Observed depth c). Scour depth d). Simulated depth of deposit

A simple probabilistic approach is employed to quantify the uncertainties in the occurrence of the runout. The Model employed shows that central part of the deposit area has the highest probability of getting runout and it reduced away from the centre part. Figure 4.33 shows that 90 percentage of deposition area had the probability of runout reaching above 80 percentage. Each pixel in Figure 4.32.a to Figure 4.32.b shows the probability that runout with depth 0-2m, 2-4m, 4-6m would reach respectively. Figure 4.32.b shown that 49 % deposition area in Kaipalli event has 80 to 100% probability of runout deposit of depth 0 m to 2 m. Less than 1.2 % of deposition area in Kaipalli event had a probability of deposit of depth above 6m.

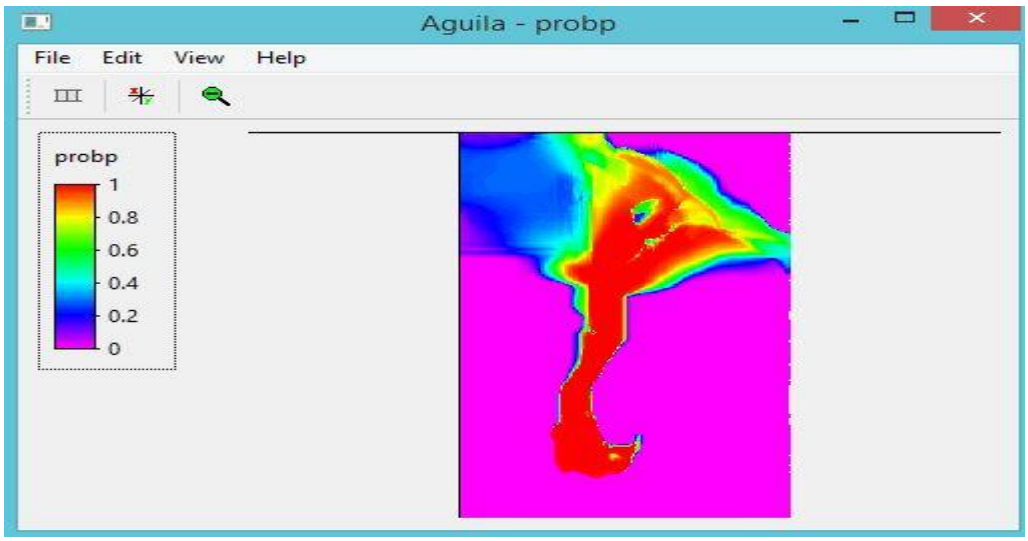

Figure 4.31 Prediction of the Probability of Runout in Deposition Zone of Kaipalli event

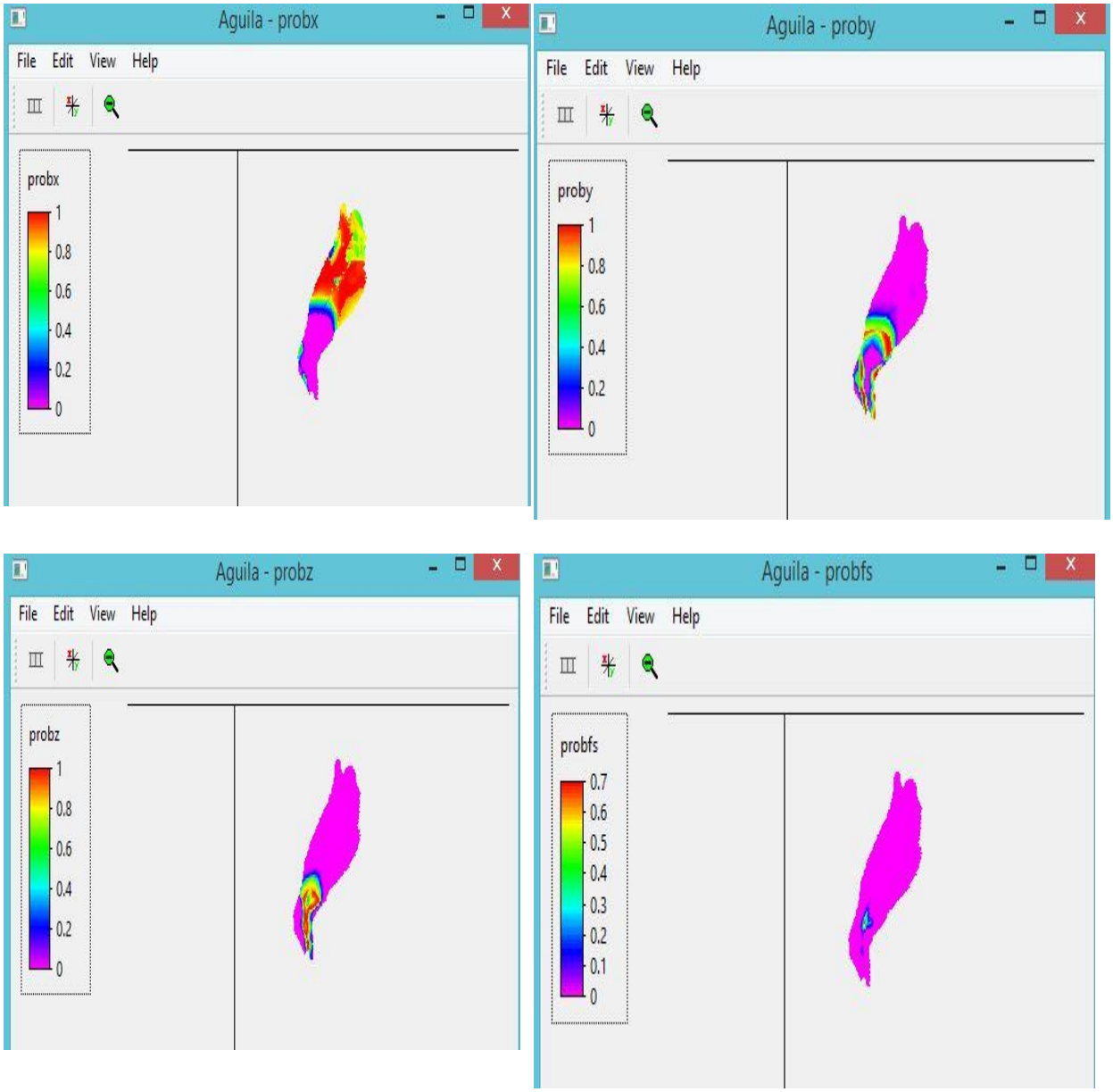

Figure 4.32 Probability of runout of (a) Depth 0m -2m (b) Depth 2m -4m (c) Depth 4m -6m (d) Depth above 6m for Kaipalli event

For each of the 2000 simulations, the maximum flow height was reported along with maximum flow velocity in transition and deposition zone. The normal distribution was fitted to the simulated outputs and shown in the Figure 4.33 to Figure 4.35. The mean for maximum flow depth and mean of maximum flow depth at point D were 6.44 m and 5.5 m respectively.. The mean maximum flow velocity was measured as 31.26 m/s. the mean velocity measured in D and R point were 3.3 m/s and 10.23 m/s respectively. Point D had lower velocity than R point which showied that the runout has higher velocity in transportation scouring zone than in the deposition zone.

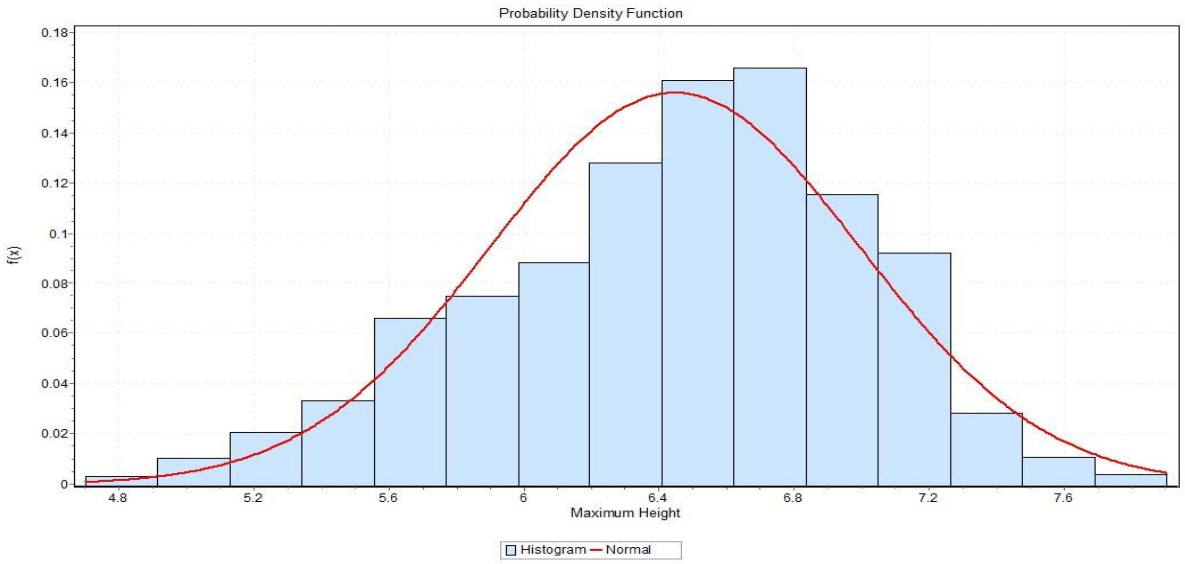

Figure 4.33 Normal distribution fitted to maximum height of the flow of Kaipalli event

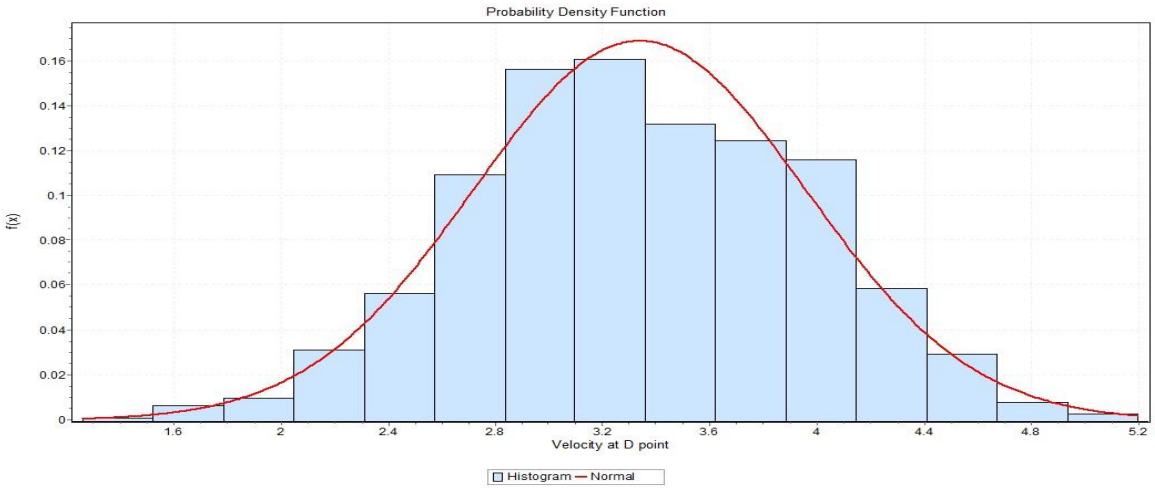

Figure 4.34 Normal distribution fitted to maximum velocity at D point of Kaipalli event

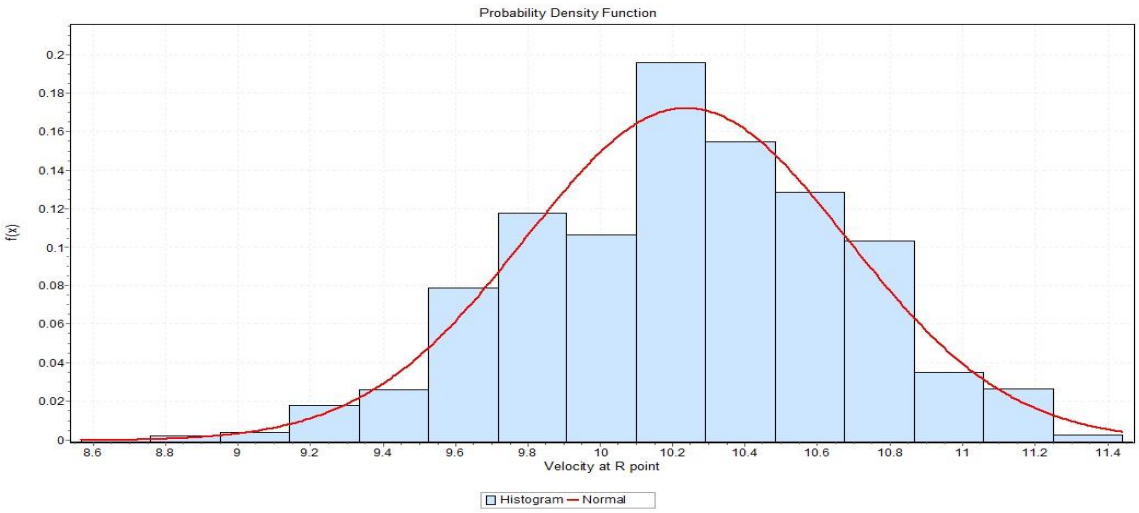

Figure 4.35 Normal distribution fitted to maximum velocity at R point of Kaipalli event

Highly influencing rheological parameters are calculated by backend analysis for both case studies. 2000 random variables are generated by Latin Hypercubic Sampling method for both cases to account the uncertainties associated with rheological parameters. Probability of the event 2004 was predicted with respect to the depth observed at D point. From the Figure 4.24 Probability of the debris height of the event 2004 is 0.35. The summary of the Monte Carlo simulation for the case studied at Peringalam and Kaipalli are shown in the Table 4.3.

Table 4.3 Summary of the results of Monte Carlo simulation

	Peringalam		Kaippali		Remark
	Mean	Std. Dev	Mean	Std. Dev	
Mean debris flow maximum height obtained with the model at point D (m)	5.39	0.49	5.5	0.75	Peringalam case mean debris flow maximum height is close to the observed value of 5.4 m
Maximum debris flow height (m)	6.407	0.53	6.44	0.54	-
Mean debris flow maximum velocity obtained with the model at point R (m/s)	13.6	0.81	10.23	0.44	Velocity is high in transition zone
Mean debris flow maximum velocity obtained with the model at point D (m/s)	5.24	1.3	3.3	0.62	Velocity is less in deposition zone
Maximum velocity (m/s)	26.49	2.4	31.26	1.46	Fast moving runout

Chapter 5

Summary and Conclusions

This chapter summaries the results obtained from the granular column collapse in erodible layer and the application of dynamic landslide runout model with entrainment to the case studies. The conclusion and contribution from the present research are also discussed in.

5.1 Summary

A pilot study on the stability of slopes was carried out based on data from Idukki district of Kerala. A detailed study of 3D Discrete Element Method study in granular column collapse on erodible bed was carried out. Open source software LIGGGHTS was used to simulate 3D Granular Column Collapse on erodible bed. 3D granular column Collapse was validated with the results of both laboratory and numerical values from literature. With dynamic entrainment analysis, new runout model was formulated and the same was applied to two case studies i.e. Peringalam and Kaipalli. Using back analysis based on the observation of field runout deposit, the material parameters for the model are calibrated. Monte-Carlo method was applied to the model to quantify the uncertainties in the model. To simulate the landslide runout, open source GIS software PCRaster was used here

In the presence of an erodible bed, different behaviour was observed between granular columns of smaller (less than 3) and larger aspect ratios (greater than 3). In larger aspect ratio cases and granular columns with erodible layer, the normalized run-out distance was about 75% higher than that of the rigid bed condition. The increase in normalised run-out duration for small aspect ratios is very less, ranging from 25% of rigid bed to almost none. The inertial effect of particles in large aspect ratio columns caused a frontal ploughing in the erodible bed, thereby initiating entrainment. The entrained particles increase the density of the flowing mass, which is shown by the increase in overall coordination number of the system. Relatively thicker deposits bearing a coordination number of 4 were encountered in the cases with erodible bed.

The kinetic energy of the system was found to be higher in the case with erodible bed when compared to rigid bed. The particles with increased kinetic energy cover longer distances, which is evident in the increased normalized run-out length for larger aspect ratio columns. However, this inertial effect of particles does not have much impact on smaller aspect ratio columns because the particle movement is controlled by inter-particle friction.

Limit equilibrium analysis was performed to study the effects of rainfall intensities, duration and slope angles on the stability of the slope. Parametric studies for varying rainfall intensities of 0.2 k_{sat}, 0.4 k_{sat} and 0.6 k_{sat} were performed to evaluate the change in pore water pressure and stability of slope. To quantify the uncertainties involved in deterministic analysis, reliability analysis was carried out to obtain the probability of failure. It was apparent that there was a difficulty in describing the initiation and propagation of landslide runout in single numerical model. So modelling propagation phase was dealt with separately.

A two dimensional numerical model which includes the effect of entrainment was formulated and used in the present study to simulate the landslide flow kinematics based on depth-averaged flow equation. Using Eulerian approach, depth of deposit, velocity and entrainment rate exerted by the flow on particular point were analysed. The entrainment model was formulated as a function of rheology, bed shear and mean velocity of the flow. The model formulated was applied to two case studies, Peringalam 2004 event and Kaipalli (2009) event. The rheological parameters were calibrated to match the simulation and observed field values. Turbulent coefficient and basal friction angle are calibrated for both case studies. Uncertainty analysis was carried out with rheological parameters and the simulated values were compared with field observed values. Monte Carlo analysis is performed to quantify the uncertainties associated with runout models due to rheological parameters. Latin hyper cubic sampling

method was adopted to model 2000 events with Monte Carlo simulation which allows one to predict the probability distribution of height and velocity which will be useful in landslide hazard analysis. These data can be useful for having hazard management to plan the mitigation of such calamities and prepare policies. Though the model predicts the depth of deposit well, it has limitations in predicting of volume of deposit. With more data on rheological parameters and studies related to critical velocity required for the entrainment of soil material in erodible layer, the reliability of the model can be improved.

5.2 Conclusions

The current study reached the following specific conclusions:

- Based on the stability analysis carried out for the slope geometry and conditions prevailing in the Western Ghats of Idukki region, it can be concluded that high intensity rainfall might trigger slope failure for short duration of rainfall also. The probability of failure increases with increase in rainfall intensity, duration and slope angle. Landslide and propagation induced by landslide are not described in a single model due to the difficulties in explaining evolution of flow and its behaviour.

- The presence of erodible bed does not affect the final run out length with respect to granular columns having smaller aspect ratios, whereas, it reveals marked variation for columns of larger aspect ratios. There is a 75 % increase in runout length for larger aspect ratio.

- The entrainment rate is found to be a function of availability of momentum in the system and depth of regolith. Rheological parameters highly affect the runout behaviour. From back analysis, the turbulent coefficient and basal friction angle have been calculated for Peringalam (250 $m/s^2$and 34^o) and Kaipalli (275 m/s^2 and 29^o) case studies.

- The present model incorporating entrainment is able to predict the depth of deposit and velocity of runout and it was in good agreement with observed values in field.

- Monte Carlo simulations were carried out with 2000 random variables of rheological parameters and the probability of debris height of Peringalam event is found to be 0.35.

- 28% deposition area in Peringalam and 49% deposition area in Kaipalli had more than 80 % probability of runout deposit of depth 0m to 2m. Less than 1% of deposition area in Peringalam and 1.2% of deposition area in Kaipalli had any probability of deposit of depth above 6m.

5.3 Contribution of the Research Work

The following are the significant contributions based on the findings of the present study:

- Attributes of Landslide Inventory from field survey have been provided for 2018 event in Adimali, Idukki district of Kerala. Unsaturated soil properties like Soil water Characteristic Curve (SWCC) and hydraulic conductivity function have been prepared with laboratory tests.

- The effect of erodible bed in flow behaviour of Granular Column Collapse (GCC) has been numerically analysed with 3D-DEM.

- A new runout model has been formulated with entrainment and the uncertainties have been quantified with model parameters. This model can be used for back analysis of debris flow.

- Two case studies have been analysed based on the new entrainment model and the uncertainties involved in the rheological parameters quantified. The results provided can be used for landslide hazard management.

5.4 Limitations

The numerical model used in this study have limitations and these limitation are also the limitations of the study.

- The granular column collapse is studied for the dry granular material. Pore fluid pressure is not considered in this study.

- Model is sensitive to the resolution of the digital elevation module (DEM). High resolution DEM is required for the reliable results.

- Entrainment model will overestimate the entrainment rate if velocity of the flowing mass is near to zero.

- Pore water pressure and problem of segregation in runout deposit is not considered.

- It is assumed that density and angle of internal friction will be constant throughout the simulation.

5.5 Future scope

Future scope for the current is presented below:

- Granular column collapse can be studied under submerged condition.

- Two phase landslide runout model can be modelled since geo-material contains solids and fluids.

- Experimental and numerical studies on the rheology of landslide runout and the selection of frictional parameters like turbulent coefficient and basal frictional angle.

- Experimental and numerical studies on deriving the process based dynamic entrainment model with the consideration of pore water pressure.

LIST OF PUBLICATIONS

Journal Articles

- Kavinkumar C, Sureka S, Rakesh J. Pillai & Heeralal Mudavath (2021) Influence of erodible layer on granular column collapse using discrete element analysis, *Geomechanics and Geoengineering*, DOI: 10.1080/17486025.2021.1928759
- Kavinkumar C, Heeralal, M and Rakesh J Pillai (2020). Numerical Assessment of Rainfall Induced Slope Failure. *Journal of Mechanics of Continua and Mathematical Sciences. Sciences*. Journal Vol – 15 No -1, January 2020.
- Kavinkumar C, Heeralal M, and Khan Mohammad Muzzaffar (2020). Numerical Assessment of Stability of Infinite Slope and Probability of Failure under Varying Rainfall Intensity. *Disaster Advances*. Vol. 13(9), September 2020.

Conferences

- Kavinkumar C, Rakesh J Pillai, Sureka S (2020) - "Investigation of dry granular flows through granular column collapse", *in proceedings of the International Conference on Triple Helix Ecosystem for Earth, Environment and Energy. PSG Institute of technology and applied research*, Coimbatore, Tamil Nadu.

- Kavinkumar C, Rakesh J Pillai, Sureka S (2020) -" Study of Dry Granular Flow Behavior with and without Erodible layer". *Indian Geotechnical Conference 2020*

REFERENCES

Anderson, M. G. and Lloyd, D. M. (1991) 'Using a combined slope hydrology-stability model to develop cut slope design charts', *Proceedings - Institution of Civil Engineers. Part 2. Research and theory*, 91, pp. 705–718. doi: 10.1680/iicep.1991.17486.

Ayachit, U. (2015) *The paraview guide: a parallel visualization application*. Kitware, Inc.

Balmforth, N. J. and Kerswell, R. R. (2005) 'Granular collapse in two dimensions', *Journal of Fluid Mechanics*, 538, p. 399.

Bandara, S., Ferrari, A. and Laloui, L. (2016) 'Modelling landslides in unsaturated slopes subjected to rainfall infiltration using material point method', *International Journal for Numerical and Analytical Methods in Geomechanics*, 40(9), pp. 1358–1380. doi: 10.1002/nag.2499.

Bandara, S. S. (2013) 'Material point method to simulate large deformation problems in fluid-saturated granular medium'. University of Cambridge Cambridge, UK.

Bateman, A. *et al.* (2007) 'Modelo bidimensional para simulación de flujos detríticos: FLATModel. Aplicación a una cuenca del Pirineo Catalán', *Ingeniería hidráulica en México*, 22(4), pp. 5–20.

Beguería, S. *et al.* (2009) 'A GIS-based numerical model for simulating the kinematics of mud and debris flows over complex terrain', *Natural Hazards and Earth System Sciences*, 9(6), pp. 1897–1909.

Berger, C., McArdell, B. W. and Schlunegger, F. (2011) 'Direct measurement of channel erosion by debris flows, Illgraben, Switzerland', *Journal of Geophysical Research: Earth Surface*, 116(1), pp. 1–18. doi: 10.1029/2010JF001722.

Berti, M. and Simoni, A. (2005) 'Experimental evidences and numerical modelling of debris flow initiated by channel runoff', *Landslides*, 2(3), pp. 171–182.

Berti, M. and Simoni, A. (2014) 'DFLOWZ: A free program to evaluate the area potentially inundated by a debris flow', *Computers & Geosciences*, 67, pp. 14–23.

Bishop, A. W. (1959) ‘The principle of effective stress’, *Teknisk ukeblad*, 39, pp. 859–863.

De Blasio, F. V., Breien, H. and Elverhøi, A. (2011) ‘Modelling a cohesive-frictional debris flow: An experimental, theoretical, and field-based study’, *Earth Surface Processes and Landforms*, pp. 753–766. doi: 10.1002/esp.2101.

Bouchut, F. *et al.* (2008) ‘On new erosion models of Savage-Hutter type for avalanches’, *Acta Mechanica*, 199(1–4), pp. 181–208. doi: 10.1007/s00707-007-0534-9.

Bouchut, F., Ionescu, I. R. and Mangeney, A. (2016) ‘An analytic approach for the evolution of the static/flowing interface in viscoplastic granular flows’, *Communications in Mathematical Sciences*, 14(8), pp. 2101–2126.

Bowman, E. T. *et al.* (2010) ‘Experimental modelling of debris flow behaviour using a geotechnical centrifuge’, *Canadian Geotechnical Journal*, 47(7), pp. 742–762. doi: 10.1139/T09-141.

Brunsden, D. (1999) ‘Some geomorphological considerations for the future development of landslide models’, *Geomorphology*, 30(1–2), pp. 13–24.

Calvetti, F., Crosta, G. and Tatarella, M. (2000) ‘Numerical simulation of dry granular flows: from the reproduction of small-scale experiments to the prediction of rock avalanches’.

De Campos, L. E. P. and Menezes, M. S. S. (1992) ‘A proposed procedure for slope stability analysis in tropical soils’, in *Landslides. International symposium*, pp. 1351–1355.

Cannon, S. H. and Savage, W. Z. (1988) ‘A mass-change model for the estimation of debris-flow runout’, *The Journal of Geology*, 96(2), pp. 221–227.

Cao, Z. *et al.* (2004) ‘Sediment Bed’, *Journal of Hydraulic Engineering*, 130(July), pp. 689–703.

Chen, H., Crosta, G. B. and Lee, C. F. (2006) ‘Erosional effects on runout of fast landslides, debris flows and avalanches: a numerical investigation’, *Geotechnique*, 56(5), pp. 305–322.

Chen, H. and Lee, C. F. (2000) ‘Numerical simulation of debris flows’, *Canadian Geotechnical Journal*, 37(1), pp. 146–160.

Chen, H. and Lee, C. F. (2004) ‘Geohazards of slope mass movement and its prevention in Hong Kong’, *Engineering Geology*, 76(1–2), pp. 3–25.

Chen, J. and Lee, C. F. (2007) ‘Landslide mobility analysis using Madflow’, *The*, pp. 857–874.

Chen, L. and Young, M. H. (2006) ‘Green- Ampt infiltration model for sloping surfaces’, *Water resources research*, 42(7).

Christen, M., Kowalski, J. and Bartelt, P. (2010) ‘RAMMS: Numerical simulation of dense snow avalanches in three-dimensional terrain’, *Cold Regions Science and Technology*, 63(1–2), pp. 1–14.

Cleary, P. W. and Campbell, C. S. (1993) ‘Self- lubrication for long runout landslides: Examination by computer simulation’, *Journal of Geophysical Research: Solid Earth*, 98(B12), pp. 21911–21924.

Cleary, P. W. and Frank, M. (2006) ‘Three-dimensional discrete element simulation of axi-symmetric collapses of granular columns’, in *Technical Report 44710*. Technische Universitat Kaiserslautern.

Cleary, P. W. and Prakash, M. (2004) ‘Discrete–element modelling and smoothed particle hydrodynamics: potential in the environmental sciences’, *Philosophical Transactions of the Royal Society of London. Series A: Mathematical, Physical and Engineering Sciences*, 362(1822), pp. 2003–2030.

Coussot, P. (1997) ‘Mudflow rheology and dynamics (IAHR monograph)’, *Balkema, Rotterdam, Netherlands*.

Crosta, G. B. *et al.* (2001) *DAMOCLES DEBRISFALL ASSESSMENT IN MOUNTAIN CATCHMENTS FOR LOCAL END-USERS GRANULAR FLOWS AND NUMERICAL MODELLING OF LANDSLIDES*.

Crosta, G. B., Imposimato, S. and Roddeman, D. (2009) ‘Numerical modelling of 2-D granular step collapse on erodible and nonerodible surface’, *Journal of Geophysical Research: Solid Earth*, 114(3), pp. 1–19. doi: 10.1029/2008JF001186.

Crosta, G. B., Imposimato, S. and Roddeman, D. G. (2003) 'Numerical modelling of large landslides stability and runout', *Natural Hazards and Earth System Sciences*, 3(6), pp. 523–538.

Cruden, D. M. (1991) 'A simple definition of a landslide', *Bulletin of the International Association of Engineering Geology - Bulletin de l'Association Internationale de Géologie de l'Ingénieur*, 43(1), pp. 27–29. doi: 10.1007/BF02590167.

Cundall, P. A. (1971) 'A computer model for simulating progressive large scale movements in blocky system', in *Proc. Int. Symp. on Rock Fractures.*, pp. II–8.

Cundall, P. A. and Strack, O. D. L. (1979) 'A discrete numerical model for granular assemblies', *geotechnique*, 29(1), pp. 47–65.

Cuomo, S. *et al.* (2014) 'Interplay of rheology and entrainment in debris avalanches: A numerical study', *Canadian Geotechnical Journal*, 51(11), pp. 1318–1330. doi: 10.1139/cgj-2013-0387.

D'Ambrosio, D., Gregorio, S. Di and Iovine, G. (2003) 'Simulating debris flows through a hexagonal cellular automata model: SCIDDICA S 3–hex', *Natural Hazards and Earth System Sciences*, 3(6), pp. 545–559.

Daerr, A. and Douady, S. (1999) 'Two types of avalanche behaviour in granular media', *Nature*, 399(6733), pp. 241–243.

Dai, F. C., Lee, C. F. and Ngai, Y. Y. (2002) 'Landslide risk assessment and management: an overview', *Engineering geology*, 64(1), pp. 65–87.

Denlinger, R. P. and Iverson, R. M. (2001) 'Flow of variably fluidized granular masses across three- dimensional terrain: 2. Numerical predictions and experimental tests', *Journal of Geophysical Research: Solid Earth*, 106(B1), pp. 553–566.

Denlinger, R. P. and Iverson, R. M. (2004) 'Granular avalanches across irregular three- dimensional terrain: 1. Theory and computation', *Journal of Geophysical Research: Earth Surface*, 109(F1).

Dhakal, A. S. and Sidle, R. C. (2004) 'Pore water pressure assessment in a forest watershed:

Simulations and distributed field measurements related to forest practices', *Water Resources Research*, 40(2).

Duncan, J. M. (2000) 'Factors of safety and reliability in geotechnical engineering', *Journal of geotechnical and geoenvironmental engineering*, 126(4), pp. 307–316.

Eckhardt, R. (1987) 'Stan ulam, john von neumann, and the monte carlo method', *Los Alamos Science*, 15(30), pp. 131–136.

Egashira, S., Honda, N. and Itoh, T. (2001) 'Experimental study on the entrainment of bed material into debris flow', *Physics and Chemistry of the Earth, Part C: Solar, Terrestrial and Planetary Science*, 26(9), pp. 645–650. doi: 10.1016/S1464-1917(01)00062-9.

Eichenberger, J., Ferrari, A. and Laloui, L. (2013) 'Early warning thresholds for partially saturated slopes in volcanic ashes', *Computers and Geotechnics*, 49, pp. 79–89. doi: 10.1016/j.compgeo.2012.11.002.

Fannin, R. J. and Wise, M. P. (2001) 'An empirical-statistical model for debris flow travel distance', *Canadian Geotechnical Journal*, 38(5), pp. 982–994. doi: 10.1139/cgj-38-5-982.

Fernández-Nieto, E. D. *et al.* (2016) 'A multilayer shallow model for dry granular flows with the μ (I)-rheology: Application to granular collapse on erodible beds', *Journal of Fluid Mechanics*, 798, pp. 643–681. doi: 10.1017/jfm.2016.333.

Fishman, G. (2013) *Monte Carlo: concepts, algorithms, and applications*. Springer Science & Business Media.

Fotheringham, S. and Wegener, M. (1999) *Spatial models and GIS: New and potential models*. CRC press.

Fourie, A. B. (1996) 'Predicting rainfall-induced slope instability.', *Proceedings of the Institution of Civil Engineers-Geotechnical Engineering*, 119(4), pp. 211–218.

Fraccarollo, L. and Capart, H. (2002) 'Riemann wave description of erosional dam-break flows', *Journal of Fluid Mechanics*, 461, p. 183.

Fredlund, D. G., Xing, A. and Huang, S. (1994) 'Predicting the permeability function for

unsaturated soils using the soil-water characteristic curve', *Canadian Geotechnical Journal*, 31(4), pp. 533–546.

Gauer, P. and Issler, D. (2004) 'Possible erosion mechanisms in snow avalanches', *Annals of Glaciology*, 38, pp. 384–392.

Girolami, L. *et al.* (2012) 'A three-dimensional discrete-grain model for the simulation of dam-break rectangular collapses: Comparison between numerical results and experiments', *Granular Matter*, 14(3), pp. 381–392. doi: 10.1007/s10035-012-0342-3.

Green, W. H. and Ampt, G. A. (1911) 'STUDIES ON SOIL PHYSICS . Studies on Soil Physics', *Journal of Agricultural Science*, 4(1), p. 1.

Griffiths, D. V, Huang, J. and Fenton, G. A. (2009) 'Influence of spatial variability on slope reliability using 2-D random fields', *Journal of geotechnical and geoenvironmental engineering*, 135(10), pp. 1367–1378.

Haddad, B. (2008) *Modelización numérica mediante elementos finitos y SPH de los geomateriales fluidificados: aplicación a los deslizamietos rápidos de ladera*. Universidad Complutense de Madrid.

Harlow, F. H. (1964) 'The particle-in-cell computing method for fluid dynamics', *Methods Comput. Phys.*, 3, pp. 319–343.

Herreros, M. I. *et al.* (2004) 'Modelos discretos y continuos para la modelización de deslizamientos rápidos de ladera', *Ingenieria Civil*, (134).

Hertz, H. (1882) 'Über die Berührung fester elastischer Körper', *Journal für die reine und angewandte Mathematik*, 92(156–171), p. 22.

Hiuhu, A. *et al.* (2015) 'Optimization of the Angle of Frog in Mouldboard Tillage Operations in Sandy Clay Soil'.

Horton, P. *et al.* (2013) 'Flow-R, a model for susceptibility mapping of debris flows and other gravitational hazards at a regional scale', *Natural hazards and earth system sciences*, 13(4), pp. 869–885.

Hsu, L., Dietrich, W. E. and Sklar, L. S. (2008) ‘Experimental study of bedrock erosion by granular flows’, *Journal of Geophysical Research: Earth Surface*, 113(2). doi: 10.1029/2007JF000778.

Hungr, O. (1995) ‘A model for the runout analysis of rapid flow slides, debris flows, and avalanches’, *Canadian geotechnical journal*, 32(4), pp. 610–623.

Hungr, O. and Evans, S. G. (2004) ‘Entrainment of debris in rock avalanches: an analysis of a long run-out mechanism’, *Geological Society of America Bulletin*, 116(9–10), pp. 1240–1252.

Hungr, O., Evans, S. G. and Hutchinson, I. N. (2001) ‘A Review of the Classification of Landslides of the Flow Type’, *Environ. Eng. Geosci*, 7, pp. 221–238.

Hungr, O. and McDougall, S. (2009) ‘Two numerical models for landslide dynamic analysis’, *Computers & geosciences*, 35(5), pp. 978–992.

Hungr, O., McDougall, S. and Bovis, M. (2005) ‘Entrainment of material by debris flows’, in *Debris-flow hazards and related phenomena*. Springer, pp. 135–158.

Hutchinson, J. N. (1986) ‘A sliding–consolidation model for flow slides’, *Canadian Geotechnical Journal*, 23(2), pp. 115–126.

Hutter, K. (2005) ‘Geophysical granular and particle-laden flows: review of the field’, *Philosophical Transactions of the Royal Society A: Mathematical, Physical and Engineering Sciences*, 363(1832), pp. 1497–1505.

Imran, J., Harff, P. and Parker, G. (2001) ‘A numerical model of submarine debris flow with graphical user interface’, *Computers & geosciences*, 27(6), pp. 717–729.

Ionescu, I. R. *et al.* (2015) ‘Viscoplastic modelling of granular column collapse with pressure-dependent rheology’, *Journal of Non-Newtonian Fluid Mechanics*, 219(February 2018), pp. 1–18. doi: 10.1016/j.jnnfm.2015.02.006.

Issler, D. and Johannesson, T. (2011) ‘Dynamical consistency constraints on entrainment and deposition in depth-averaged models of snow avalanches and other gravity mass flows’, *Preprint*.

Iverson, R. M. (2003) ‘The debris-flow rheology myth’, *Debris-flow hazards mitigation: mechanics, prediction, and assessment*, 1, pp. 303–314.

Iverson, R. M. *et al.* (2011) ‘Positive feedback and momentum growth during debris-flow entrainment of wet bed sediment’, *Nature Geoscience*, 4(2), pp. 116–121. doi: 10.1038/ngeo1040.

Iverson, R. M. (2012) ‘Elementary theory of bed-sediment entrainment by debris flows and avalanches’, *Journal of Geophysical Research: Earth Surface*, 117(3), pp. 1–17. doi: 10.1029/2011JF002189.

Iverson, R. M. and Denlinger, R. P. (2001) ‘Flow of variably fluidized granular masses across three- dimensional terrain: 1. Coulomb mixture theory’, *Journal of Geophysical Research: Solid Earth*, 106(B1), pp. 537–552.

Iverson, R. M., Logan, M. and Denlinger, R. P. (2004) ‘Granular avalanches across irregular three-dimensional terrain: 2. Experimental tests’, *Journal of Geophysical Research: Earth Surface*, 109(F1), pp. 1–16. doi: 10.1029/2003jf000084.

Iverson, Richard M. and Ouyang, C. (2015) ‘Entrainment of bed material by Earth-surface mass flows: Review and reformulation of depth-integrated theory’, *Reviews of Geophysics*, 53(1), pp. 27–58. doi: 10.1002/2013RG000447.

Iverson, Richard M and Ouyang, C. (2015) ‘Entrainment of bed material by Earth- surface mass flows: Review and reformulation of depth- integrated theory’, *Reviews of Geophysics*, 53(1), pp. 27–58.

Iverson, R. M., Reid, M. E. and Lahusen, R. G. (1997) ‘DEBRIS-FLOW MOBILIZATION’, pp. 85–138.

Iverson, R. M., Schilling, S. P. and Vallance, J. W. (1998) ‘Objective delineation of lahar-inundation hazard zones’, *Geological Society of America Bulletin*, 110(8), pp. 972–984.

Jaeger, H. M. and Nagel, S. R. (1992) ‘Physics of the granular state’, *Science*, 255(5051), pp. 1523–1531.

Jakob, M., Bovis, M. and Oden, M. (2005) ‘The significance of channel recharge rates for

estimating debris-flow magnitude and frequency', *Earth Surface Processes and Landforms*, pp. 755–766. doi: 10.1002/esp.1188.

Jiang, L. and LeBlond, P. H. (1993) 'Numerical modelling of an underwater Bingham plastic mudslide and the waves which it generates', *Journal of Geophysical Research: Oceans*, 98(C6), pp. 10303–10317.

De Joode, A. and Van Steijn, H. (2003) 'PROMOTOR-df: a GIS-based simulation model for debris flow hazard prediction', *Rickenmann D, Chen*, pp. 1173–1184.

Kang, C. and Chan, D. (2018) 'Numerical simulation of 2D granular flow entrainment using DEM', *Granular Matter*, 20(1), pp. 1–17. doi: 10.1007/s10035-017-0782-x.

Kelfoun, K. and Druitt, T. H. (2005) 'Numerical modelling of the emplacement of Socompa rock avalanche, Chile', *Journal of Geophysical Research: Solid Earth*, 110(B12).

Kesseler, M., Heller, V. and Turnbull, B. (2018) 'A laboratory-numerical approach for modelling scale effects in dry granular slides', *Landslides*, 15(11), pp. 2145–2159.

Kuriakose, S. L. *et al.* (2009) 'Catena Prediction of soil depth using environmental variables in an anthropogenic landscape , a case study in the Western Ghats of Kerala , India', *Catena*, 79(1), pp. 27–38. doi: 10.1016/j.catena.2009.05.005.

Kuriakose, S. L. (2010) 'Physically based dynamic modelling of the effects of land use changes on shallow landslide initiation in the Western Ghats, Kerala, India', in. ITC.

Kwan, J. S. H. and Sun, H. W. (2006) 'An improved landslide mobility model', *Canadian Geotechnical Journal*, 43(5), pp. 531–539.

Kwan, J. S. H. and Sun, H. W. (2007) 'Benchmarking exercise on landslide mobility modelling–runout analyses using 3dDMM', in *Proceedings of the 2007 International Forum on Landslide Disaster Management. Edited by Ho and Li. Hong Kong Geotechnical Engineering Office*, pp. 945–966.

Lacaze, L., Phillips, J. C. and Kerswell, R. R. (2008) 'Planar collapse of a granular column: Experiments and discrete element simulations', *Physics of Fluids*, 20(6), p. 63302.

Lagrée, P.-Y., Staron, L. and Popinet, S. (2011) ‘The granular column collapse as a continuum: validity of a two-dimensional Navier-Stokes model with a [mu](I)-rheology’, *Journal of Fluid Mechanics*, 686, p. 378.

Li, K. S. and Lumb, P. (1987) ‘Probabilistic design of slopes’, *Canadian Geotechnical Journal*, 24(4), pp. 520–535. doi: 10.1139/t87-068.

Lin, J. and Wu, W. (2012) ‘Numerical study of miniature penetrometer in granular material by discrete element method’, *Philosophical Magazine*, 92(28–30), pp. 3474–3482.

Lube, G. *et al.* (2004) ‘Axisymmetric collapses of granular columns’, *Journal of Fluid Mechanics*, 508, p. 175.

Lube, G. *et al.* (2005) ‘Collapses of two-dimensional granular columns’, *Physical Review E - Statistical, Nonlinear, and Soft Matter Physics*, 72(4). doi: 10.1103/PhysRevE.72.041301.

Lumb, P. (1975) ‘Slope failures in Hong Kong’, *Quarterly Journal of Engineering Geology*, 8(1), pp. 31–65. doi: 10.1144/GSL.QJEG.1975.008.01.02.

Luna, B. Q. *et al.* (2012) ‘Analysis of debris flow behavior with a one dimensional run-out model incorporating entrainment’, *Engineering Geology*, 128, pp. 63–75. doi: 10.1016/j.enggeo.2011.04.007.

Lusso, C. *et al.* (2017) ‘Two-dimensional simulation by regularization of free surface viscoplastic flows with Drucker–Prager yield stress and application to granular collapse’, *Journal of Computational Physics*, 333(February 2018), pp. 387–408. doi: 10.1016/j.jcp.2016.12.036.

Malet, J.-P., Remaître, A. and Maquaire, O. (2004) ‘Runout modelling and extension of the threatened area associated with muddy debris flows/Modélisation de l’écoulement et extension de la zone exposée à des laves torrentielles boueuses’, *Géomorphologie: relief, processus, environnement*, 10(3), pp. 195–209.

Mangeney-Castelnau, A. *et al.* (2005) ‘On the use of Saint Venant equations to simulate the spreading of a granular mass’, *Journal of Geophysical Research: Solid Earth*, 110(9), pp. 1–17. doi: 10.1029/2004JB003161.

Mangeney, A. *et al.* (2010) ‘Erosion and mobility in granular collapse over sloping beds’, *Journal of Geophysical Research: Earth Surface*, 115(3), pp. 1–21. doi: 10.1029/2009JF001462.

Martin, N. *et al.* (2017) ‘Continuum viscoplastic simulation of a granular column collapse on large slopes: μ (I) rheology and lateral wall effects’, *Physics of Fluids*, 29(1), p. 13301.

McCoy, S. W. *et al.* (2013) ‘Field measurement of basal forces generated by erosive debris flows’, *Journal of Geophysical Research: Earth Surface*, 118(2), pp. 589–602. doi: 10.1002/jgrf.20041.

McDougall, S. (2006) ‘A new continuum dynamic model for the analysis of extremely rapid landslide motion across complex 3D terrain’. University of British Columbia.

McDougall, S. and Hungr, O. (2004) ‘A model for the analysis of rapid landslide motion across three-dimensional terrain’, *Canadian Geotechnical Journal*, 41(6), pp. 1084–1097.

McDougall, S. and Hungr, O. (2005) ‘Dynamic modelling of entrainment in rapid landslides’, *Canadian Geotechnical Journal*, 42(5), pp. 1437–1448. doi: 10.1139/t05-064.

MEDINA, V., BATEMAN, A. and HÜRLIMANN, M. (2008) ‘A 2D finite volume model for bebris flow and its application to events occurred in the Eastern Pyrenees’, *International Journal of Sediment Research*, 23(4), pp. 348–360. doi: 10.1016/S1001-6279(09)60006-8.

Medina, V., Hürlimann, M. and Bateman, A. (2008) ‘Application of FLATModel, a 2D finite volume code, to debris flows in the northeastern part of the Iberian Peninsula’, *Landslides*, 5(1), pp. 127–142. doi: 10.1007/s10346-007-0102-3.

Mein, R. G. and Larson, C. L. (1973) ‘Modelling infiltration during a steady rain’, *Water resources research*, 9(2), pp. 384–394.

Meunier, M. and Ancey, C. (2004) ‘Towards a conceptual approach to predetermining long-return-period avalanche run-out distances’, *Journal of Glaciology*, 50(169), pp. 268–278.

Mitchell, J. K. and Soga, K. (2005) ‘Soil composition and engineering properties’, *Fundamentals of soil behavior*, pp. 83–108.

Modenese, C., Utili, S. and Houlsby, G. T. (2012) ‘A numerical investigation of quasi-static conditions for granular media’, in *Discrete Element Modelling of Particulate Media*, pp. 187–195.

Muntohar, A. S. and Liao, H. J. (2010) ‘Rainfall infiltration: Infinite slope model for landslides triggering by rainstorm’, *Natural Hazards*, 54(3), pp. 967–984. doi: 10.1007/s11069-010-9518-5.

Ng, C. W. W. and Shi, Q. (1998) ‘A Numerical Investigation of the Stability of Unsaturated Soil Slopes Subjected to Transient Seepage’, *Computers and Geotechnics*, 22(1), pp. 1–28. doi: 10.1016/S0266-352X(97)00036-0.

O’Brien, J. S., Julien, P. Y. and Fullerton, W. T. (1993) ‘Two-dimensional water flood and mudflow simulation’, *Journal of hydraulic engineering*, 119(2), pp. 244–261.

O’Sullivan, C. (2011) *Particulate Discrete Element Modelling, Particulate Discrete Element Modelling*. doi: 10.1201/9781482266498.

Padrós, C. B. (2014) ‘Discrete element simulations with LIGGGHTS’, *Zienkiewicz Centre for Computational Engineering*.

Pastor, M. *et al.* (2002) ‘Modelling tailings dams and mine waste dumps failures’, *Geotechnique*, 52(8), pp. 579–591.

Pastor, M. *et al.* (2009) ‘A depth- integrated, coupled SPH model for flow- like landslides and related phenomena’, *International Journal for numerical and analytical methods in geomechanics*, 33(2), pp. 143–172.

Pirulli, M. *et al.* (2003) ‘Rock avalanche run out prediction: combined application of two numerical methods’, in *10th ISRM Congress*. International Society for Rock Mechanics and Rock Engineering.

Pirulli, M. (2005) ‘Numerical modelling of landslide runout, a continuum mechanics approach’, *Unpublished Ph. D. Dissertation, Politecnico di Torino*.

Pirulli, M. and Mangeney, A. (2008) ‘Results of back-analysis of the propagation of rock avalanches as a function of the assumed rheology’, *Rock Mechanics and Rock Engineering*,

41(1), pp. 59–84.

Pitman, E B *et al.* (2003) ‘A model of granular flows over an erodible surface’, *Discrete & Continuous Dynamical Systems-B*, 3(4), p. 589.

Pitman, E Bruce *et al.* (2003) ‘Computing granular avalanches and landslides’, *Physics of fluids*, 15(12), pp. 3638–3646.

Poisel, R. and Preh, A. (2008) *3D landslide run out modelling using the particle flow code PFC3D*. na.

Potyondy, D. O. and Cundall, P. A. (2004) ‘A bonded-particle model for rock’, *International Journal of Rock Mechanics and Mining Sciences*, 41(8), pp. 1329–1364. doi: https://doi.org/10.1016/j.ijrmms.2004.09.011.

Pouliquen, O. (1999) ‘Scaling laws in granular flows down rough inclined planes’, *Physics of fluids*, 11(3), pp. 542–548.

Quan Luna, B. R. (2012) *Dynamic numerical run out modelling for quantitative landslide risk assessment, University of Twente*.

Rahardjo, H. *et al.* (2007) ‘Factors Controlling Instability of Homogeneous Soil Slopes under Rainfall’, *Journal of Geotechnical and Geoenvironmental Engineering*, 133(12), pp. 1532–1543. doi: 10.1061/(asce)1090-0241(2007)133:12(1532).

Rahardjo, H. and Fredlund, D. G. (1995) ‘Procedures for slope stability analyses involving unsaturated soils’, in *Developments in deep foundations and ground improvement schemes*, pp. 33–56.

Rickenmann, D. (1999) ‘Empirical relationships for debris flows’, *Natural hazards*, 19(1), pp. 47–77.

Rickenmann, D. *et al.* (2006) ‘Comparison of 2D debris-flow simulation models with field events’, *Computational Geosciences*, 10(2), pp. 241–264.

Rifai, R. (2008) ‘Spatial modelling and risk assessment of Sidoarjo mud volcanic flow’, in. ITC.

Roddeman, D. (2001) ‘Tochnog user’s manual—a free explicit/implicit finite element program’, *Available from tochnog. sourceforge. net [accessed 23 July 2006]*.

Roux, J.-N. and Combe, G. (2002) ‘Quasistatic rheology and the origins of strain’, *Comptes Rendus Physique*, 3(2), pp. 131–140.

Sassa, K. (1988) ‘Special lecture: Geological model for the motion of landslides’, in *International symposium on landslides. 5*, pp. 37–55.

Savage, S. B. and Hutter, K. (1989) ‘The motion of a finite mass of granular material down a rough incline’, *Journal of fluid mechanics*, 199, pp. 177–215.

Savage, S. B. and Hutter, K. (1991) ‘The dynamics of avalanches of granular materials from initiation to runout. Part I: Analysis’, *Acta Mechanica*, 86(1), pp. 201–223.

Seki, K. (2007) ‘SWRC fit – a nonlinear fitting program with a water retention curve for soils having unimodal and bimodal pore structure’, *Hydrology and Earth System Sciences Discussions*, 4(1), pp. 407–437. doi: 10.5194/hessd-4-407-2007.

Shen, W. *et al.* (2018) ‘A modified finite difference model for the modelling of flowslides’, *Landslides*, 15(8), pp. 1577–1593. doi: 10.1007/s10346-018-0980-6.

Sheridan, M. F. *et al.* (2005) ‘Evaluating Titan2D mass-flow model using the 1963 Little Tahoma peak avalanches, Mount Rainier, Washington’, *Journal of Volcanology and Geothermal Research*, 139(1–2), pp. 89–102.

Shi, B., Zhang, Y. and Zhang, W. (2018) ‘Analysis of the entire failure process of the rotational slide using the material point method’, *International Journal of Geomechanics*, 18(8), p. 4018092.

Soundararajan, K. K. (2015) ‘Multi-scale multiphase modelling of granular flows’. University of Cambridge.

Sovilla, B., Burlando, P. and Bartelt, P. (2006) ‘Field experiments and numerical modelling of mass entrainment in snow avalanches’, *Journal of Geophysical Research: Earth Surface*, 111(3), pp. 1–16. doi: 10.1029/2005JF000391.

Staron, L. and Hinch, E. J. (2005) ‘Study of the collapse of granular columns using DEM numerical simulation’, *arXiv preprint physics/0501022*.

Staron, L. and Lajeunesse, E. (2009) ‘Understanding how volume affects the mobility of dry debris flows’, *Geophysical Research Letters*, 36(12).

Takahashi, T. (2007) *Debris flow: mechanics, prediction and countermeasures*. Taylor & Francis.

Tang, H. *et al.* (2019) ‘Measurement of restitution and friction coefficients for granular particles and discrete element simulation for the tests of glass beads’, *Materials*, 12(19). doi: 10.3390/ma12193170.

Thompson, E. L. and Hupper, H. E. (2007) ‘Granular column collapses: Further experimental results’, *Journal of Fluid Mechanics*, 575(June 2015), pp. 177–186. doi: 10.1017/S0022112006004563.

Utili, S., Zhao, T. and Houlsby, G. T. (2015) ‘3D DEM investigation of granular column collapse: evaluation of debris motion and its destructive power’, *Engineering geology*, 186, pp. 3–16.

VanDine, D. F. and Bovis, M. (2002) ‘History and goals of Canadian debris flow research, a review’, *Natural Hazards*, 26(1), pp. 67–80.

Vijith, H. *et al.* (2014) ‘Shallow landslide initiation susceptibility mapping by GIS-based weights-of-evidence analysis of multi-class spatial data-sets: A case study from the natural sloping terrain of Western Ghats, India’, *Georisk*, 8(1), pp. 48–62. doi: 10.1080/17499518.2013.843437.

Voellmy, A. (1955) ‘Die Zerstorungs-Kraft von lawinen, Sonderdruck aus der Schweiz’, *Bauzeitung*, 73, pp. 159–165.

Whitman, R. V (2000) ‘Organizing and evaluating uncertainty in geotechnical engineering’, *Journal of Geotechnical and Geoenvironmental Engineering*, 126(7), pp. 583–593.

Wicklein, E. and Papanicolaou, A. N. (2000) ‘Sediment Transport Modelling in Mountain Streams’, in *Building Partnerships*, pp. 1–10.

Yang, G. and Wang, X. (2012) ‘Discrete element modelling for granular materials’, *Electronic Journal of Geotechnical Engineering*, 17, pp. 2463–2474.

Zenit, R. (2005) ‘Computer simulations of the collapse of a granular column’, *Physics of Fluids*, 17(3), p. 31703.

Zhan, T. L. T. and Ng, C. W. W. (2004) ‘Analytical analysis of rainfall infiltration mechanism in unsaturated soils’, *International Journal of Geomechanics*, 4(4), pp. 273–284.

Zhang, Y. and Campbell, C. S. (1992) ‘The interface between fluid-like and solid-like behaviour in two-dimensional granular flows’, *Journal of Fluid Mechanics*, 237, pp. 541–568.

Zhao, T. (2014) *Investigation of landslide-induced debris flows by the DEM and CFD*. Oxford University, UK. Available at: https://ora.ox.ac.uk/objects/uuid:316cb3fc-dfc6-4e5a-bc0d-298e298c9c5b.

Zhao, T. (2017) *Coupled DEM-CFD analyses of landslide-induced debris flows*. Springer.

Zhu, Y. H. *et al.* (2008) ‘Research on cohesive sediment erosion by flow: An overview’, *Science in China, Series E: Technological Sciences*, 51(11), pp. 2001–2012. doi: 10.1007/s11431-008-0232-4.